REPUBLIC OF TURKEY

GAZİANTEP UNIVERSITY

GRADUATE SCHOOL OF NATURAL & APPLIED SCIENCES

INVESTIGATION OF IMPACT BEHAVIOR OF THE NANO-SCALED PARTICLE FILLED HYBRID COMPOSITE PLATES

Ph.D. THESIS

IN

MECHANICAL ENGINEERING

BY

NURETTİN FURKAN DOĞAN

JULY 2019

JULY 2019 Ph.D. in Mechanical Engineering NURETTİN FURKAN DOĞAN

INVESTIGATION OF IMPACT BEHAVIOR OF THE NANO-SCALED PARTICLE FILLED HYBRID COMPOSITE PLATES

Ph.D. Thesis

in

Mechanical Engineering

Gaziantep University

Supervisor

Assoc. Prof. Dr. Ahmet ERKLİĞ

by

Nurettin Furkan DOĞAN

July 2019

REPUBLIC OF TURKEY
GAZİANTEP UNIVERSITY
GRADUATE SCHOOL OF NATURAL & APPLIED SCIENCES
MECHANICAL ENGINEERING

Name of the Thesis : Investigation of Impact Behavior of The Nano-Scaled Particle Filled Hybrid Composite Plates
Name of the Student : Nurettin Furkan DOĞAN
Exam Date : 05.07.2019
Approval of the Graduate School of Natural and Applied Sciences

Prof. Dr. A. Necmeddin YAZICI
Director

I certify that this thesis satisfies all the requirements as a thesis for the degree of Doctor of Philosophy.

Prof. Dr. Mustafa GÜNAL
Head of Department

This is to certify that we have read this thesis and that in our consensus/majority opinion it is fully adequate, in scope and quality, as a thesis for the degree of Doctor of Philosophy.

Assoc. Prof. Dr. Ahmet ERKLİĞ
Supervisor

Examining Committee Members:	Signature
Assoc. Prof. Dr. Recep EKİCİ	....
Assoc. Prof. Dr. Ahmet ERKLİĞ	....
Assoc. Prof. Dr. Ö. Yavuz BOZKURT	....
Assist. Prof. Dr. M. Veysel ÇAKIR	....
Assist. Prof. Dr. Mehmet BULUT	....

I hereby declare that all information in this document has been obtained and presented in accordance with academic rules and ethical conduct. I also declare that, as required by these rules and conduct, I have fully cited and referenced all material and results that are not original to this work.

Nurettin Furkan DOĞAN

ABSTRACT

INVESTIGATION OF IMPACT BEHAVIOR OF THE NANO-SCALED PARTICLE FILLED HYBRID COMPOSITE PLATES

DOĞAN, Nurettin Furkan
Ph.D. in Mechanical Engineering
Supervisor: Assoc. Prof. Dr. Ahmet ERKLİĞ
July 2019
126 pages

The present study aims to investigate the ability of graphene nanoplatelets (GnPs) inclusion effects on mechanical (tensile and flexural) and low-velocity impact (LVI) characteristics of glass, aramid, basalt and carbon fiber reinforced hybrid/non-hybrid composites. A high speed of mechanical stirrer was used for mixing of epoxy with GnPs particles at different GnPs weight contents (0, 0.1, 0.25, and 0.5 wt %), and the mixture of the GnPs enriched resin was applied to the fiber fabrics for different lay-up conditions by using the hand-layup and vacuum assisted hand lay-up method. Impact tests were performed by using a drop weight impact machine at the impact energy of 30J, and load to time/displacement history responses were evaluated and reported. Damage characteristics of the composite samples after the low-velocity impact tests were characterized and compared according to GnPs contents. In this way, the combined effects of GnPs loading and glass/aramid, glass/basalt, glass/carbon fiber hybridizations were investigated in detail. Results showed from this study that incorporation of GnPs particles at the certain concentrations significantly affected the impact resistance and mechanical properties of fiber reinforced hybrid/non-hybrid composites. However, excessive GnPs particle addition into the epoxy resin caused a reduction in mechanical and impact properties as a result of particle agglomeration with reducing load transferring from particle to matrix resin.

Key Words: Low velocity impact, Glass, Aramid, Basalt, Carbon, Graphene nano platelets (GnPs).

ÖZET

NANO KATKILI HİBRİT KOMPOZİT PLAKALARIN DARBE DAVRANIŞLARININ İNCELENMESİ

DOĞAN, Nurettin Furkan
Doktora Tezi, Makine Mühendisliği
Danışman: Doç. Dr. Ahmet ERKLİĞ
Temmuz 2019
126 sayfa

Bu çalışma, grafen nanoparçacıkların (GnPs) cam, aramid, bazalt ve karbon fiber takviyeli hibrit / hibrit olmayan kompozitlerin mekanik (gerilme ve eğilme) ve düşük hız etkisi (LVI) özellikleri üzerindeki etkilerini araştırmayı amaçlamaktadır. Farklı GnPs ağırlık muhtevasında (ağırlıkça %0, 0.1, 0.25 ve 0.5) GnP parçacıkları ile epoksi karışımı yüksek hızlı mekanik karıştırıcı vasıtasıyla karıştırıldı ve farklı tabaka dizilimleri için elyaf kumaşlara GnP katılmış reçine karışımı uygulandı. El yatırması ve vakum destekli el yatırması yöntemi kullanılarak kompozit plakaların üretimleri gerçekleştirildi. Darbe testleri, 30J darbe enerjisi için bir ağırlık düşürmeli darbe makinesi kullanılarak yapıldı ve yük / yer değiştirme/ zaman diyagramları oluşturuldu ve incelendi. Düşük hızlı darbe testlerinden sonra kompozit numunelerin hasar özellikleri karakterize edildi ve GnP ağırlık oranlarına göre karşılaştırıldı. Bu şekilde, GnP'lerin modifikasyonu ve cam / aramid, cam / bazalt, cam / karbon fiber hibridizasyonunun birleşik etkileri ayrıntılı olarak incelenmiştir. Bu çalışmadan elde edilen sonuçlar, GnP partiküllerinin belirli konsantrasyonlarda dahil edilmesinin, fiber takviyeli hibrit / hibrit olmayan kompozitlerin darbe direncini ve mekanik özelliklerini önemli ölçüde etkilediğini gösterdi. Bununla birlikte, epoksi reçinesi içine aşırı GnPs partikül ilavesi, partikülden matris reçineye yük transferini azaltan partikül topaklanmasının bir sonucu olarak mekanik ve darbe özelliklerinde bir azalmaya neden olmuştur.

Anahtar Kelimeler: Düşük hız etkisi, Cam, Aramid, Bazalt, Karbon, grafen nanoparçacık (GnP).

'To my beloved parents, my wife and my daughter'

ACKNOWLEDGEMENTS

I would like to thank my supervisor Assoc. Prof. Dr. Ahmet ERKLİĞ for his guidance, enthusiasm and friendly advice throughout the study. I am sincerely grateful for his encouragement and motivation.

I would like to express my deepest regards and respects to the Ph.D. thesis monitoring committee members Assoc. Prof. Dr. Recep EKİCİ and Assoc. Prof. Dr. Ö. Yavuz BOZKURT for their suggestions and support throughout my thesis study.

I would like to express my love and gratitude to my wife for her support, always best wishes.

I would like to take this opportunity to express my gratitude to my parents for their spiritual support and encouragement.

Many thanks also to my friend Research Asst. Özkan ÖZBEK for his support in laboratory studies and assistantship duties.

This work is supported by Gaziantep University Scientific Research Projects Coordination Unit through project MF.DT.18.08.

TABLE OF CONTENTS

Page

LIST OF TABLES

LIST OF FIGURES

LIST OF ABBREVIATIONS

GnPs	Graphene nanoplatelets
LVI	Low velocity impact
FRP	Fiber reinforced polymer
GFRP	Glass fiber reinforced polymer
AFRP	Aramid fiber reinforced polymer
BFRP	Basalt fiber reinforced polymer
CFRP	Carbon fiber reinforced polymer
SEM	Scanning electron microscopy

CHAPTER 1

INTRODUCTION

1.1 General Introduction

Composite materials are used not only in the modern world but also in the structures made by the ancient Mesopotamian civilizations dating back to 4900 BC. These civilizations used bricks made of mud and straw to build their homes, and these bricks they used were good examples of composite materials. Since then, the choice of suitable materials in engineering design has a critical role. Ensuring security conditions and optimizing designs support this role. The need for suitable materials has been started to be removed by means of fiber-reinforced polymer (FRP) composites with the production of high strength fibers and advances in polymer chemistry. Together with these developments, fiber-reinforced polymer composites are used at high rates in aviation, marine, automobile industries due to their great advantages over traditional monolithic engineering materials [1, 23, 24].

1.2 An Overview of Composite Materials

A composite material can be defined as the combination of two or more material in macroscopic level to benefit the superior properties of each material to reach a new material having desired properties. For example, in some designs, the high strength of the material may be required with the lightness of the material. It may not always be possible to have a material to respond to these demands. On the other hand, composite materials can respond to these demands with having different material combinations, configurations, ratio. Composite materials have some advantages over conventional materials (Figure 1.1). These advantages can be summarized as follows [1]:

- Excellent strength-to-weight and stiffness-to-weight ratios can be achieved by composite materials.
- Laminate patterns and ply build-up in a part can be tailored to give the required mechanical properties in various directions.

- Complex double-curvature parts with a smooth surface finish can be made in one manufacturing operation.
- Composites offer excellent resistance to corrosion, chemical attack, and outdoor weathering, etc. Composites can retain their shape and size when they are hot or cool, wet or dry.
- Composites have low thermal conductivity.

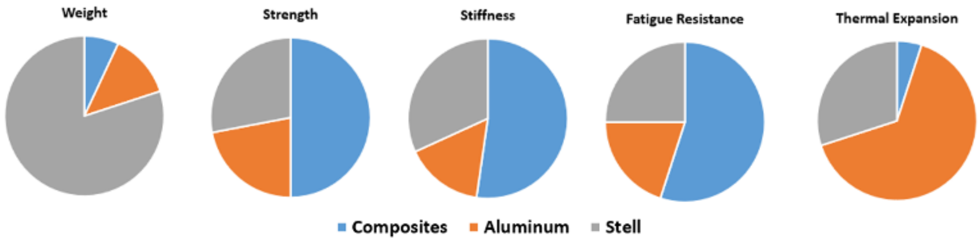

Figure 1.1 Comparison between composite materials and conventional engineering materials [2].

However, composites have some drawbacks and limitations compared to conventional engineering materials also [1-3]:

- The production process of composite materials can be complex and expensive.
- Mechanical characterization of the composite materials is more complex than metals due their anisotropic behavior.
- Composites have poor impact resistance. Delamination and cracks which formed mostly as a result of impact loading are internal and may require some special inspection techniques.
- Laminated composites exhibit poor resistance to out-of-plane loading.
- Since composites are constructed by different layers, they can delaminate between layers.
- Also, disposal of composite materials is difficult compared to traditional materials.

Composite material consists of two main elements as matrix (continuous phase) and reinforcement (discontinuous phase) material. Matrix has the duty of holding reinforcement material (fiber) together, distributing the load regularly on the fibers and protecting the fiber against environmental effects [3]. Fiber is the main strength element in the composite material structure. The classification of composite materials is done in two different ways. In the first one, matrix type is used for classification in Figure 1.2. According to this method composites classified into three group as a polymer, ceramic or metal-based composites. In the second way, reinforcement geometry as fiber, particulate and flake is used to classify the composite materials in Figure 1.3 [1, 4].

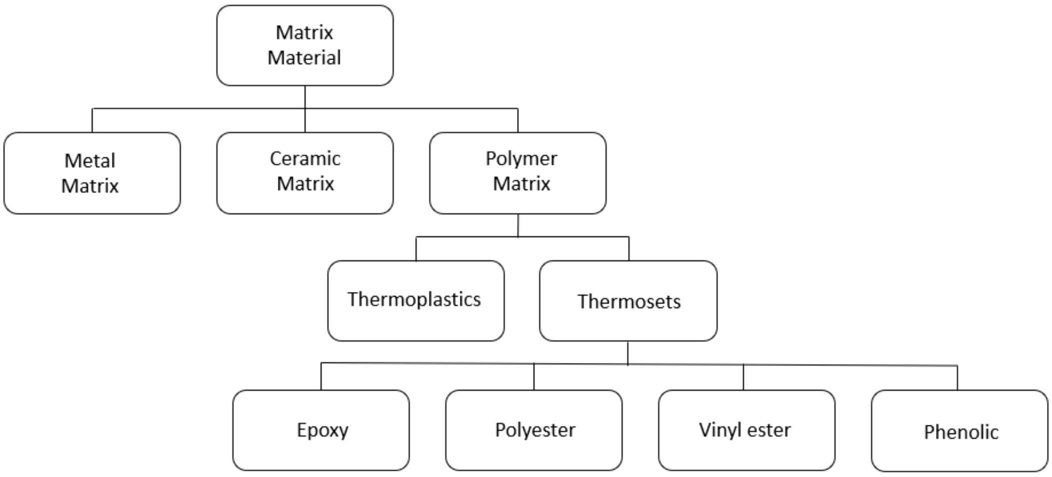

Figure 1.2 Composite material classification according to matrix type [1, 4].

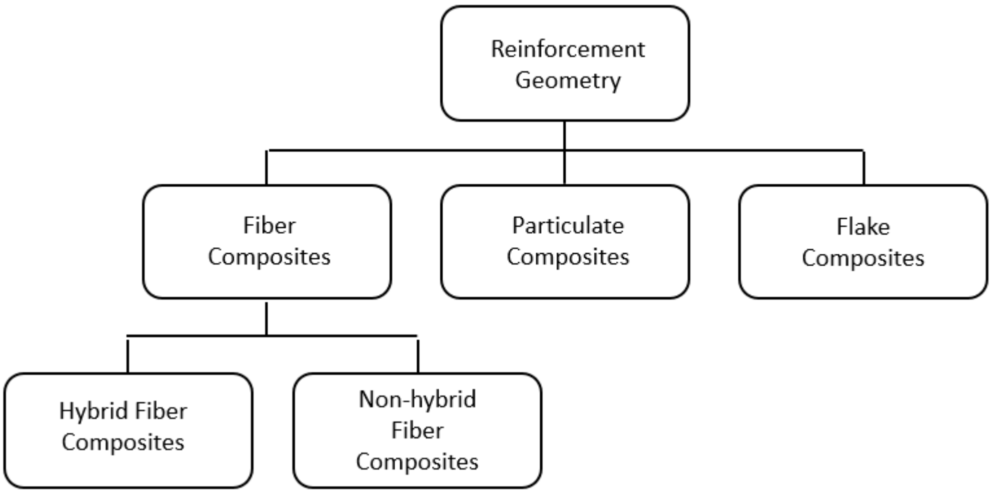

Figure 1.3 Composite material classification according to reinforcement type [1, 4].

Polymer matrix are divided into two categories: *thermoplastics* and *thermosets*. Thermoplastic polymers can melt or soften with heating and they can flow under heat and pressure. In the room temperature, thermoplastics harden and becomes plastic. On the other hand, thermosets are cured with the help of chemical curing agents. Once they cured to become plastic, they can never soften or dissolve due to their cross-linked form of molecule network. Epoxy, polyester, vinyl ester and phenolic are commonly used thermoset polymers as matrix material in composites. Epoxy is the most frequently used thermoset matrix material type especially in aerospace industry where the weight of the structure is critical. Epoxy is a polymer which contains an epoxide group (an oxygen atom and two carbon atoms in Figure 1.4) in its chemical structure. Epoxy resins have higher cost than polyesters, but they have better moisture resistance, higher thermal resistance (i.e. maximum in use capacity), higher adhesion with glass fibers, and lower shrinkage on curing properties. The many types of epoxy can be produced using various chemical agents. For example, diluents are used to decrease the viscosity of epoxy polymer [2].

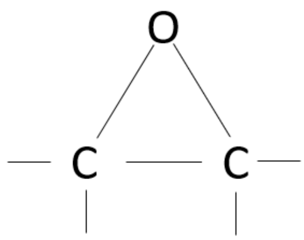

Figure 1.4 Chemical structure of an epoxide group.

Table 1.1 Properties of thermoset resins [1, 2, 25].

Resin Types	Characteristics
Epoxies	Expensive
	Higher temperature resistance than polyester and vinyl ester.
	Better moisture resistance
	Low shrinkage on curing
Polyesters	Cheap
	High processing flexibility
	High shrinkage on curing
Vinyl esters	Tougher than polyesters
	Better moisture resistance than polyesters
Polyimides	Very high temperature resistance
	Requires elevated-temperature post cure
Phenolics	Good for high temperature applications with smoke and fire resistance
	Difficult to process

Since their superior strength to weight ratio, especially fiber reinforced polymer (FRP) composites have attracted great interest in the aerospace, automobile, marine and defense industries applications. Fiber types in FRP composites vary from glass, carbon, aramid and graphite fibers as well as natural fibers like basalt, jute, kenaf, hemp, bamboo and flax [5]. Using textile technology, these fibers are used as glass, carbon, aramid or hybrid woven fabrics in composite materials, and woven fabric technology is highly popular due to their cost efficiency and high processability. The mechanical properties of fabric composites depend on the fiber (yarn), matrix properties, as well as material structural properties, i.e. number of fabric and weaving type [6]. Different fabrics can be produced by using different weaving patterns with the same fiber type. Typical fabric weaving patterns can be seen in Figure 5.

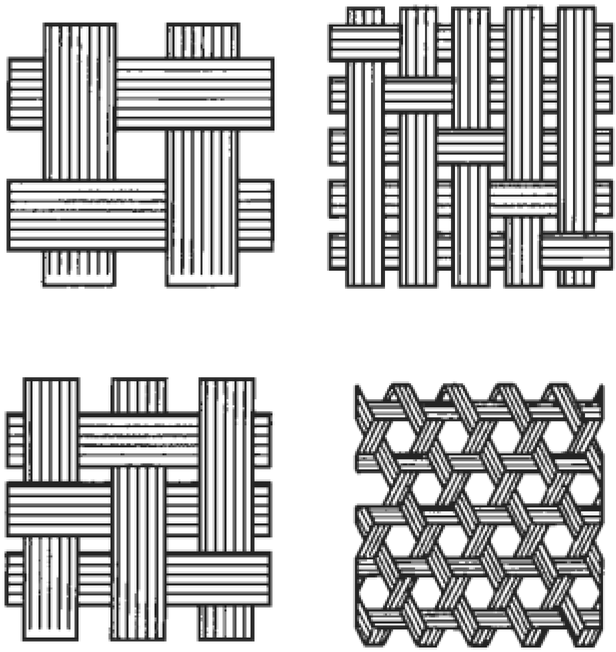

Figure 1.5 Typical fabric weaving patterns: (a) plain, (b) satin, (c) twill and (d) triaxial [6].

Glass fibers are mainly silica based and contain other minerals (oxides of calcium, sodium, aluminum, magnesium, boron etc.). According to their additives, glass fibers are designated with E, S and C. For example, S-glass contains high silica content and can be applicable for higher temperature applications. Most of the glass fibers in the market is E-glass which E is designated to high electrical insulation property of fiber. E-glass fiber have high strength and moderate tensile modulus values. Glass fibers have low density and high strength value. On the other hand, elastic modulus of glass fiber is quite low. Glass fibers are very cheap, and are used into wide application area as glass fiber reinforced polymer (GFRP), but generally they are used in the structures that are not constantly loaded. Because, GFRP are susceptible to static fatigue which occurs the material constantly bear a load for a long time period [2,6,8].

Carbon and graphite fibers are carbon element-based fibers and they have high application area in aerospace and automobile industry due to their high modulus and strength, high electrical conductivity, low thermal expansion and high chemical resistance properties. In molecular structure of carbon fiber, carbon atoms are aligned as a plane which parallel to the axis of the fiber and thus have superior properties. Carbon fibers have more than 50 type with different strength, stiffness and cost properties in the market [2, 25, 26].

Aramid fibers have low density, high stiffness and strength in tension properties but poor compressive properties (Some of the types of aramid fibers only have a compressive strength up to 1/8 of their tensile strength) [2]. Kevlar 29 is used to make ballistic vest due to its high strain to failure property [14]. Furthermore, the aramid fiber has good vibration damping properties and is very sensitive to ultraviolet light.

In FRP composites, fibers can be used individually and be used two or more together as “hybrid fibers”. With the hybrid fibers usage, it becomes possible to combine the advantages of different fibers while reducing their less desirable properties of the material. As an example, carbon fiber reinforced composites show high strength and low-density properties, unless they have poor impact resistance. With hybridization by using glass fiber, impact resistance of composite can be improved while excellent strength property can be hold.

Despite good mechanical properties of reinforcement materials, brittle nature of matrix materials (especially polymeric systems) is a major drawback and limits the usage of composite material in load-bearing applications. Matrix modification with the incorporation of micro/nano scaled filler material is one of the methods to overcome these weak features of the matrix as well as increasing electrical/thermal conductivity or fire resistance properties. In general, the unique property of nano-fillers (e.g. strength, hardness, etc.) and the unique combination of the low concentration are required to affect the properties of the polymers constitute the most important advantage of the nano-particle addition to the polymer matrices. Mostly used nanoparticles that used with composites are graphene nano platelets (GnPs), carbon nanotube (CNT), nanoclay, nano graphene, nano silica etc. [15-20].

Enhancement in mechanical properties of FRP composites is mostly related with the interfacial adhesion between fiber/matrix/particle. As a definition, nanoparticles are particles with at least one dimension below 1 μm (or 100 nm). And it is known that decreasing particle size offers increasing surface/volume ratio. So that, to increase the surface area of particles particle dimensions must be decreased which lead to increase interfacial interaction between fiber/matrix/particle [21]. Schematically explanation can be seen in Figure 1.6.

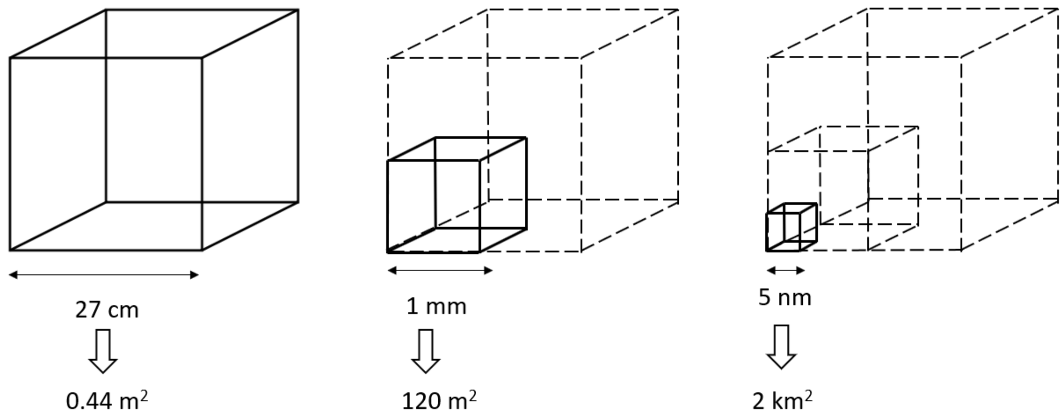

Figure 1.6 Schematic illustration of the increasing surface area with decreasing particle dimension [21].

Recently, carbon-based nano materials such as carbon nanotubes (CNTs), nano graphite and nano graphene or graphene nano platelets (GnPs) have attracted huge attention by the researchers due to their outstanding thermal, electrical and mechanical properties.

1.3 Composite Laminates under Low-velocity Impact (LVI)

The damage characteristics of composite materials under impact loading are complex phenomenon that is affected by various factors ranging from the content of composite material to lamina sequence, and they are associated with the energy absorption of the composite material, occurring in the whole of matrix cracking, fiber breakage and delamination.

Impact damage in metals can be easily determined due to the damage initiates at the impact surface; however, in composite materials damage starts at the non-impacted surface or in the form of internal delamination. In addition, impact damage in metals is often not considered as a threat due to their ductile nature which metals may absorb a large amount of energy. On the other hand, most composites are in brittle nature and can absorb energy just in their elastic deformation, not within plastic deformation. In addition, internal damage can be significant, and it can reduce the load-bearing capacity of composite structure. Even if the structure continues to carry the load after impact damage, the damaged area will continue to spread in the structure and eventually lead to catastrophic damage to the entire structure. Thus, studies on the impact behavior of composites have a vital importance in safety of engineering designs [7].

1.3.1 Definition of Low-velocity Impact

Impact can be defined as the loading that is applied on a structure which occurs in short, middle and long time periods. Impact loading is classified into three groups according to the velocity of the impact action [8-10]:

- Low-velocity impact (velocities of 1-10 m/s)
- Intermediate-velocity impact (velocities of 10-50 m/s)
- High-velocity (Ballistic) impact (velocities of 50-1000 m/s)

Some researchers defined the low-velocity impact related with not only with the impactor velocity, but also with the material property. They stated the stress wave through the material thickness played no significant role in stress distribution. In addition to that comment, Abrate and Davies and Robinson [11, 12] proposed an ultimate compressive strain ε_c equation, assuming that a cylindrical region under the impactor was subjected to a uniform strain as the stress wave propagates along the material thickness:

$$\varepsilon_C = \frac{v_i}{v_s} \tag{1.1}$$

where v_i is the impact velocity and v_s is the speed of sound in the material.

The high-velocity impact response of the material occurs in a very short period as the stress wave propagates through the material thickness, leading to local damage. The boundary conditions can be ignored in this type of impact loading since the stress wave does not reach the boundary of the structure when the impact loading has been completed. In low velocity impact, the whole structure absorbs the impact energy of the projectile because the contact time is long enough for the respond of complete structure, and most of the impact energy is absorbed elastically (Figure 1.7).

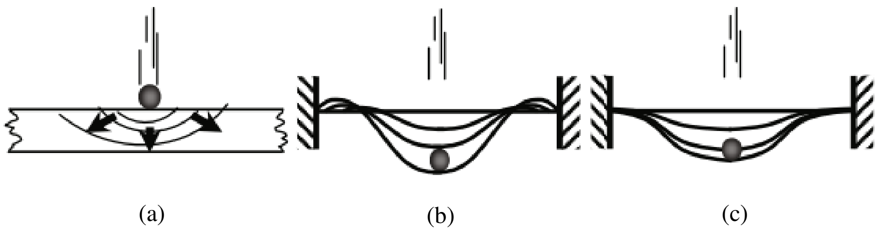

Figure 1.7 Impact response of bodies to (a)Ballistic, (b)Intermediate and (c) Low velocity impact loadings [13, 30, 31].

Charpy impact, Izod impact and drop weight impact testing are commonly performed tests for low velocity impact testing. Izod and Charpy impact tests are performed by placing a notched/unnotched specimen into machine. In these tests, the pendulum is raised up a certain height, released to strike on the specimen and bounced to a measured height (Figure 1.8). Both of test method work with pendulum mechanism, but difference is that Charpy impact test specimen is supported as simple beam, and Izod test specimen is supported as a cantilever.

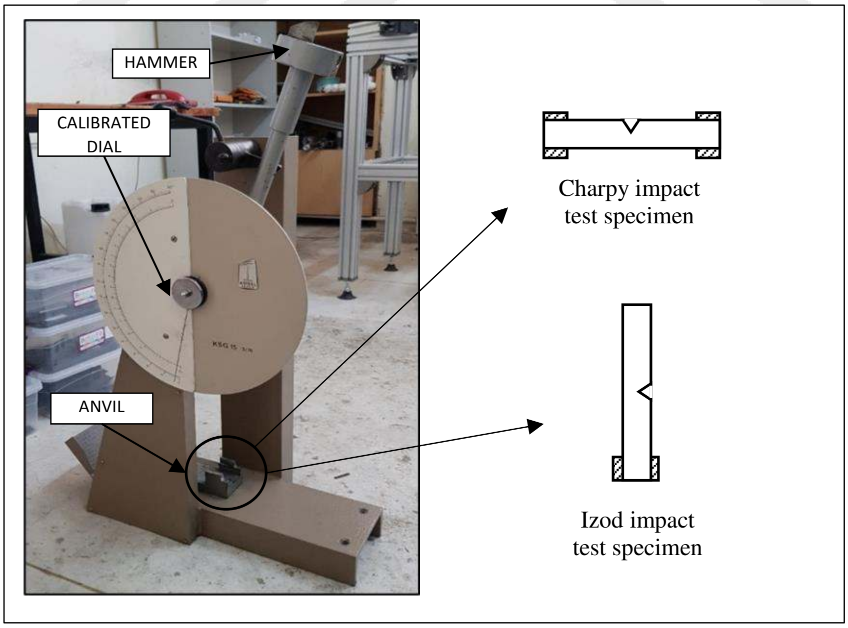

Figure 1.8 Charpy and Izod impact test rigs.

In drop weight impact test (Figure 1.9), the specimen is subjected to impact load by using free-falling mass from a certain height to simulate the low-velocity impact. The advantages of this test method include the adjustment of impactor geometry, weight and impact energy. A hemi-spherical shaped impactor is generally used in these tests, but if it is desired this can be in another form and diameter.

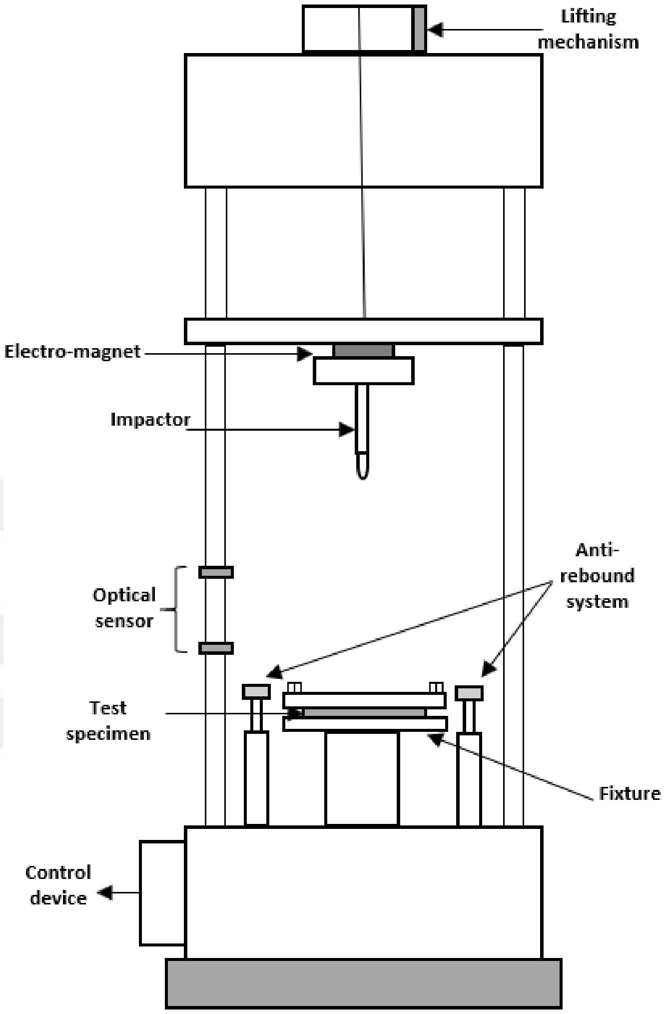

Figure 1.9 Drop weight impact test rig.

1.3.2 Failure Modes under Low-velocity Impact

Failure modes induced by impact in fiber reinforced composites are directly related with the fiber and matrix properties as well as fiber/matrix interphase region [23, 25]. Bonding strength in fiber/matrix interphase is the most important parameter for load bearing capacity of the whole composite body. Load transfer between fiber and matrix, as well as between fibers occurs in fiber/matrix interphase region. Thus, better load transfer and interfacial bonding mean better mechanical properties for FRP composite material. Besides that, there are numerous parameters that affect the impact response of composites like plate thickness, tensile and flexural modulus of composite, resin toughness, impactor mass and geometry [13].

Due to the anisotropic and heterogeneous form of FRP composite laminates, failure modes under impact load vary, and often occur interpedently in the following modes: (1) matrix mode, (2) debonding and/or delamination mode, (3) fiber mode and (4) penetration.

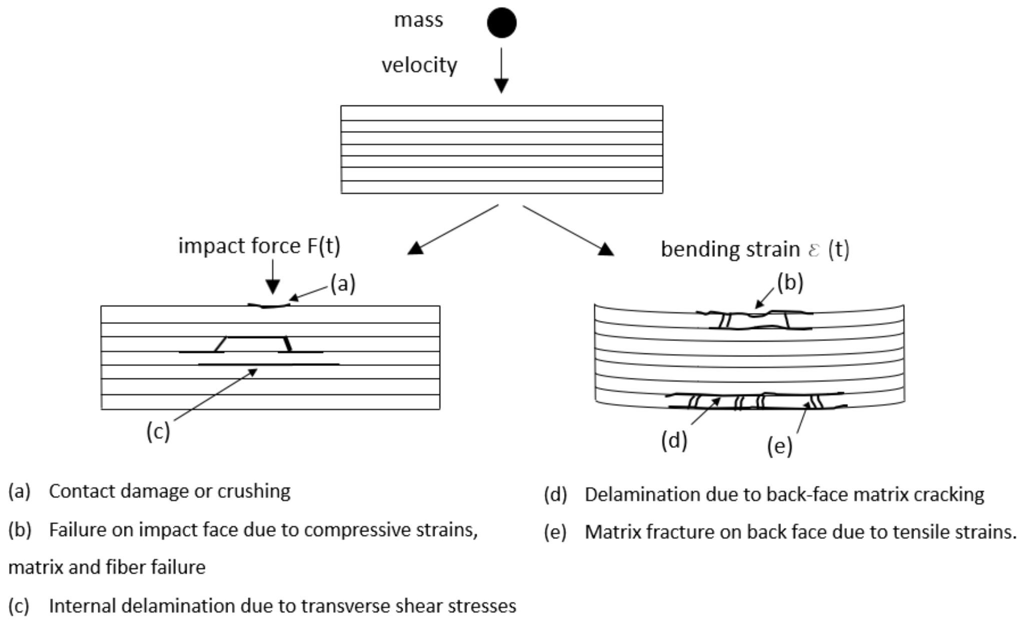

Figure 1.10 Failure modes in LVI [88].

Matrix cracking occurs due to tension, compression or shear and is triggered by LVI load. Matrix cracking usually initiates delamination and fiber/matrix debonding. Matrix cracks on the impact side of the composite laminate are called shear crack due to high transverse shear stress related to contact force applied by the impactor. The cracks on the back side of the impacted side of laminate are called a bending crack. The bending crack is formed perpendicular to the laminate and is formed due to high bending stress on the back side of laminate. These cracks are highly related with the flexural deformation of the composite laminate [13].

Delamination is the failure mode which occurs as a separation of fabric plies as a result of bending stiffness difference between fiber and matrix. Thus, delamination failure is directly proportional with bending stiffness of the plies. Also, it is related with the thickness of ply, stacking sequence and material behavior. The bending stress in the laminate is the major cause of this failure type. In addition, delamination failure is generally initiated by the matrix crack which results high out-of-plane normal stresses and high interlaminar shear stress on the interface [13, 22].

Delamination failure is followed by the fiber failure which can be considered as the precursor of catastrophic failure of whole structure. After the impact loading, the impact failure process continues in the form of matrix crack, delamination and fiber failure. This shows that, with the end of the matrix protection in the composite material, the matrix material cannot transfer the load uniformly over the structure which leads stress concentration and destructive failures such as fiber breakage have begun. Fiber failure modes generally occur in two ways: fiber breakage and fiber buckling. On the non-impacted side of plate, fiber breakage (rupture) occurs due to high bending stress, however fiber buckling failure occurs due to high contact stress on the impacted side [23].

Penetration mode is a catastrophic failure mode and occurs when the fiber failure reaches a critical size, resulting in a complete perforation of the composite material.

1.4 Research Objectives and Tasks

In parallel with the increase in the use of modern composite materials, the need for information about the basic mechanical properties of these materials is increased. However, mechanical properties of fiber-reinforced composite materials need to be improved in order to meet the needs of today's technology. These properties of FRP composites can be changed in three ways; fiber hybridization, matrix modification by adding micro/nano particles and fiber surface treatments. Fiber is the main load-bearing element in FRP composites and mechanical properties of the whole composite material is mainly affected by the fiber property. The process of fiber hybridization and changing the fabric stacking sequence ensures that the composite materials have the desired properties.

In addition, fiber/matrix interphase is important region to ensure proper load transfer between fibers. In order to improve fiber/matrix interfacial load transfer (or adhesion), fiber surface treatment and adding micro/nano fillers to the matrix are the most used methods in literature. A good dispersed nanofillers in matrix will improve load transfer and reduce the stress concentration points in matrix due high specific surface areas and aspect ratios [27- 29].

In this perspective, this study will mainly be focused on the impact behavior of fiber hybridization and nanofiller inclusion in polymer matrix composite laminates. Four types of fiber (glass, carbon, aramid and basalt) and a single type nanofiller of GnPs (graphene nanoplatelets) were used as reinforcement toughening material. Epoxy resin was used to as matrix in produced hybrid composite laminates. Hybrid composite laminates were produced binary combinations of fabrics with various stacking sequences. Also, four different weight content of nanofiller (0, 0.1, 0.25, 0.5 wt%) filled epoxy resin was used in laminate productions. Mechanical properties of produced composite laminates were measured experimentally by means of tensile and 3-point bending tests. LVI response of hybrid/non-hybrid laminates was investigated with drop-weight impact test using impact energy 30 J. Following mechanical tests, fracture photographs and SEM images of fractured samples were also examined in order to understand failure modes.

Main contributions of this PhD project are:

- To investigate the mechanical properties of fiber hybridized and nanoparticle filled polymer composite materials.
- To characterize the effect of fiber hybridization and matrix modification on the LVI behavior of fiber reinforced polymer composites by conducting drop-weight impact test.
- To establish a relation between fabric stacking sequence, nanofiller inclusion and LVI behavior of hybrid composite laminates.

1.5 Outline of the Thesis

This thesis presents the PhD project titled "Investigation of Impact Behavior of The Nano-Scaled Particle Filled Hybrid Composite Plates". The report consists of five chapters and in Chapter 1, general introduction, basic concepts of composite materials, the definition of low-velocity impact, and the importance of the thesis are given. Chapter 2 presents the literature survey into three sub-headers. Information about the properties of the materials used in the fabrication of composite plates and composite production methods are given in Chapter 3. In addition, in Chapter 4 tensile and flexural tests which used to investigate the mechanical properties of produced composite plates are also given in the same chapter. In Chapter 5, a detailed investigation of the effect of fiber hybridization and matrix modification on the LVI response of composite plates is given with fractographs and SEM images. Finally, the general discussions and future works are given in Chapter 6 and Chapter 7.

CHAPTER 2

LITERATURE REVIEW

2.1 Introduction

The impact behavior of fiber reinforced composites had been a major limitation in their industrial application due to their limited out-of-plane mechanical characteristics. The impact behavior of fiber reinforced composites has been a major limitation in industrial applications due to their non-planar mechanical characteristics. Therefore, the development of the mechanical characteristics of composite materials has been done extensively by the researchers. This chapter summarizes the existing research studies related to current Ph.D. project.

2.2 Studies on Low-velocity Impact Behavior of Composite Laminates

Studies on the effects of fiber hybridization and matrix modification on the low-velocity impact properties of fiber reinforced composites are presented under three headings.

2.2.1 Studies on Hybrid Fiber Reinforced Composite Laminates without Nanoparticle

Hasan et al [32] manufactured jute and glass hybrid fiber reinforced polyester composite laminates by different stacking sequences. They studied the impact and tensile properties of manufactured composites and stated that the fabric stacking sequence affected the impact behavior of composite laminates. According to the experimental results hybrid composite sample which glass fabric was on outer layers showed the highest impact strength. However, they also noticed that the fabric stacking sequence had no effect on the tensile strength of the hybrid composite samples.

Behnia et al. [33] studied the effect of stacking sequence and notch angle on low velocity impact behavior of hybrid composites by using Charpy impact test. They used aramid-basalt, aramid-carbon, carbon-basalt, glass-basalt and individual fiber reinforced composites with different sequences. They stated that basalt/carbon hybrid composites have higher energy absorption capacity when the outer layer is basalt, for glass-basalt hybrid when basalt fiber in the middle. Also, increasing notch angle from 45 to 75 degree decreased the energy absorption capacity of composite with most of stacking sequence.

Lee et al. [34] studied the low velocity impact response of graphite-glass/epoxy and graphite-Kevlar/epoxy hybrid composite laminates numerically. Finite element analysis was used to analyze the impact behavior of hybrid composite laminates. They have concluded that bending and impact behavior of the composite dominantly depend on the material properties of the impacted surface. They have shown that the fractional energy loss is low when the impacted surface is graphite and it is three times higher when the impacted surface is Kevlar.

Agarwal et al. [35] investigated the effect of fabric stacking sequence on the mechanical properties of glass/carbon hybrid FRP composites. They concluded that the glass/carbon/glass aligned samples has the highest tensile strength and the hybrid sample with carbon/glass/carbon fabric alignment has the highest impact strength.

Park et al. [36] investigated the impact behavior aramid/glass fiber hybrid composite laminates and tried to evaluate this behavior using the delamination area. When the aramid layer was at the impacted surface hybrid composite exhibited higher impact energy and wider delamination area. They attributed this result to the flexible aramid layer which bends during impact which leads the laminate to deform largely during contact.

In another one of their studies, Park et al. [37] studied on the effect of stacking sequence on the impact behavior aramid/glass fiber hybrid composite laminates. After experiments, they concluded that the position of the aramid fiber layer strongly affected the impact behavior of the hybrid composite. The composite showed higher impact energy when the aramid layer on the impacted surface.

Naik and colleagues [38] investigated the impact behavior and post-impact compressive characteristics of carbon-glass/epoxy hybrid composites with drop weight testing method. They compared these behaviors with the different stacking sequences and glass-only and carbon-only laminates. After experiments, they concluded that glass-carbon hybrid composites have lower notch sensitivity compared to only glass or carbon composites. In hybrid composites, when the glass fabric on the impacted surface impact duration was higher than the reverse configuration. Also, hybrid composites give higher post impact compressive strength and lower notch sensitivity with the carbon layer outside configuration.

Hosur et al. [39] studied on the low velocity impact response of carbon-glass/epoxy hybrid laminates with four different layer configurations. They applied the drop weight impact test with different energy levels from 10-40 J and reached the conclusions: hybrid composites showed stiffness more than S2-glass/epoxy laminates, less than carbon-epoxy laminates and when glass layer on the back-surface impact response of hybrid composite enhanced due to high strain values of glass fibers.

Gustin et al. [40] investigated the low velocity impact response of Kevlar-carbon hybrid fiber sandwich composites and reached the conclusions that the addition of hybrid to outface of laminate improve the energy absorption capacity and average peak force about 5% and 14% respectively, addition of Kevlar improved the maximum absorbed energy and average peak force about 10%.

Wang et al. [41] investigated the effect of the fiber arrangement in 3D woven aramid-basalt/epoxy hybrid composites on the low velocity impact response. They concluded that the interply hybrid composite had lower peak load and higher energy absorption than intraply hybrid composite.

Sayer M. et al. [42] studied the impact behavior of glass-carbon/epoxy hybrid composite plates experimentally with different impact energies from 25 J to 75 J and reached some conclusions: when carbon layer on the impacted surface, energy absorption capacity is less than glass layer on top. Also, they worked on another study [43] the impact behavior of the aramid-glass and aramid-carbon/epoxy hybrid laminates with two different stacking sequences. Results showed that the stacking sequence has an important role in the impact response of composite plates.

Sevkat and colleagues [44] compared the results of drop weight impact of glass-graphite/epoxy hybrid composite panels experimentally and numerically. They used four different stacking sequence and four different energy levels (47, 60, 71, 122J) in their experiments. They had the results as: the hybrid composite had the impact resistance between glass only and graphite only composite plates. Also, the finite element results showed good agreement with the experimental results.

Enfedaque and colleagues [45] studied the low velocity impact behavior of carbon-glass/epoxy hybrid laminates under impact energies from 30 to 245J with drop weight impact test. Thus, hybridization of carbon fiber/epoxy composite with glass fibers increased the peak load by 10% and energy dissipated by 25%.

Sevkat et al. [46] experimented the effect of the impactor geometry on the drop weight impact response of glass-graphite/epoxy hybrid laminates. Two different stacking sequenced hybrid composites were impacted using spherical, flat-ended cylindrical and straight line Charpy impactors. They also compared their experimental results with the finite element models. They concluded that the glass fiber on the impacted surface, composite sustained higher impact load and larger delamination. Larger contact area produced larger initial peak and maximum force, bigger delamination between layers.

Sarasini et al. [47] experimentally investigated the low velocity impact behavior and residual post-impact behavior of the aramid-basalt/epoxy hybrid composites. They applied falling dart impact test on the different stacking sequenced plates with energy levels of 5, 12.5 and 25 J. Also, they used the four-point bending test to examine the post impact properties of the composites. Results showed that when the basalt fiber is on the outside surface, hybrid composite exhibited a better energy absorption capability than inside configuration.

Sarasini and colleagues [48] studied the low velocity impact behavior of basalt-carbon/epoxy hybrid composites. Drop weight impact test was performed on their study with three different energies of 5, 12.5 and 25J on the composite laminates with different stacking sequences. They also investigated the post-impact properties of hybrid composite. Basalt fiber hybridization causes larger global deformation, thus a wider damage area and energy absorption after impact tests. Also, basalt hybridization allows to peak load enchantment with no penetration on the surface.

Valença et al. [49] investigated the mechanical behavior of Kevlar fiber reinforced and glass-Kevlar reinforced epoxy composite by performing tensile, bending and impact tests. Hybrid composite showed the best results of ratio between impact energy and specific yield strength based on experiments.

Bandaru et al. [50] studied the low velocity impact behavior of 3D angle-interlock Kevlar-basalt/polypropylene (PP) composite by using drop weight impact test with the energy level of 240 J. They compared the LVI responses of hybrid PP composites by means of peak force, energy absorption and damage modes. They concluded that the peak force of hybrid laminate is higher than Kevlar PP composite and less than basalt PP composite laminate. Also, energy absorption capacity of hybrid laminates is higher than Kevlar and basalt/polypropylene composites.

Cheon et al. [52] investigated the low velocity impact energy absorption characteristics of glass fiber hybrid composite by performing Charpy impact test. They used polyethylene fabric, polypropylene fabric, not-silane-treated glass fibers and Kevlar fibers for hybridization process of glass fiber. According to study, when unidirectional Kevlar fiber was embedded into glass/epoxy composite, the impact energy absorption capacity was 80% higher, also, when not-silane-treated glass fiber was embedded into pure one, energy absorption capacity was 40% higher than pure glass/epoxy composite laminate.

Murugan et al.[53] studied the effect of fiber hybridization on the dynamic and static mechanical properties of fiber reinforced composite plates. They used E-glass and carbon plain fabrics, and epoxy resin in composite plate production. According to their experimental results, when E-glass fabric was on the outer layers, hybrid composite laminates had higher tensile and impact strength, while composite laminate with carbon fabric in the core layers had higher flexural strength, storage and loss modulus values.

In one study, Erkliğ and Bulut [54] investigated the effects of fabric stacking sequence on the LVI resistance and damage tolerance of Kevlar/glass/epoxy hybrid composites by performing Charpy impact tests. They stated that, when Kevlar fabric was on impacted side hybrid samples exhibited higher absorbed energy with lower damage propagation.

Bozkurt et al. [55] manufactured Basalt/Aramid/epoxy hybrid composites to study hybridization effects on the LVI behavior of composite with different fabric stacking configurations. It was reported that impact response of FRP composite were dominantly affected by the fabric type on the impacted surface of the hybrid sample.

When the above-mentioned studies are examined, it was seen that the effect of fiber hybridization on LVI behavior of composite materials has been studied extensively. In these studies, it was observed that epoxy resin was used with aramid, basalt, carbon and glass fabrics.

2.2.2 Studies using Non-Hybrid Fiber Reinforced Composite Laminates with Nanoparticle

The use of nanoparticles as a reinforcement material for composite materials has become increasingly widespread. Nanoclay, CNT and nano silica are generally used particles in the studies.

Hosur et al. [56] experimented the effect of the nanoclay content in the carbon/epoxy composites on the low-velocity impact response. Drop weight impact test with different energy levels of 10, 20 and 30J is used to characterize the low velocity impact response. In results, 1 wt% nanoclay content had the best results in terms of damage area, nanoclay addition resulted stiffer and more localized damage area in composite laminates. They attributed the localization of damage area to increased stiffness and damage propagation resistance of composite laminates.

Iqbal et al. [57] investigated the impact damage resistance of carbon fiber reinforced epoxy with nanoclay filler using low velocity impact and compression after impact tests. In experiments, they fabricated carbon/epoxy composite with 0, 3 and 5 wt% content of nanoclay and applied drop weight impact test with 15, 20, 25 and 30J impact energy levels. In the study, they concluded that up to 3 wt% nanoclay incorporation with the epoxy decreased the impact damage size compared to full carbon-epoxy laminates. Addition of 3 wt% nanoclay in matrix improved the impact damage resistance in terms of impact energy.

In another study, Khan et al. [58] studied the effect of nanoclay on the mechanical and fracture behavior of carbon fiber/epoxy composites. Charpy impact and quasi-static compact tension tests performed to measure fracture toughness of the samples. Highest impact fracture toughness is reached when the nanoclay content is 3 wt%. At higher contents of filler toughness tend to decrease.

In order to analyze the effect of MWCNT on the low velocity impact and after impact behavior of CFRP laminates, Kostopoulos et al. [59] used 0.5 wt% MWCNT for matrix modification. Impact tests were performed per ASTM D5628-07 by drop weight impact machine with 2, 8, 12, 16 and 20J impact energy levels. According to results, authors stated that there was no radical difference in delamination area and absorbed energy when enhanced laminates compared with pristine laminates. Also, they mentioned that the effect of CNT can be higher in the high velocity impact.

Ashrafi et al. [60] investigated the mechanical performance of epoxy/carbon fiber laminate composites reinforced with single-walled carbon nanotubes in weight percentages of 0.1 and 0.2. They performed drop weight impact and compression after impact (CAI) tests. 0.1 wt% nanoparticle incorporation in epoxy resin resulted in a 5% reduction of the impact damage area.

In another study, Alhazov et al. [61] carried out the absorbed energy capacities of laminated glass plies reinforced with carbon nanotube (0, 0.5, 1 and 1.5 wt%) by performing Charpy impact test with the impact energy of 1.1J. They found that the 341% increasing in the energy absorption capacity at 1.5 wt% CNT additive.

Soliman and colleagues [62] studied the low velocity impact behavior of thin woven carbon fabric composites filled by addition of MWCNTs with 0.5, 1 and 1.5wt%. The test samples are subjected to impact with the levels of energy 15, 24, 30, 60 and 120J. They investigate the load-displacement curves, velocity and energy absorption behaviors of the laminates. They mentioned that the samples showed same peak force and 50% improvement of penetration energy below the penetration limit with 1.5 wt% addition. Above the penetration limit, penetration energy decreased when the impact energy increased.

Reis et al. [63] studied the impact response of Kevlar fiber/epoxy reinforced with nanoclay by wt% of 1.5, 3 and 6. Low velocity impact tests are performed using drop weight impact test with energy levels of 6, 12 and 21 J. They concluded that the 6 wt% nanoclay filled laminates showed the best performance in terms of elastic redemption and penetration resistance.

In another study, Reis et al. [64] studied the impact response of Kevlar fiber/epoxy reinforced with cork powder and nanoclay. They used the drop weight impact test with the impact energy levels of 6, 12 and 21 J. They mentioned that the filler effect was positive in the maximum impact load, however it was negative in displacement. The maximum load increased about 4.5% in laminates with cork powder, 10.4% in laminates with cork/clay and 16.1% in laminates filled with nanoclay for 21 J impact energy. They obtained the best result for elastic recuperation in the laminates filled with nanoclay and was 40.1% improvement occurred. On the other hand, damaged area increased with the incorporation of nanoclay. And, damaged area increased 29% with nanoclay addition. Besides, cork addition resulted a decreasing in damaged area about 20%.

In order to analyze the low velocity impact response of carbon nanofiber (CNF) filled glass fiber reinforced polyester composites, Hossain et al. [65] performed drop weight impact test with 10, 20 and 30J impact energies. They prepared the samples 0.1, 0.2 and 0.3 wt% of CNF filled to polyester resin per ASTM D3763 standard. They concluded that the peak load increased with the increasing of impact energy and peak load was higher in laminates filled with CNF than conventional samples. Also, absorbed energy decreased with the infusion of CNF. The 0.2 wt% filled GFR composite had the highest peak load and lowest absorbed energy.

Alomari and colleagues [66] studied the low velocity impact characteristics of Kevlar/polyester enhanced with nanoclay (4.3wt% and 9.4wt%). They used the drop weight impact test to investigate the impact energy absorption characteristics of samples. They concluded that the nanoclay addition resulted the improve in impact resistance of composites. Composite delamination aggravated with the 9.4 wt% nanoclay addition.

Rahman et al. [67] investigated the low velocity impact properties of carbon nanofiber filled carbon fiber/epoxy composites by using drop weight impact test with different energy levels of 10, 20 and 30J. They analyzed the impact surface with SEM, ultrasonic C-scan. After tests, they concluded that the peak load significantly increased with the nano material inclusion by 11%, 14% and 17% at energy levels of 10J, 20J and 30J respectively. Damage initiation energy is also increased by 35%, 33% and 52% at each energy levels. Also, damage area reduction was investigated with the presence of carbon nanofiber after C-scan studies of authors.

In another study, Siegfried et al. [68] investigated the impact residual impact properties of carbon fiber/epoxy composites reinforced with CNT. The low velocity impact behavior was conducted by using drop weight impact test per ASTM D7136 standard with the impact energy of 6.9 and 26.8J. From their observation, the mean of the delamination area for the CNT modified specimens was larger compared to the reference composite. The differences of the absorbed energy between the tested materials were limited and no major trend can be noticed.

Sivasaravanan and colleagues [69] manufactured glass fiber reinforced epoxy composites to investigate the effect of different nanoclay contents of 1, 2, 3, 4 and 5 wt% addition in epoxy matrix on the impact behavior by using Charpy and Izod impact tests per ASTM D256. As conclusions, 5 wt% of nanoclay additive in epoxy showed best results based on impact tests. After this percentage, the material became brittle and preparing process became very hard.

In one study, Taraghi et al. [70] investigated the low velocity impact response of Kevlar fiber/epoxy reinforced MWCNT's at low (-40°C) and ambient (27°C) temperatures. Impact tests were performed by drop weight test per ASTM D5628 with different energy levels from 20 to 80J. They presented some conclusions as: absorbed energy increased about 35% with 0.5 wt% MWCNT's at ambient temperature, increased about 34% with 0.3 wt% MWCNT's at low temperature.

Islam et al. [71] studied the characterization of CFR-epoxy composites filled with nanoclay and carbon nanotubes by applying 3-point bending test, dynamic mechanical analysis and low velocity impact test. Low velocity impact tests performed with 30 and 40J energy levels. They concluded that the nanoparticles modified samples showed higher impact energy absorption capacity and MWCNT's filled samples had better impact resistance than other samples.

Boumbimba et al. [72] investigated the low velocity impact of the glass fiber/epoxy modified tri-block copolymer (nanostrength) matrix. Drop tower impact test is performed at impact energies of 5.7, 9.6 and 13.4J to analyze the impact behavior. In epoxy resin, the nanostrength weight concentration was 10%. After impact tests, they concluded that the impact resistance increased, and it was more significant at high energy level. Also, the threshold penetration is increased with the presence of tri-block copolymer.

Boroujeni et al. [73] studied the high velocity impact behavior of hybrid ZnO nanorod-carbon nanotube reinforced carbon fiber/ epoxy composites. They also investigated the delamination damage of hybrid CFRP laminates by using SEM. They reached a 21% of improvement in impact energy absorption capacity with the addition of ZnO nanorods and MWCNTs.

Rafiq and colleagues [74] studied the impact resistance of glass fiber-epoxy with nanoclay filler. They subjected the samples to low velocity impact with energy levels from 10 to 50J. At the end of the study, its concluded that the addition of 1.5 wt% nanoclay resulted in the improvement of 23% in the peak load and 11% increase in stiffness of the composite.

Meybodi et al. [75] experimented a study on low velocity impact behavior of glass/epoxy composite reinforced with various contents of nanoclay. The effect of nanoclay types and manufacturing method of composite also investigated. They practiced the drop weight impact test on the samples filled with 0, 3, 5 and 7 wt% of nanoclay. They made some conclusions which are: no significance difference in peak load with content of nanoclay; delamination area decreased one to third when change in content from 3 wt% to 7 wt%; samples fabricated with vacuum resin transfer method(VARTM) had less damage area and more energy absorption than hand lay-up method samples.

Singh et al. [76] studied the impact response of quasi-isotropic asymmetric carbon fiber/epoxy filled with multiwalled carbon nanotubes (MWCNT's) on low velocity impact damage. The composite laminates embedded with 0, 2, and 5 wt% MWCNT's and subjected to drop weight impact test with 94.14J impact energy level per ASTM D7136 standard. After experiments, they reached 13.53% improvement in energy absorption capacity and damage area reducing with 2 wt% of MWCNT's filler content.

Taraghi et al. [77] studied the effect of MWCNT's filled foam-core sandwich panels with Kevlar fiber reinforced epoxy face sheet on the low velocity impact response. Impact tests performed per ASTM D5628 by using drop tower impact test machine for different levels of energy (10, 20, 30, 40 and 50J). They used 0 and 5 wt% of MWCNTs into resin. Their results showed that the addition of nanoparticle, the rebounding, perforation thresholds, penetration thresholds and the absorbed energy increased with the addition of 5 wt% MWCNTs.

Rostamiyan et al. [78] studied the modelling and optimizing tensile and impact strength properties of glass fiber/epoxy composite reinforced with nano silica (SiO_2) and nanoclay. They performed the Izod impact test per ASTM D256 to evaluate the impact strength of material. According to test results, they mentioned that the best impact strength obtained in 4.03 wt% nano silica and 5 wt% nanoclay introduced laminates.

Mohan et al. [79] investigated the medium velocity impact response of nanoclay filled glass fiber/epoxy composite laminates. The various weight percentages (0, 1, 2, 3 and 5 wt%) of nanoclay is introduced epoxy resin. They also investigated the effect of fiber orientation and weight fraction on the mechanical properties of laminates.

Ahmad and colleagues [80] studied the effect of nano silica particle inclusion in glass fiber reinforced composites on the mechanical and thermal properties with different weight percentages of nano material. They conducted the Charpy impact test to evaluate the low velocity impact response of material and stated that the absorbed energy increases with the nano silica content, and they interpreted as a result of delay in the fracture due to pulling and breaking mechanism between matrix and fibers.

Kamar et al. [81] studied the ability of graphene nanoplatelets (0, 0.25 and 1 wt%) to improve the interlaminar mechanical properties of glass-reinforced composites. Drop weight impact test is conducted with different impact energies to evaluate the low velocity impact property of samples. They concluded that the increasing content of nanoparticles resulted the increasing in energy absorption capability.

In one study, Haq et al. [82] studied the LVI response of glass fiber / PVC foam reinforced sandwich composites with GnPs inclusion. They manufactured the sandwich plate in form of GnPs filled PVC foam on skin layers and glass fiber sheet in core layers. They compared the LVI results of GnPs doped composite laminates with the pristine ones. According to their study, GnPs doped specimens have greater absorbed impact energy values with less damage compared to pristine samples.

In another study, Ávila et al. [83] investigated the effect of graphene and nanoclay addition in epoxy matrix on the post fire behavior under dynamic loading. They manufactured carbon/epoxy composite by hand lay-up with vacuum assisted curing method. They stated that the addition of nanoparticles resulted in enhanced fire resistance and addition of nanoclay particle in composite increased the peak force in post-fire low velocity impact test about 11.69%.

2.2.3 Studies using Hybrid Fiber Reinforced Composite Laminates with Nanoparticle

Gokuldass and Ramesh [84] experimentally investigated the effect of nano-silica and micro rubber particles incorporation in epoxy resin on the mechanical and LVI behavior of intraply glass/Kevlar fiber reinforced composites. The researchers used intraply and mono fabrics that they weave from glass and Kevlar fibers. They studied the effect of fiber hybridization and matrix modification on tensile and flexural strength, fracture toughness and impact energy absorption behaviors on composite laminates. According to their experimental results, intraply hybrid fabric reinforced composites had higher mechanical strength than pure epoxy and mono-fabric reinforced epoxy composites. Flexural strength and modulus values were increased with fiber hybridization, micro-rubber and nano-silica addition. Also, LVI behavior of composites were enhanced with fiber hybridization, as well as micro and nano filler addition.

Kavitha and colleagues [85] studied the size scale effects on the post impact properties of hybrid glass-carbon/epoxy nano-composites. The epoxy reinforced with 0, 0.5, 1, 1.5, 2 and 2.5 wt% of nanoclay addition and the low velocity impact test is performed with drop weight impact machine at two velocities of 3.78 and 4.49 m/s. They concluded that the addition of 1.5 wt% nanoclay provides highest tensile strength and Young's modulus. Also, authors revealed that the ply-level scaled specimen absorbs more impact energy compared to sub-laminate scaled specimen.

Mohanty et al. [86] investigated the effect of nano alumina particles on the impact and flexural behavior of short glass/carbon fiber reinforced epoxy hybrid laminates with Charpy impact test method. They performed the test with the impact energy of 11J. In composite test samples, they used epoxy resin incorporated with alumina nano particles (1, 2, 3, 4 and 5 wt%) and chopped glass/carbon fibers. As conclusion, they stated that the addition of 2 wt% alumina nano particle the impact energy absorption is increased.

In another study, Asaee et al. [87] experimentally investigated the LVI response and damage mechanism of fiber-metal hybrid laminates with GnPs. They manufactured fabric-metal layered composite laminates by using 3D E-glass fabrics which sandwiched by two magnesium alloy sheets and epoxy resin filled with GnPs. According to their results, composite specimens with GnPs exhibited improved impact response. After 1 wt% GnPs, the ductility and energy absorption capacity of specimens were decreased. They attributed the degradation to the agglomeration of nano particles which lead to inhomogeneous particle dispersion in epoxy resin.

2.3 Conclusions on Literature Review

A comprehensive review of the literature on the effects of fiber modification and matrix modification on the impact behavior of materials in fiber reinforced composites is presented in this section. The following comments can be made as a result of this literature review:

- Glass, carbon, aramid and basalt fibers were used as reinforcement elements for the studies on the impact behavior of fiber reinforced composite materials.
- In addition to the mentioned fibers, natural fibers such as jute and kenaf were used as reinforcement elements.
- In most of the studies on the LVI behavior of hybrid FRP composites, the fibers were used in the form of binary combinations. And, in these studies, main parameters such as fabric stacking sequence, impact energy and impactor geometry were frequently examined.
- The effects of nanoparticle additives on LVI behavior of composite materials have been investigated in many studies. In these studies, nanoparticles such as CNT, nano-clay and nano silica have been investigated by adding to composite materials by different methods.
- It is understood that the effect of GnPs nanoparticle on the mechanical, electrical and thermal properties of composite materials has yet to be investigated.
- However, it has been found that studies on the effect of matrix modification with nanoparticles in addition to fiber hybridization, on the mechanical properties of composite materials are also very few.

The main objective of this thesis is to investigate the effect of graphene nanoplatelets inclusion on the low velocity impact behavior of hybrid composites. The specific goals of this study are:

- To produce hybrid FRP composite plates using binary fiber fabric combinations (glass/basalt, glass/carbon, glass/aramid) in addition to FRP composites of a single kind of fiber fabric reinforced.
- To use different fabric stacking sequence to observe the effect of hybridization in hybrid fiber fabric reinforced composite plates produced.
- Adding GnP in different amounts (0, 0.1, 0.25 and 0.5 wt%) to epoxy polymer resin used in composite plate production.
- To utilize tensile and flexural tests, for the determination of the mechanical properties of composite materials produced.
- To apply drop-weight impact tests, for the determination of the low-velocity impact behavior of composite materials produced.
- To investigate the effects of fiber hybridization and matrix modification on the tensile, bending and low-velocity impact behaviors of composite materials by using experimental results.
- To examine the composite samples using SEM images and fractographs.

CHAPTER 3

COMPOSITE PLATE PRODUCTION AND MECHANICAL TESTS

3.1 Introduction

In this chapter, detailed information about the production methods of the composite plates used in the experiments, the properties of the materials used in the production and the tests performed for the characterization of the mechanical properties of the plates are given.

3.2 Composite Plate Production

3.2.1 Materials

In this study, plain woven basalt fabric (supplied from Tila Kompozit, Istanbul, Turkey), plain woven S-glass fabric, plain woven carbon fabric and twill woven aramid fabric (supplied from Dost Kimya, Istanbul, Turkey) were used as reinforcement phase in the composite plates as shown in Figure 3.1. The areal density of fabrics is 200, 202, 200 and 173 g/m^2 respectively as presented in Table 3.1.

Figure 3.1 Fibers used in composite plate production.

Table 3.1 Mechanical and physical properties of reinforcements [55, 89].

Material	Specifications	Dimensions
Glass Fabric	Areal density (g/m^2)	202
	Fibre thickness (mm)	0.15
	Tensile strength (MPa)	3000-5000
	Elastic modulus (GPa)	72-82
Aramid Fabric	Areal density (g/m2)	173 g/m2
	Fibre thickness	0.17 mm
	Tensile strength (MPa)	2750-3000
	Elastic modulus (GPa)	82-124
Basalt Fabric	Areal density (g/m^2)	200 g/m^2
	Fibre thickness	0.28 mm
	Tensile strength (MPa)	2000-2300
	Elastic modulus (GPa)	90-92
Carbon Fabric	Areal density (g/m^2)	200 g/m^2
	Fibre thickness	0.17 mm
	Tensile strength (MPa)	2500-3000
	Elastic modulus (GPa)	200-700
Graphene Nano Platelets	Density	50 kg/m^3
	Fibre thickness	5-8 nm
	Surface area	120-150 m^2/g
	Diameter	5 µm

GnPs were supplied from Grafen Chemical Industries Co., Ankara, Turkey, and they were used as main toughening nano particle in the epoxy resin. GnPs consist of a few layers of graphene stacked together with exhibiting a particle diameter of 5 µm. Graphene layer thickness was varied from 5 to 8 nm, and surface area ranges from 120 to 150 m2/g as given in Table 3.1.

Resin systems consist of Epikote Resin MGS L285 (with curing agent Epikure MGS H285) and MGS L160 (with curing agent Epikure MGS H260S) which display good filler acceptance due to their low surface tension. They were supplied from Dost Kimya Company, Istanbul, Turkey. Table 3.2 illustrates the physical properties of resin system components.

Table 3.2 Physical properties of resins systems.

Component	Density (g/cm3)	Viscosity (mPa.s)	Mixing Ratio (Epoxy: Hardener)
MGS L285	1.18-1.23	600-900	100:40 [a]
MGS L160	1.13-1.17	700-900	100:35 [b]
MGS H285[a]	0.94-0.97	50-100	-
MGS H260s[b]	0.93-0.97	80-100	-

Two different methods were utilized in the production of composite plates used throughout the study. In the early stages of thesis, vacuum assisted hand lay-up method was used to produce composite laminates in which glass and basalt fabrics were combined. In later production, hand lay-up method with hot press was used.

3.2.2 Vacuum Assisted Hand Lay-up Method

Vacuum-assisted hand lay-up method was used for manufacturing of glass, basalt, glass/basalt and basalt/glass test samples, and schematic illustration for production process is shown in Figure 3.2. Totally 16 composite laminates of glass and basalt fiber reinforced epoxy with 4 different stacking sequences and GnPs filler content were produced by using this method. Production steps of the vacuum assisted hand lay-up method can be summarized as follows:

- Fiber fabrics were cut in desired sizes with (0/90) fiber orientation.
- For the resin system, the epoxy (MGS L160) was mixed with different proportions (0, 0.1, 0.25, 0.5 wt%) of the GnPs particles at 8000 rpm for 5 minutes. The mixture was then mixed with the hardener (MGS H260s) and stirred at 8000 rpm for 5 minutes.
- Then, fiber fabrics were placed on the thin release film with applying resin mixture enriched by GnPs particles in order to wetting fabrics uniformly. This procedure was continued for each group of the composite samples.
- A peel ply and resin infusion mesh were placed over the wetted fibers, and finally vacuum bag was sealed onto mesh.
- A vacuum check was made to detect any leaks in the vacuum bagging.
- After the wetting of the fibers for impregnation, they were subjected to curing process under the vacuum pressure of 700 mmHg at temperature of 45 °C for 1 h, and then remained 5 h to reach room temperature.

- Then, composite laminate was removed from vacuum bagging.
- Finally, a post-curing operation was conducted on the samples for 2 h under 45 °C temperature.

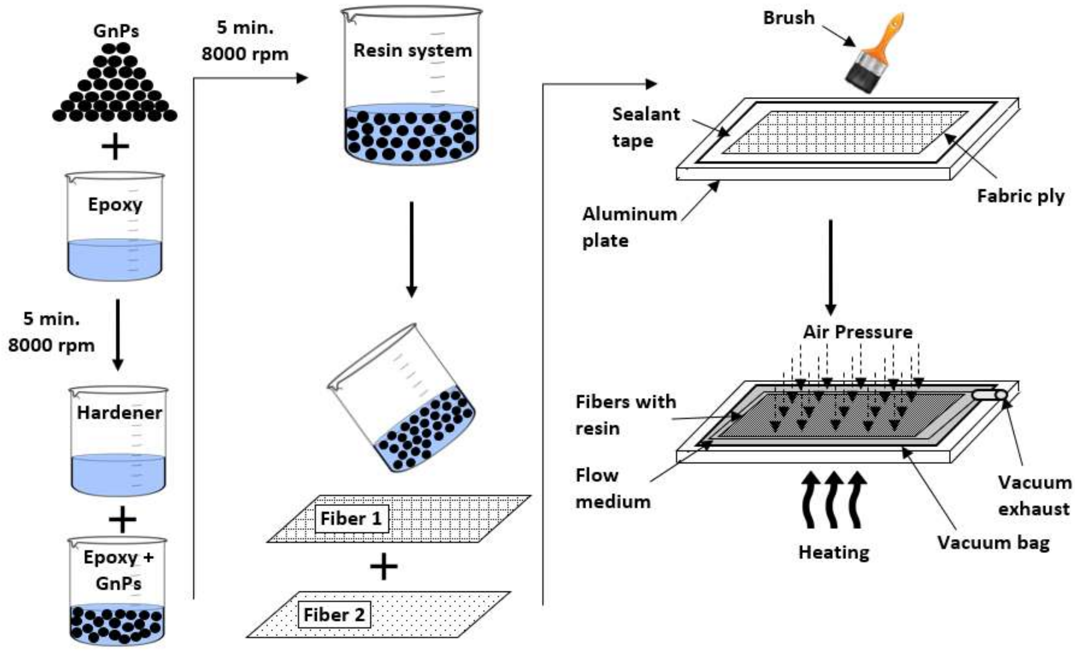

Figure 3.2 Schematic illustration of vacuum assisted hand lay-up method.

In addition to reference composites, S-glass fabric reinforced epoxy composite "G" and basalt fabric reinforced epoxy composite "B", two symmetric hybrid arrangements were produced in first stacking sequence $(G_3/B_3)_S$ which is called as "GB" and second $(B_3/G_3)_S$ which is called as "BG".

3.2.3 Hand Lay-up Method

The second production method seen in Figure 3.3 was the hand lay-up method. 32 composite laminates of glass, aramid and carbon fiber reinforced epoxy with 4 different stacking sequences and GnPs filler content were produced by using this method. The method was utilized according to following steps:

- Fiber fabrics were cut in desired sizes with (0/90) fiber orientation.
- For the resin system, the epoxy (MGS L285) was mixed with different proportions (0, 0.1, 0.25, 0.5 wt%) of the GnPs particles at 8000 rpm for 5 minutes. The mixture was then mixed with the hardener (MGS H285) and stirred at 8000 rpm for 5 minutes.

- First, plies were laid on to a thin release agent one ply for each step on production desk, and the resin mixture was distributed uniformly over the layers by roller, the same procedure was repeated for all twelve layers.
- Then, the composite plate was placed between hot mold press for curing process then left under 0.3 MPa pressure and 75 °C temperature for 1 h.
- At the end of production, composite material left to cooling for 2 h under same pressure.

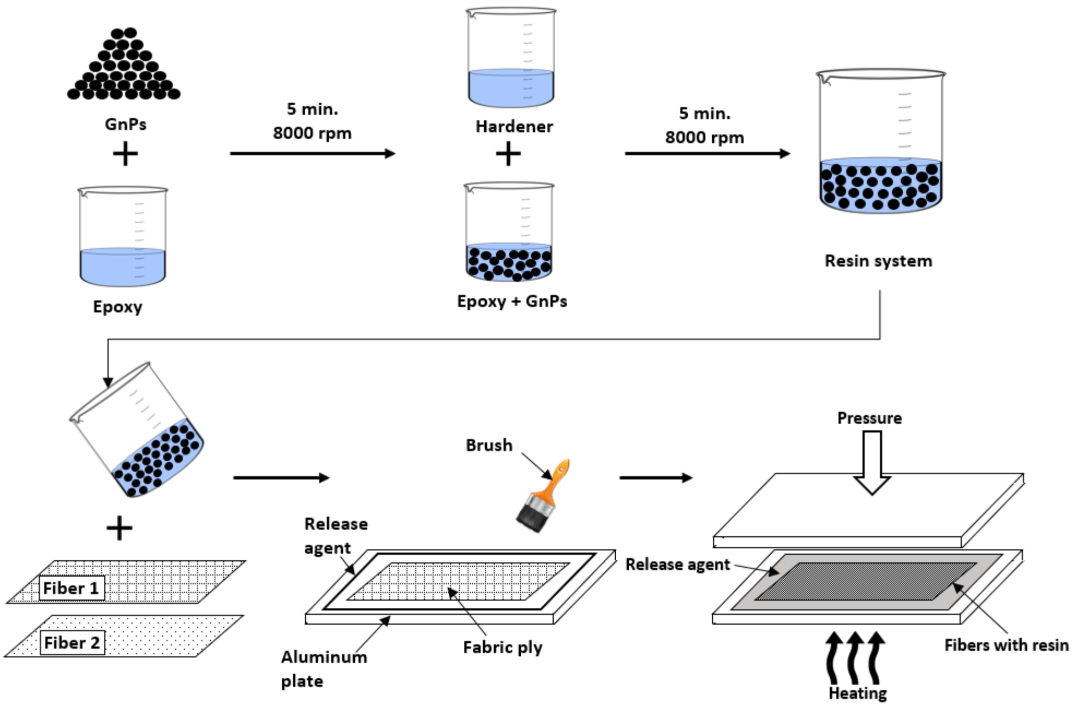

Figure 3.3 Schematic illustration of hand lay-up method.

In the study, a total of 48 plates were produced for each single fabric types and each binary fiber combination (glass / basalt, glass / carbon, glass / aramid) with different filler content (0, 0.1, 0.25, 0.5 wt%) as seen in Figure 3.4. The mass fractions of the hybrid composites which are determined by using following equation are presented in Table 3.3.

$$W_f = \frac{w_f}{w_c} \tag{3.1}$$

Where:

w_f= weight of fiber,

w_c= weight of composite.

Four symmetric hybrid configurations were produced; in first one "AG" sandwich-like sequence with six glass layers (core) and three aramid layers (skins) for each side of the composite laminate while second hybrid configuration "GA" six layers of aramid (core) and three glass layers (skins) in each side of laminate were stacked. In the same order, two hybrid configurations were also made using glass and carbon fabrics which were designated as "GC" and "CG". In addition to hybrid configurations, non-hybrid configurations were also manufactured as S-glass fabric reinforced epoxy composite "G", aramid fabric reinforced epoxy composite "A", and carbon fabric reinforced epoxy composite "C".

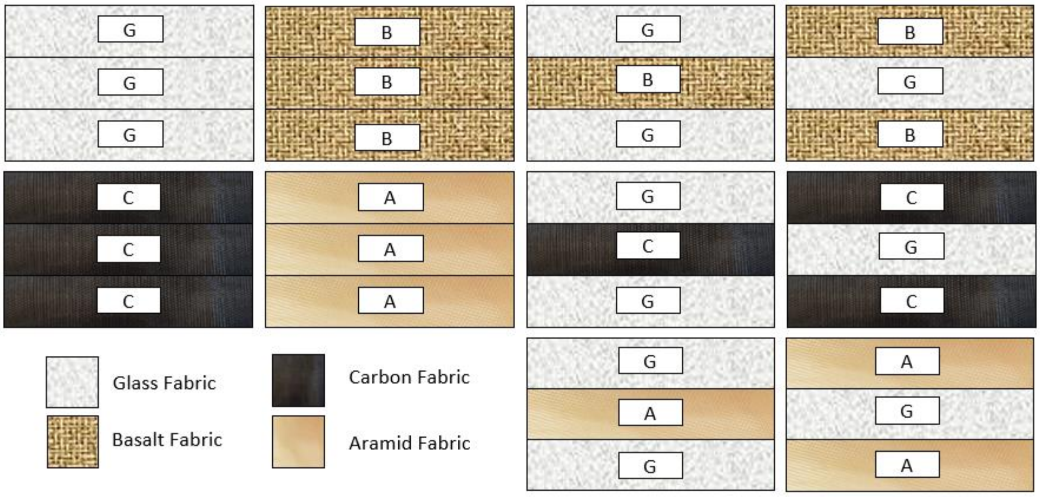

Figure 3.4 Fabric stacking sequences.

Table 3.3 Fiber mass fractions of hybrid composite specimens.

	Fiber mass fraction (%)			
Specimen	$w_{f,G}$	$w_{f,A}$	$w_{f,B}$	$w_{f,C}$
G	64.92	0.00	0.00	0.00
A	0.00	44.84	0.00	0.00
B	0.00	0.00	67.76	0.00
C	0.00	0.00	0.00	58.28
GA	33.47	33.14	0.00	0.00
AG	32.62	32.30	0.00	0.00
GB	33.94	0.00	33.60	0.00
BG	32.94	0.00	32.62	0.00
GC	31.98	0.00	0.00	31.98
CG	31.12	0.00	0.00	31.12

3.3 Mechanical Analysis

3.3.1 Specimen Preparation

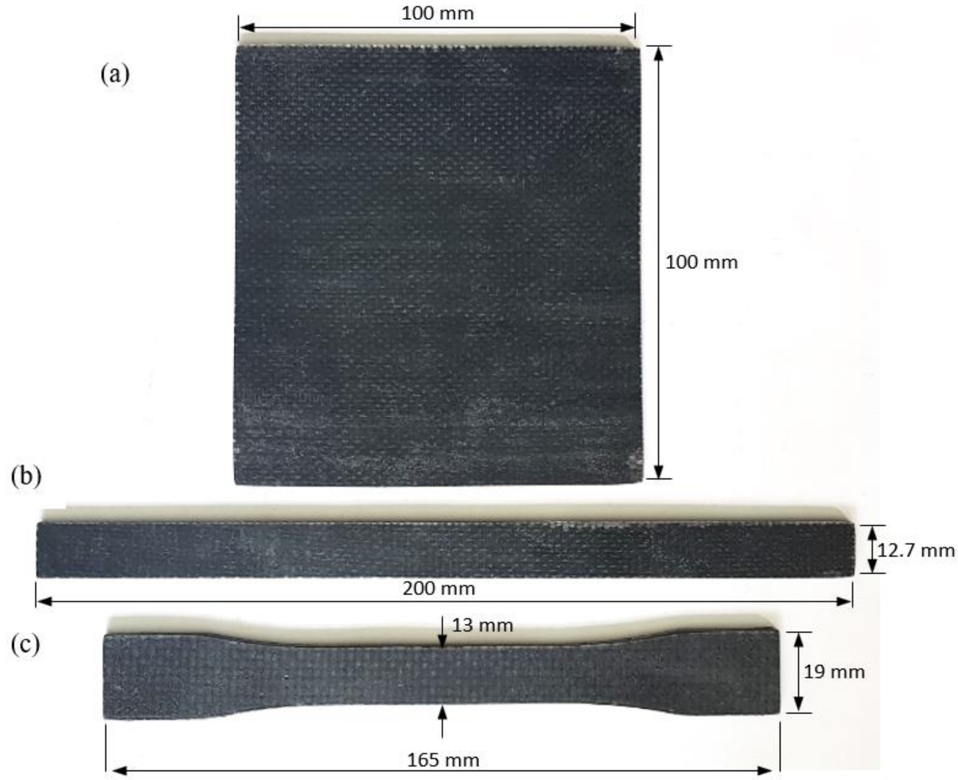

Figure 3.5 Produced composite test samples: (a)low velocity impact, (b) flexural, (c) tensile test samples.

The plates were cut in accordance with the tests required for the mechanical characterization of the produced composite plates as shown in Figure 3.5. AUTOCAD drawing software was used to draw the test specimen forms. Later, the drawings were made suitable for CNC cutting with ARTCAM software. The cutting process was carried out by means of CNC milling machine. All composite plates produced were cut according to ASTM D6264 [91], D790 [92] and D638 [93], respectively, for the drop impact, flexural and tensile tests.

3.3.2 Tensile Test and Test set-up

The uniaxial tension test as shown in Figure 3.6, was conducted using Shimadzu testing machine AG-X series (Kyoto, Japan) at room temperature to estimate the effect of nano filler on the tensile properties of the prepared composite samples according to ASTM D638 standard [93]. Also, with the help of axial extensometer (Epsilon Tech. 3542), axial displacement values were measured. The test was carried out at 2 mm/min crosshead speed.

Figure 3.6 Tensile test set-up and test specimens.

3.3.3 Flexural Test and Test set-up

To investigate the effect of the GnPs filler on the flexural behavior of the hybrid / non-hybrid composite plates, a three-point bending test was performed using the Shimadzu test machine AG-X series (Kyoto, Japan) at room temperature according to the ASTM D790 standard. The experiments were carried out at the crosshead speed, which was calculated by the equation given below and was directly related to the sample thicknesses [92]:

$$R = ZL^2/6d \tag{3.2}$$

where:

R= rate of crosshead motion (mm/min),

L= support span (mm),

d= depth of the beam (mm),

Z= rate of straining of the outer fiber (mm/mm/min).

The flexural stress (σ_f), strain (ε_f) and modulus (E_f) were calculated from test data using following equations [92]:

$$\sigma_f = \frac{3PL}{2bd^2}\left[1 + 6\left(\frac{D}{L}\right)^2 - 4\left(\frac{D}{L}\right)\left(\frac{d}{L}\right)\right] \tag{3.3}$$

$$\varepsilon_f = \frac{6Dd}{L^2} \tag{3.4}$$

$$E_f = \frac{L^3}{4bd^3}\frac{\Delta P}{\Delta x} \tag{3.5}$$

where:

P= the load at a given point on the load-deflection curve (N),

b and *d* = width and depth of the beam (mm),

D= the maximum deflection before failure (mm),

ΔP/Δx= the slope of the linear region of the load–deflection curve (N/mm).

Figure 3.7 Three-point bending test set-up and test specimens.

3.3.4 Drop Weight Impact Test and Test set-up

Drop weight impact tests were conducted to determine the effect of GnPs dispersion on the low-velocity impact behavior of fiber reinforced composite laminates according to ASTM D7136/7136M [90] standard at room temperature. Test specimens were cut in size of 100 x 100 mm, having quasi-isotropic structure according to ASTM D6264/6264M [91] standard.

During impact event, the force response of the structure was recorded by mounting a piezoelectric force sensor (ICP M202B ® quartz force ring) having maximum force capacity of 44.48 kN under the impactor. A hemispherical tipped cylindrical shape of steel impactor with 12.7 mm diameter was used during the impact tests. The samples were clamped in the frame with 76.2 mm diameter of circular opening, which exposed to impact. The impact tests were carried out same conditions with impact energy of 30J, which resulting from impact velocity of 3.4 m/s with a total impactor weight of 5 kg. The actual velocity of total impactor was evaluated by optical sensors located just above 25 mm from the sample surface.

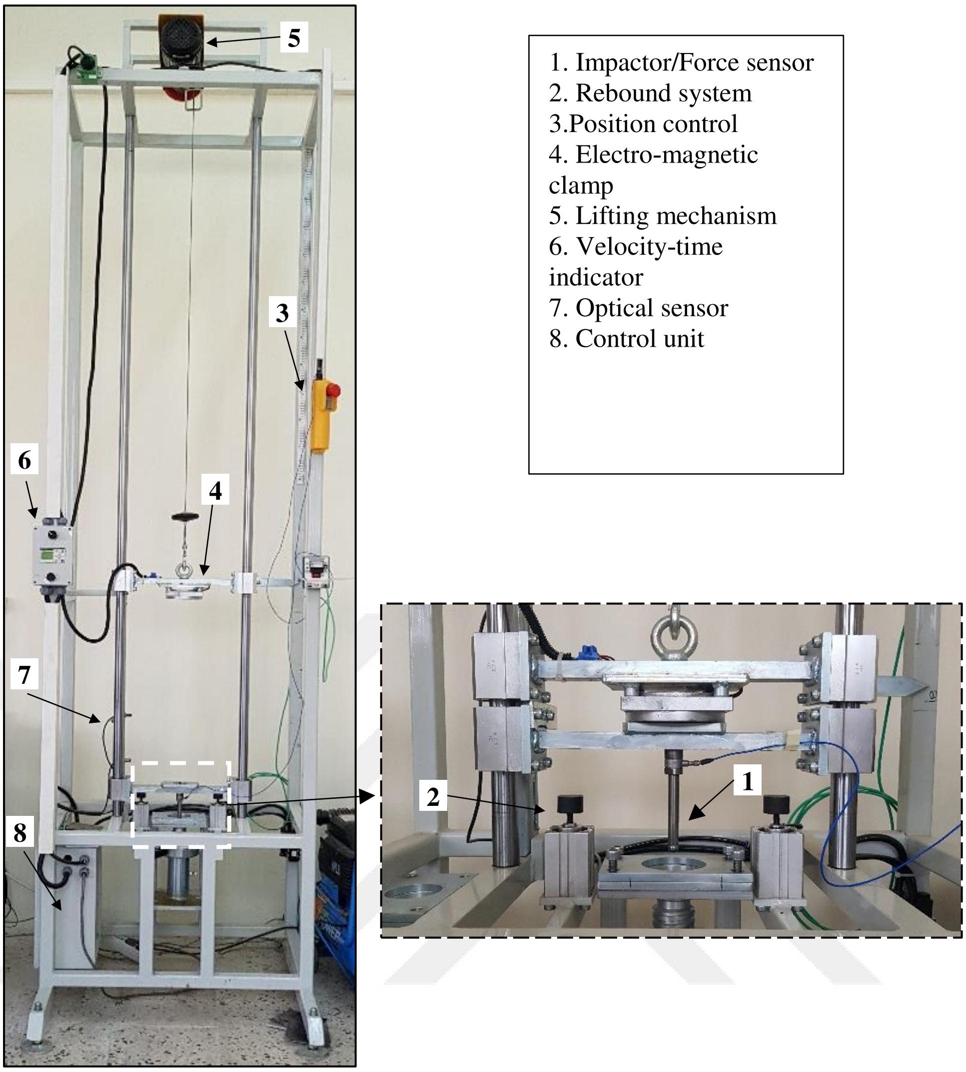

Figure 3.8 Drop weight impact test set-up.

The velocity, deformation, and absorbed energy values were obtained from the area under the force-displacement curves. The velocity–time versus force–time values during the impact change according to Eq. 3.6:

$$v(t) = v_i + gt - \int_0^t \frac{F(t)}{m} dt \tag{3.6}$$

where *t* is the time, *v* is the velocity of impactor, *g* is the acceleration due to gravitation, and *m* is the total mass of the impactor unit. If the impact device monitoring generates the impact force, the Eq. 3.7 has incorporated to represent the deformation of impactor from the initiation of impact event.

$$\delta(t) = v_i(t) + \frac{1}{2}gt^2 - \int_0^t \left(\int_0^t \frac{F(t)}{m} dt \right) dt \tag{3.7}$$

Using Eq. 3.6 and 3.7, the absorbed energy has been calculated as given in Eq.3.8:

$$E_a(t) = \frac{m(v_i^2 - v(t)^2)}{2} + mg\delta(t) \tag{3.8}$$

CHAPTER 4

RESULTS AND DISCUSSION ON MECHANICAL TESTS

4.1 Introduction

In this section, the results of the mechanical tests which are conducted to the determination of the basic mechanical properties of the produced composite plates are presented. The results of mechanical tests including tensile and flexural tests are given in terms of fiber hybridization and matrix modification.

4.2 Tensile Test Results and Damage Characterization

In order to determine the tensile strength and modulus of the produced composite samples, uniaxial tensile test was performed at least five test specimens. The effect of fiber hybridization and matrix modification on tensile behavior of composite plates was investigated in terms of tensile stress and tensile modulus under separate headings. In addition, the test results were interpreted by performing damage characterization of the test samples.

4.2.1 Effect of Fiber Hybridization and Stacking Sequence on the Tensile Behavior of Composite Laminates

Figure 4.1 shows the stress-strain histories of the hybrid/non-hybrid fiber reinforced composite samples. In the figure, the stress-strain diagrams of the aramid, basalt, carbon and glass reinforced composite plates are given together with the stress-strain diagrams of the hybrid fiber-reinforced composite plates of glass/aramid, glass/basalt, and glass/carbon. In addition, the tensile behavior of the composite laminates is given in Table 4.1 with respect to fiber type.

It was seen that the highest tensile strength value was recorded as 715.80 MPa in CFRP and the lowest tensile strength value was recorded as 312.35 MPa in BFRP. Also, the highest tensile modulus value was recorded as 43.32 GPa for CFRP and the lowest tensile modulus value was recorded as 13.39 GPa for BFRP.

(a)
(b)
(c)

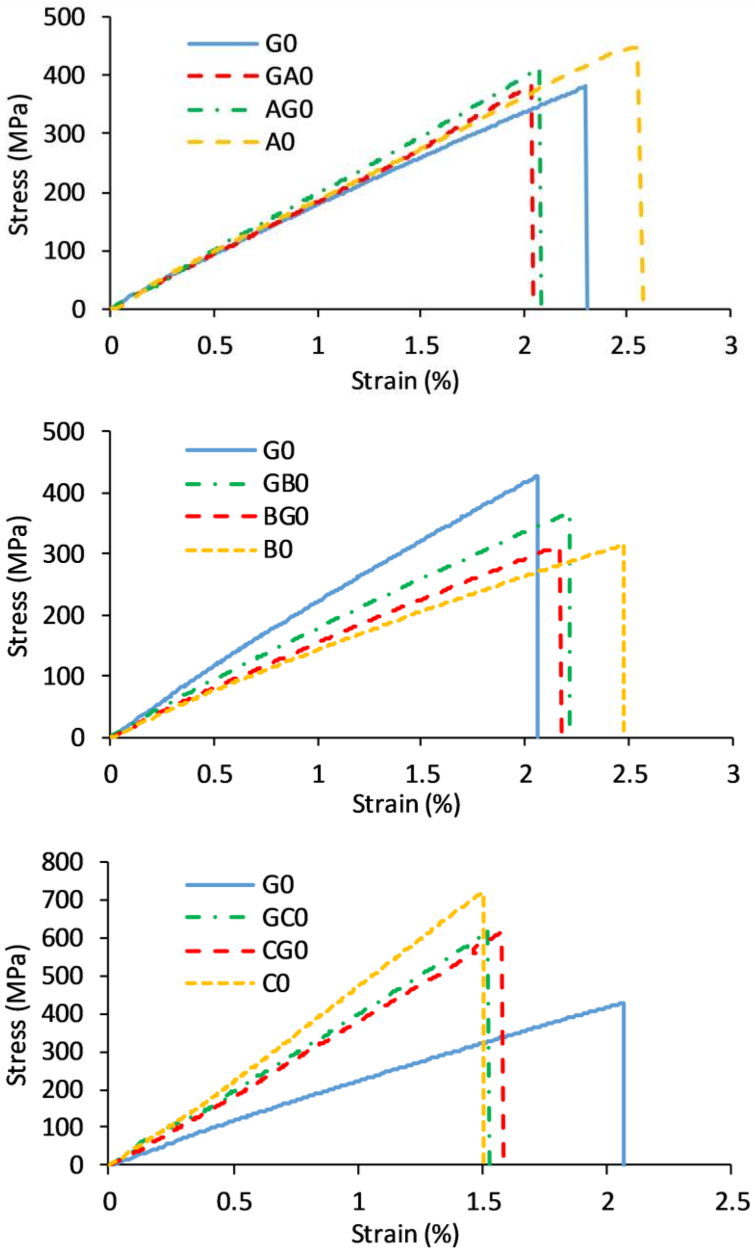

Figure 4.1 Stress-strain diagrams of fiber hybridized composite samples without GnPs addition under axial tensile load.

4.2.1.1 Glass / Aramid Fiber Reinforced Composite

Tensile strength and modulus values of unmodified aramid fiber reinforced composite samples (A0) were recorded as 449.78 MPa and 18.97 GPa as given in Table 4.1. Aramid fiber hybridization was resulted as improvement in tensile behavior of GFRP composite plates which is similar to study in reference [94] as seen in Figure 4.1 (a) and Table 4.1. When glass fiber was placed on the skin, and aramid fiber was in placed in core, hybrid composite material with unmodified epoxy showed the better tensile strength compared to the other hybrid configurations.

Improvement in tensile strength value of G0 sample was 9.97% for AG0 sample and 3.02% for GA0 composite sample. This may be due to the fact that the bonding between the aramid fabrics is stronger than the others, and that this strong bond in the interface gives higher tensile strength to the hybrid composite sample.

Table 4.1 Tensile properties of unmodified composite samples with different stacking sequences.

Sample code	**Tensile strength (MPa)**	**Tensile modulus (GPa)**	**Tensile strain (mm/mm)**
G0	370.10	16.02	0.0235
A0	449.78	18.97	0.0232
B0	312.35	13.39	0.0260
C0	715.80	43.32	0.0131
GA0	381.27	17.40	0.0210
AG0	407.03	19.12	0.0226
GB0	367.50	16.40	0.0241
BG0	313.02	13.59	0.0246
GC0	620.70	36.73	0.0161
CG0	613.20	37.65	0.0167

4.2.1.2 Glass / Basalt Fiber Reinforced Composite

The tensile test results of the glass / basalt hybrid composites used in the second hybrid configuration are given in Table 4.1 and Figure 4.1 (b). Tensile strength and modulus values of basalt fiber reinforced composite samples (B0) were recorded as 312.35 MPa and 13.39 GPa. When glass fiber was placed on the skin, and basalt fiber was in the core, hybrid composite material with unmodified epoxy showed the better tensile strength compared to the other hybrid configurations. Tensile strength and modulus values were 367.5 MPa and 16.4 GPa for GB0 sample, 313.02 MPa and 13.59 GPa for BG0 sample. Improvement in tensile strength was 17.65% for GB0 and 0.2% for BG0 compared to B0 sample. Thus, when glass / basalt fabrics were used, there was significant difference between the tensile strength values in different stacking sequences.

4.2.1.3 Glass / Carbon Fiber Reinforced Composite

Figure 4.1 (c) demonstrates the tensile test results of the third hybrid type glass / carbon fiber reinforced hybrid composites. Tensile strength and modulus values were recorded as 715.80 MPa and 43.32 GPa in unmodified carbon fiber reinforced composite sample (C0). Also, tensile strength and modulus values were 620.70 MPa and 36.73 GPa for GC0 sample, 613.20 MPa and 37.65 GPa for CG0 sample, respectively. It can be understood that the carbon fiber hybridization was improved tensile behavior of glass fiber reinforced composite samples. Improvement in tensile strength and modulus values were 67.7% and 129.27% for GC0 sample, 65.68% and 135% for CG0 sample. It can be concluded that tensile strength was greater in composite sample which glass fiber was placed on skin and carbon fiber was placed in core. Same behavior was obtained by Agarwal et al [35]. It was also observed that the elongation of the hybrid composites was reduced despite the increase in strength and modulus due to the lower strain value of the carbon fiber.

4.2.2 Effect of Graphene Nano Platelets Inclusion on the Tensile Behavior of Composite Laminates

Although the tensile properties of the fiber-reinforced composite materials have been known to be dominated by continuous fiber when measured in the longitudinal direction, the GnPs contribution to the tensile strength of the composite samples has been investigated. The variation of tensile properties with varying content of GnPs are presented in Tables 4.2- 4.4., and stress-strain curves are displayed in Figures 4.3, 4.7, and 4.11. First, it is observed that the small amount of GnPs additive significantly affects the tensile strength of the produced composite materials. Both GnPs modified and unmodified samples have shown brittle behavior according to stress-strain curve and have increasing trend until 0.1 wt% in terms of strength and modulus.

Generally, the ability of a fiber/matrix interface to transmit elastic deformation is largely dependent on interface stiffness and bonding strength. It can be concluded from Table 4.2 that the 0.1 wt% content of GnPs slightly increases the tensile strength and modulus by 6.1% and 11.29% for glass fiber (G) reinforced composite samples. In addition, maximum elongation value was reached at this content. However, excessive GnPs loading created a reverse effect on the stress and modulus with a decreasing trend. Previous studies [95- 97] reported a better tendency of composite material up to a certain amount of graphene content, such as tensile strength, bending strength, and fracture toughness, whereas a higher tendency to decrease mechanical properties in higher graphene content was reported. This is due to the fact that the particles formed serious aggregation when high amounts of graphene are used.

Figure 4.2 demonstrates the fractured specimens of glass fiber (G) reinforced composite samples with increasing GnPs content and it is observed that the failure modes are mainly in type of fiber rupture, matrix crack and delamination. The increasing content of GnPs resulted high fiber debonding especially in weft direction. It may be interpreted as a result of poor interfacial bonding between fibers and fiber/matrix material due to poor functionalization of GnPs particles in the polymer matrix.

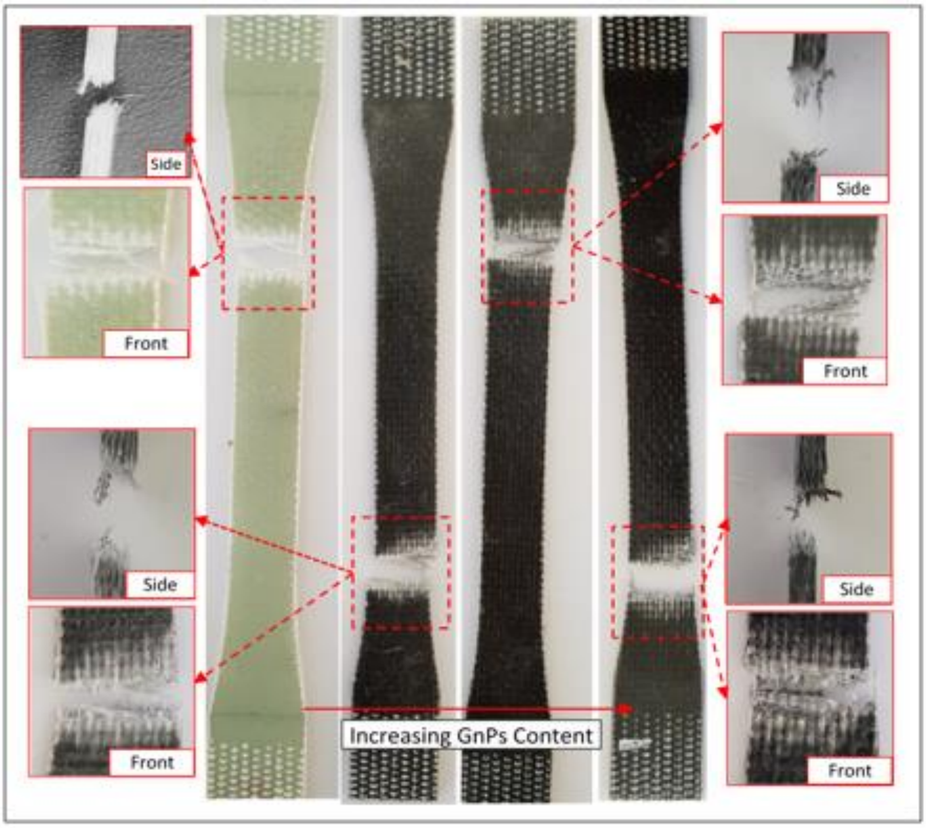

Figure 4.2 Tensile damage figures for GFR samples with various GnPs content.

4.2.2.1 Glass / Aramid Fiber Reinforced Composite

When the tensile test results of Aramid fiber (A) reinforced composites given in Table 4.2 and Figure 4.3 (d) are examined, 0.1 wt% content of GnPs was found to resulted slightly increase in the tensile strength from 449.78 MPa to 456.48 MPa by 6.5 %. Also, maximum elongation value was recorded at this filler content. After this content fluctuating results were observed showing the inhomogeneous distribution of nanoparticles.

In addition to these results, when glass/aramid hybrid composites were examined, it is seen that 0.1 wt% GnPs content causes an increase in tensile strengths and modules of composite materials. As seen in Table 4.2, tensile strength values of hybrid glass/aramid fiber reinforced composite samples were recorded as 381.27 MPa and, 407.03 MPa in unmodified samples; 406.3 MPa and 428.8 MPa in 0.1wt% filled specimens GA and AG hybrid composites respectively. Improvement in tensile strength values were measured as 6.5% and 5.3% in 0.1 wt% filled composite samples. Furthermore, it was observed that the tensile strength was higher than that of the opposite configuration when the aramid fiber is on skin and glass fiber is in core. At higher GnPs contents (0.25 and 0.5 wt%), a decreasing trend was recorded for tensile strength values compared to specimens with 0.1 wt% GnPs. These conclusions were attributed to agglomeration in graphene particles at high particle contents hence inhomogeneous particle dispersion and stress concentration in matrix material which can lead to crack initiation/propagation and consequently lower strength values in composite material [98, 99].

Figures from 4.4 to 4.6 depict the fractured photographs of A, GA, and AG composite samples with increasing GnPs content in the matrix. It was observed that the failure modes were mainly in type of fiber rupture, matrix crack and delamination. The increasing content of GnPs resulted high fiber debonding especially in weft direction. The reason of this result can be the poor interfacial bonding between fibers and fiber/matrix material due to inhomogeneous distribution of nano particles in the polymer matrix.

Table 4.2. Tensile properties of hybrid/non-hybrid glass/aramid fiber reinforced composite samples with various GnPs content.

Sample code	Tensile strength (MPa)	Tensile modulus (GPa)	Tensile strain (mm/mm)	Sample code	Tensile strength (MPa)	Tensile modulus (GPa)	Tensile strain (mm/mm)
G0	370.10	16.20	0.0235	**A0**	449.78	18.97	0.0232
G01	392.55	18.03	0.0240	**A01**	456.48	18.74	0.0241
G025	372.08	19.24	0.0214	**A025**	412.17	18.56	0.0204
G05	372.10	18.90	0.0225	**A05**	445.35	19.55	0.0240
GA0	381.27	17.40	0.0210	**AG0**	407.03	19.12	0.0226
GA01	406.30	18.50	0.0221	**AG01**	428.80	18.37	0.0245
GA025	379.80	18.05	0.0220	**AG025**	379.66	15.92	0.0241
GA05	390.90	18.00	0.0228	**AG05**	375.79	18.36	0.0203

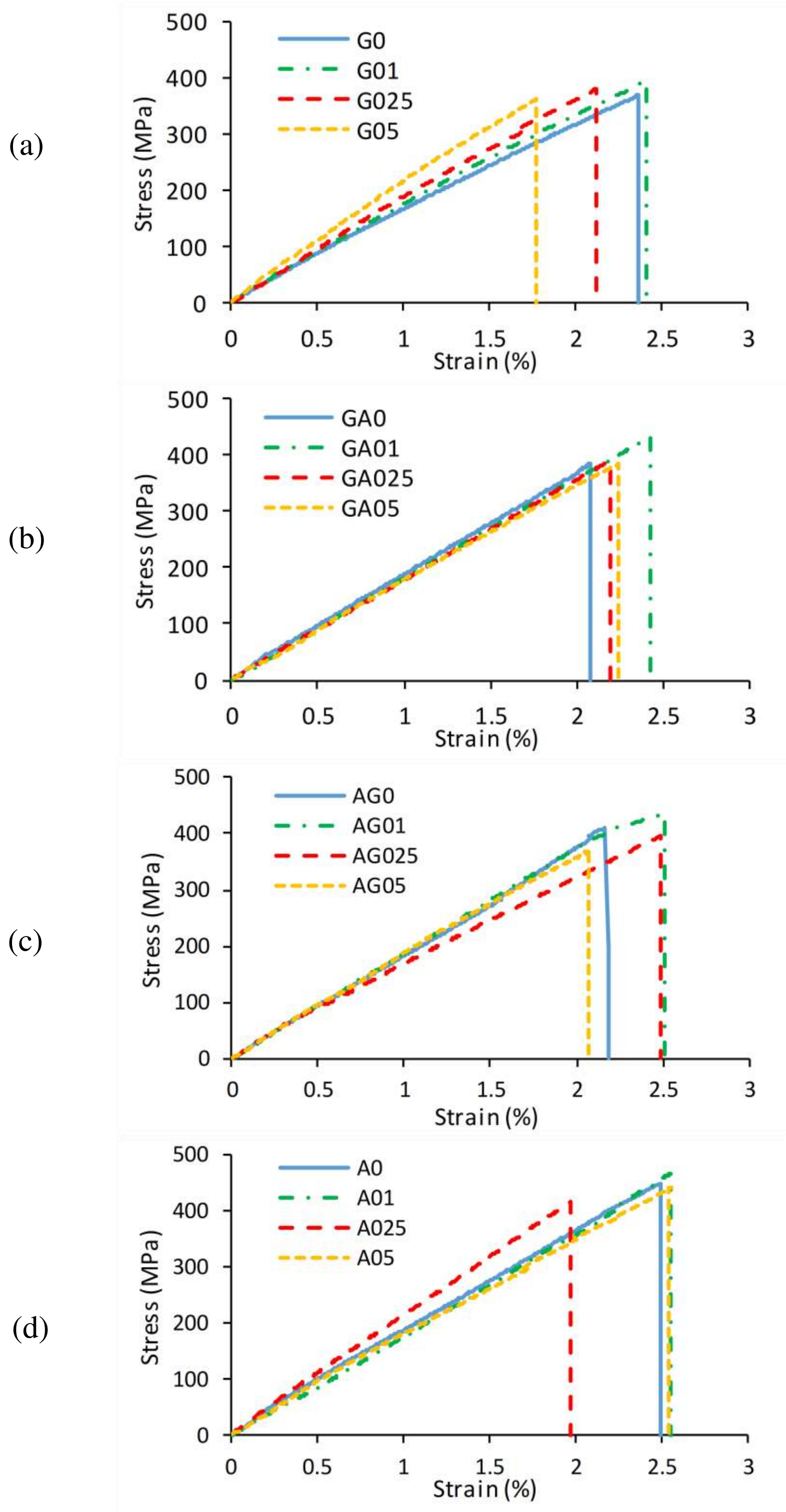

Figure 4.3 Stress-strain diagrams of hybrid/non-hybrid glass/aramid fiber reinforced composite samples with various GnPs addition under axial tensile load.

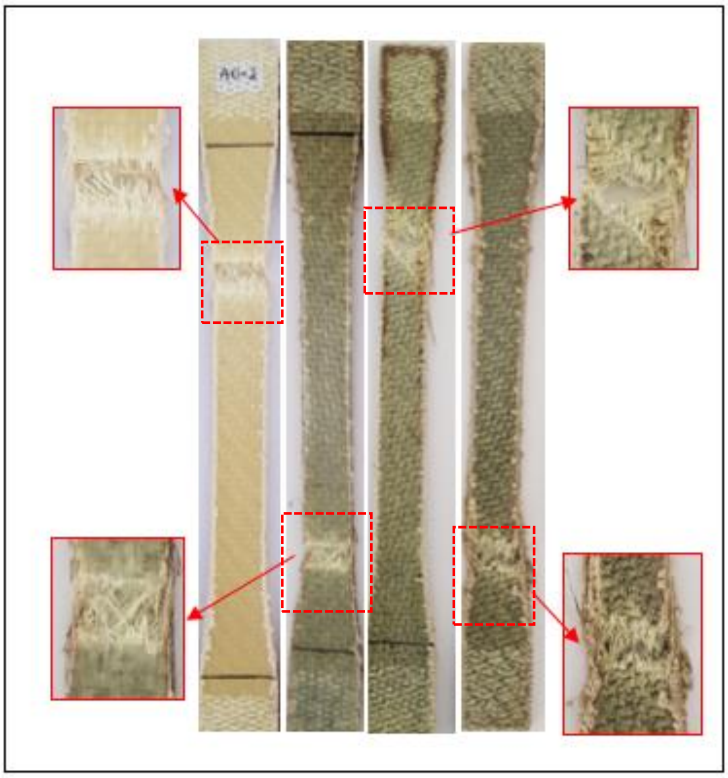

Figure 4.4 Tensile damage figures for AFR samples with various GnPs content.

Figure 4.5 Tensile damage figures for GAFR samples with various GnPs content.

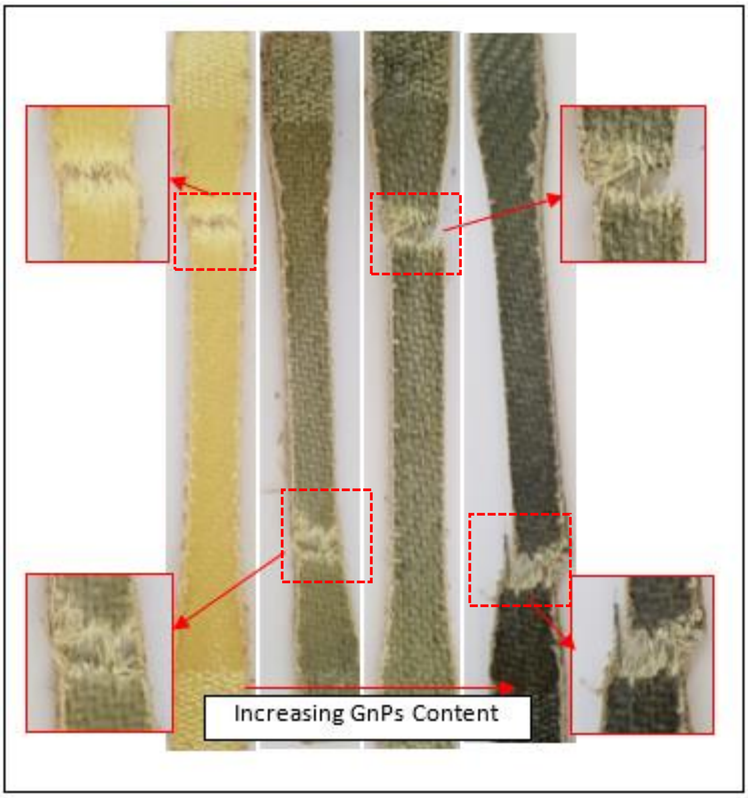

Figure 4.6 Tensile damage figures for AGFR samples with various GnPs content.

4.2.2.2 Glass / Basalt Fiber Reinforced Composite

As can be seen in Table 4.3, tensile strength of basalt fiber (B) reinforced composite samples were slightly increased from 315.9 MPa to 321.18 MPa by 1.67% with the content of 0.1 wt% GnPs. However, increased elongation values were obtained which were accompanied by decreasing tensile modulus values with the increasing content of GnPs nanoparticles to the materials which indicates the increasing ductility of the composite sample as seen in Figure 4.7 (a).

Table 4.3 Tensile properties of hybrid/non-hybrid glass/basalt fiber reinforced composite samples with various GnPs content.

Sample code	Tensile strength (MPa)	Tensile modulus (GPa)	Tensile strain (mm/mm)	Sample code	Tensile strength (MPa)	Tensile modulus (GPa)	Tensile strain (mm/mm)
G0	370.10	16.20	0.0235	**B0**	315.90	13.39	0.0260
G01	392.55	18.03	0.0240	**B01**	321.18	12.89	0.0267
G025	372.08	19.24	0.0214	**B025**	233.35	10.63	0.0244
G05	372.10	18.90	0.0225	**B05**	268.19	10.80	0.0280
GB0	367.50	16.40	0.0241	**BG0**	313.02	13.59	0.0243
GB01	404.34	16.50	0.0237	**BG01**	389.27	16.80	0.0255
GB025	281.72	14.10	0.0224	**BG025**	291.98	13.30	0.0221
GB05	285.35	13.80	0.0227	**BG05**	310.96	13.40	0.0240

In addition to these results, in Table 4.3, tensile strength values of hybrid glass/basalt fiber reinforced composite samples were recorded as 367.5 and, 298.55 MPa for unmodified samples; 404.34 and, 389.27 MPa for 0.1 wt% GnPs filled GB and BG composites, respectively. It can be understood from the test results, GNP filler content significantly influenced the tensile strength of the composite and compared with unmodified samples tensile strength values were increased by 10% in GB and 24.36% in BG with 0.1 wt% GnPs addition. An increasing the GnPs content after 0.1 wt% followed by a decreasing trend in strength values as seen in Figure 4.7. This suggested the following conclusion: Both combining effects of GnPs inclusion resulting in better load transfer between particle and matrix, and high tensile strength of a fiber as well as high mechanical performance of basalt fibers revealed the high mechanical performances which could be arranged with changing fiber position, GnPs content or fiber fractions.

The fractured photographs of B, GB, and BG composite samples with increasing GnPs content in the matrix was depicted in figures from 4.8 to 4.10. Fiber rupture, matrix cracking and delamination type failures were observed in fractured samples. In these samples, it was obvious that the increased content of GnPs particles especially after 0.1 wt% resulted in the enlargement of delaminated areas which indicates the poor interfacial bonding between fibers and matrix material due to agglomerations of nanoparticles in the polymer matrix.

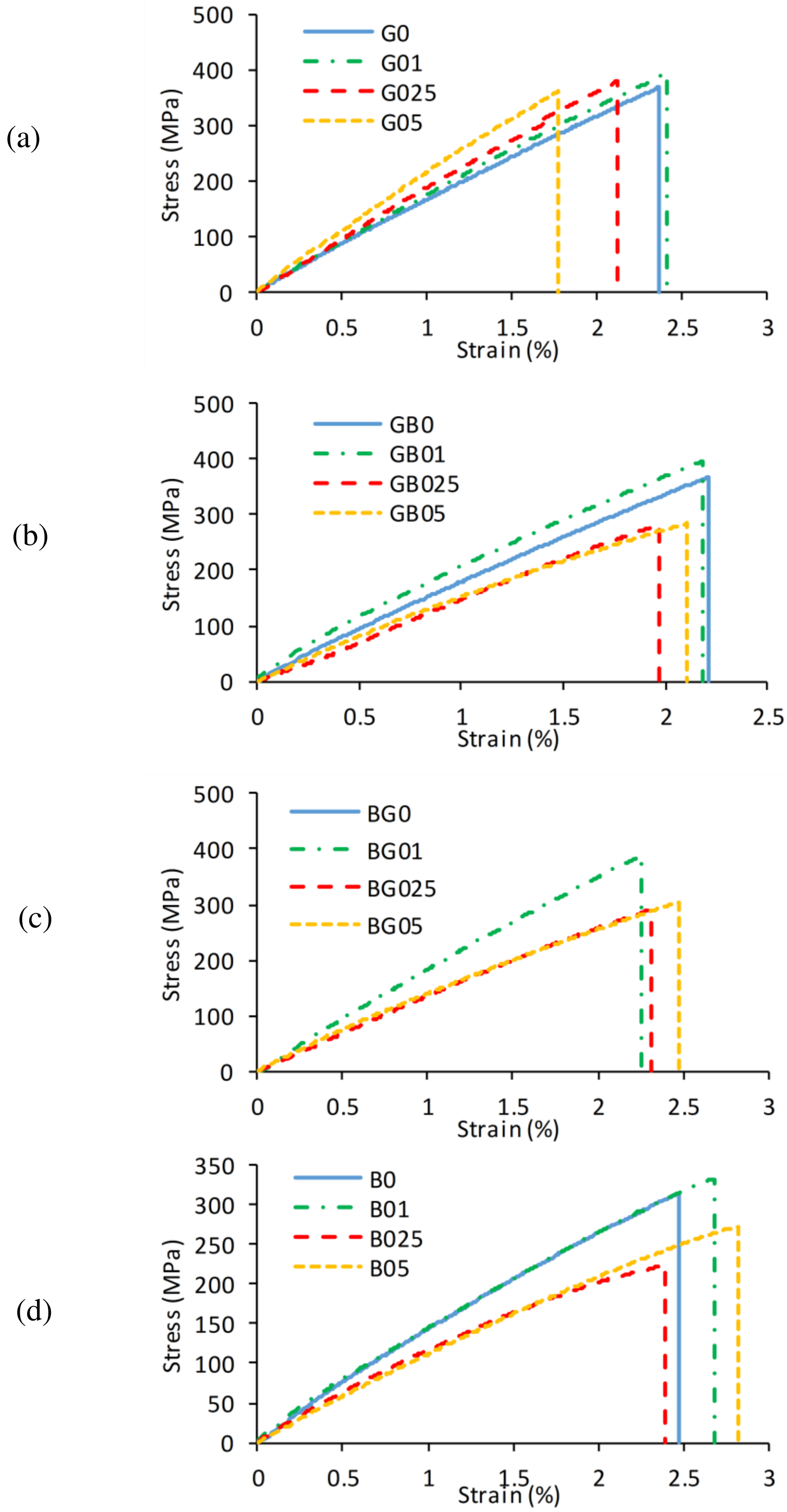

Figure 4.7 Stress-strain diagrams of hybrid/non-hybrid glass/basalt fiber reinforced composite samples with various GnPs addition under axial tensile load.

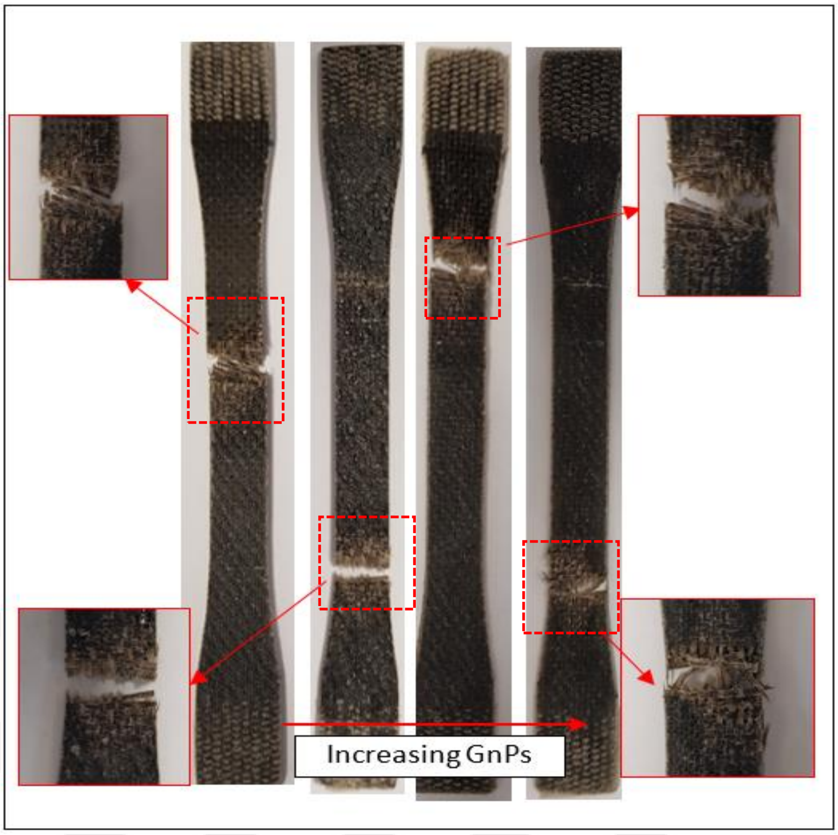

Figure 4.8 Tensile damage figures for BFR samples with various GnPs content.

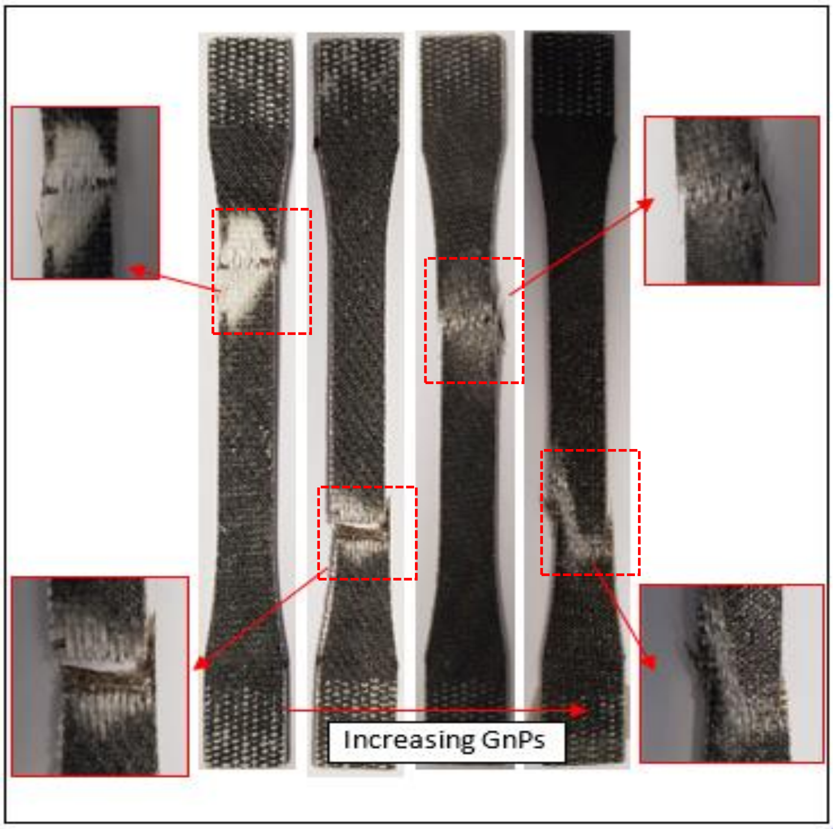

Figure 4.9 Tensile damage figures for GBFR samples with various GnPs content.

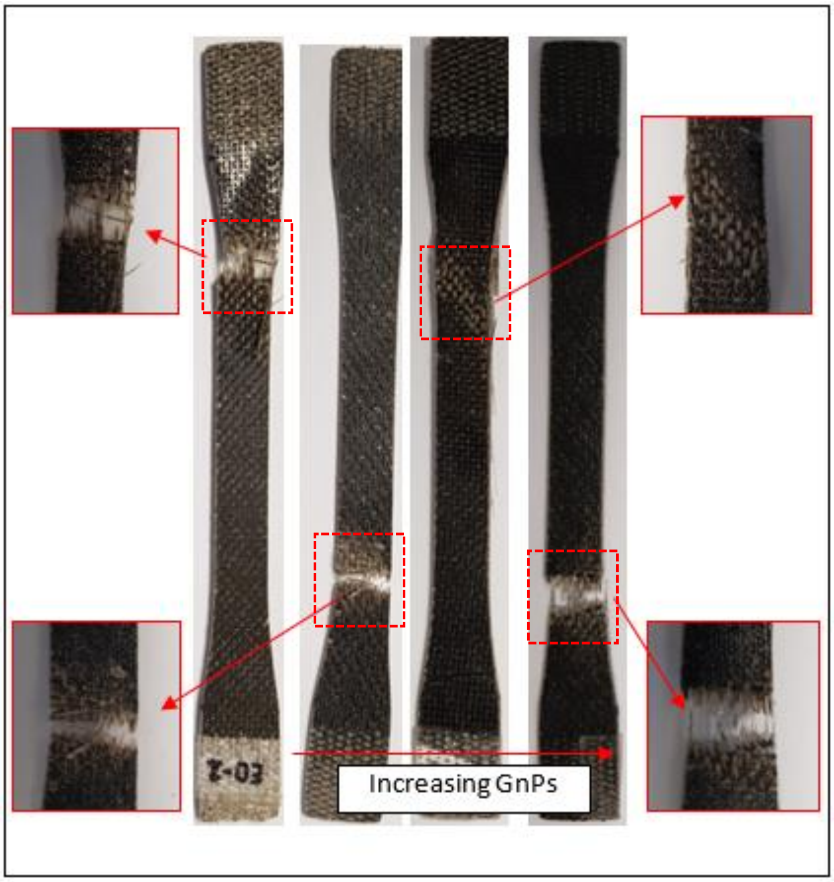

Figure 4.10 Tensile damage figures for BGFR samples with various GnPs content.

4.2.2.3 Glass / Carbon Fiber Reinforced Composite

Figure 4.11 shows a comparison of stress-strain histories of the GnPs particle modified and unmodified carbon/epoxy and glass/epoxy samples. Samples have shown the brittle nature both GnPs modified and unmodified samples. GnPs modified test samples indicate the higher nonlinear response when comparing other samples, and addition of GnPs particles reduces these nonlinearities for carbon/glass hybrid samples. The resulting maximum values of tensile stress, elastic modulus, and strain values were presented in Table 4.4.

Table 4.4 Tensile properties of hybrid/non-hybrid glass/carbon fiber reinforced composite samples with various GnPs content**.**

Sample code	Tensile strength (MPa)	Tensile modulus (GPa)	Tensile strain (mm/mm)	Sample code	Tensile strength (MPa)	Tensile modulus (GPa)	Tensile strain (mm/mm)
G0	370.10	16.20	0.0235	**C0**	715.80	43.32	0.0131
G01	392.55	18.03	0.0240	**C01**	748.40	43.65	0.0150
G025	372.08	19.24	0.0214	**C025**	780.10	45.10	0.0149
G05	372.10	18.90	0.0225	**C05**	788.20	45.79	0.0161
GC0	620.70	36.73	0.0161	**CG0**	613.20	37.65	0.0167
GC01	622.10	36.76	0.0165	**CG01**	635.50	32.93	0.0174
GC025	627.20	38.10	0.0163	**CG025**	625.20	33.99	0.0151
GC05	630.20	36.57	0.0176	**CG05**	625.90	39.90	0.0165

Carbon fiber (C) reinforced composites have clearly showed better tensile strength and modulus than glass fiber reinforced composites [100, 101]. The maximum result of tensile strength value was recorded with improvement of 10.2 % from the GnPs modified carbon fiber reinforced composites at GnPs content of 0.5 wt%. In addition, incorporation of GnPs at 0.5 wt% into the carbon/epoxy composites increased the tensile modulus by 4.6 % which indicates a good functionalization of the GnPs within the epoxy resin, and maximum elongation was increased by 22.9 % at this GnPs content. From these findings, brittleness and load bearing capacity of the GnPs modified unmodified carbon/epoxy samples increases as increasing GnPs content in the epoxy resin, with providing a better load transferring between particles and matrix. However, excessive GnPs loading created a reverse effect on the stress and modulus, and this was attributed to the poor load transferring from particles to the matrix as a result of agglomeration effects. As a general known fact, the mechanical properties of particle filled composite materials is directly affected by the homogenous distribution of particulate fillers into matrix material and improved load transfer between particle, fiber and matrix interface [102].

For the carbon/glass hybrid samples, it is evident that incorporation of GnPs particles did not contribute a significant effect on tensile strength with 3.5 % improvement at the GnPs content of 0.1 wt % when carbon fibers were placed at outer layers (CG). However, a little variation in terms of tensile strength and modulus of hybrid samples when glass fibers were seen placed at the outer layers (GC) while modifying epoxy resin by GnPs particles. The reason of this was explained the stacking sequence of the glass and carbon fibers in the lamina, and addition of GnPs particles as a secondary reinforcement contributed the reduction of stress, strain and modulus resulting in closer results.

The fractured photographs of C, GC, and CG composite samples under tensile loading and with increasing GnPs content in the matrix was presented in figures from 4.12 to 4.14. Fiber rupture, matrix cracking and delamination type failures were observed in fractured samples. In Figure 4.12, it can be clearly seen fiber pull out, rupture and delamination failures in fractured surfaces. And, obviously delaminated regions increased with the increased GnPs content. These findings were also seen in Figure 4.13. In these visual investigations, the negative effects of nanoparticle homogeneity on interlaminar load transfer were noteworthy. In addition, it was seen that the skin and core materials of the fiber hybridized GC and CG samples were clearly delaminated and the fiber ruptures in the material were independent from each other. This can be interpreted as the obvious difference between the tensile strain capabilities of carbon and glass fibers, as can be seen in the Table 4.4.

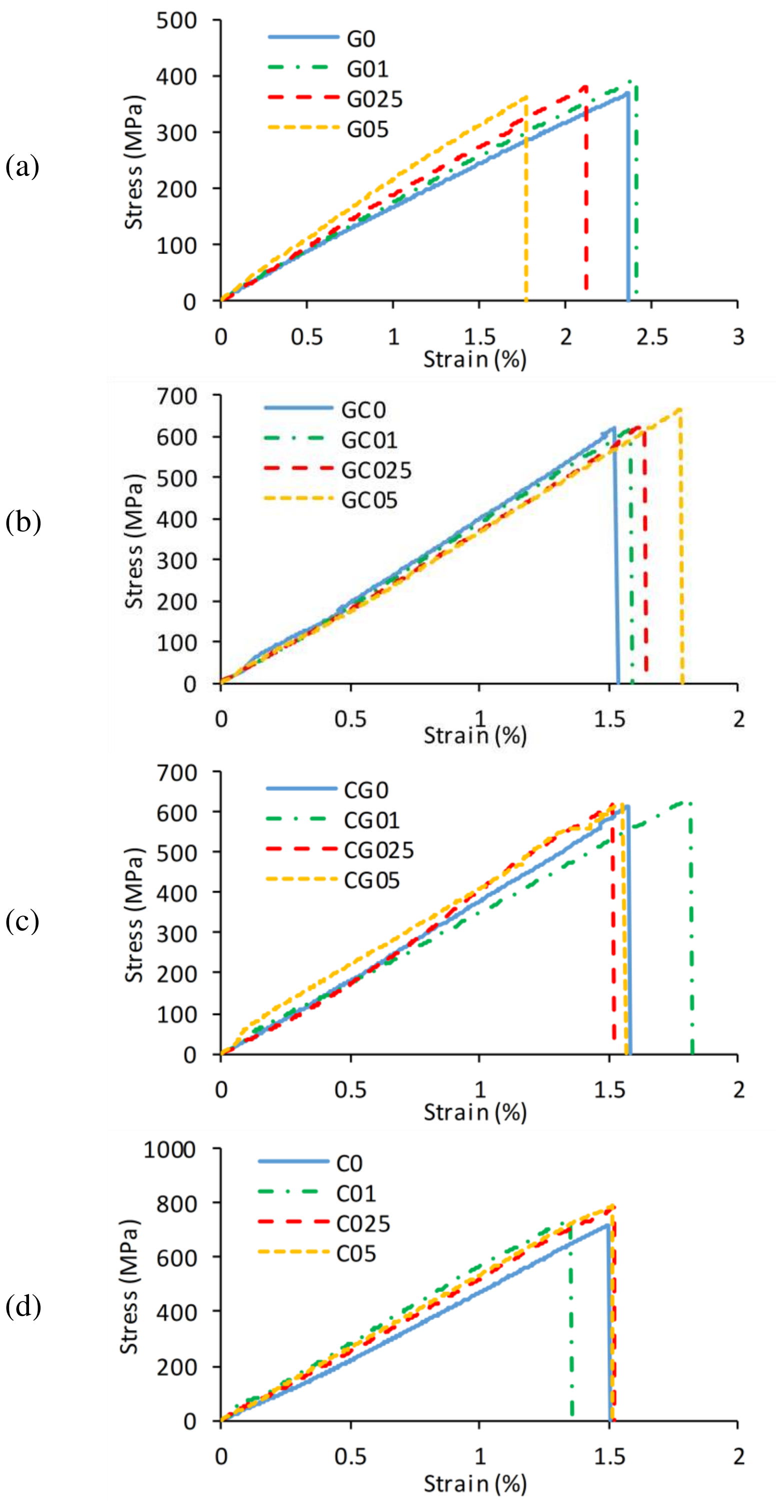

Figure 4.11 Stress-strain diagrams of hybrid/non-hybrid glass/carbon fiber reinforced composite samples with various GnPs addition under axial tensile load.

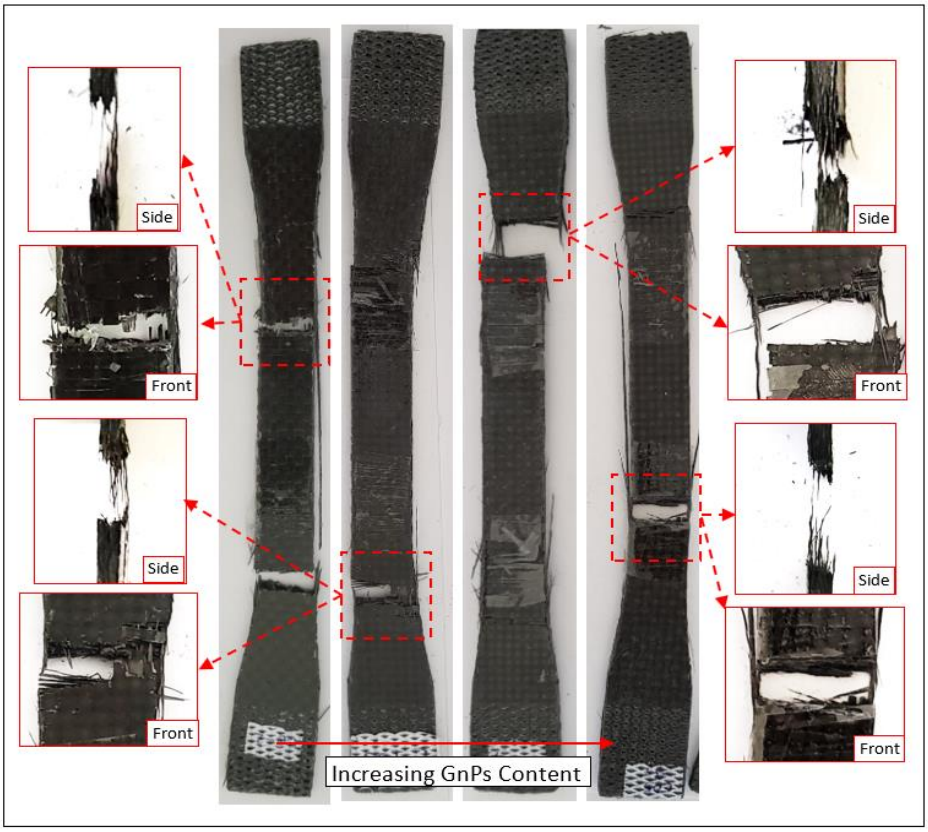

Figure 4.12 Tensile damage figures for CFR samples with various GnPs content.

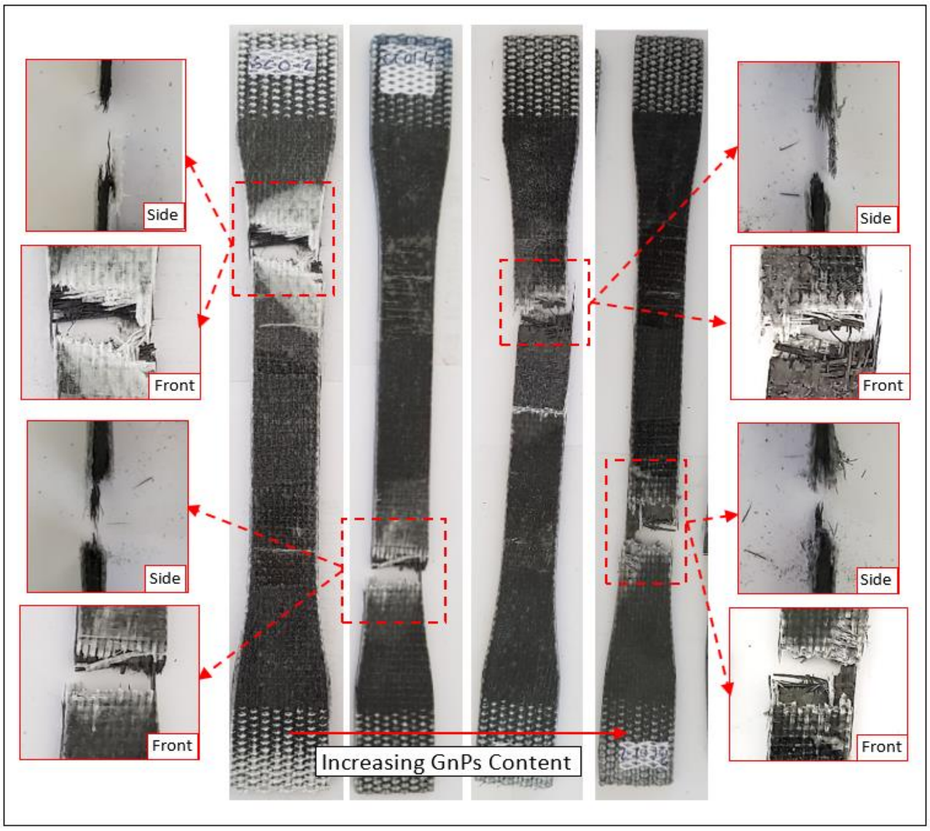

Figure 4.13 Tensile damage figures for GCFR samples with various GnPs content.

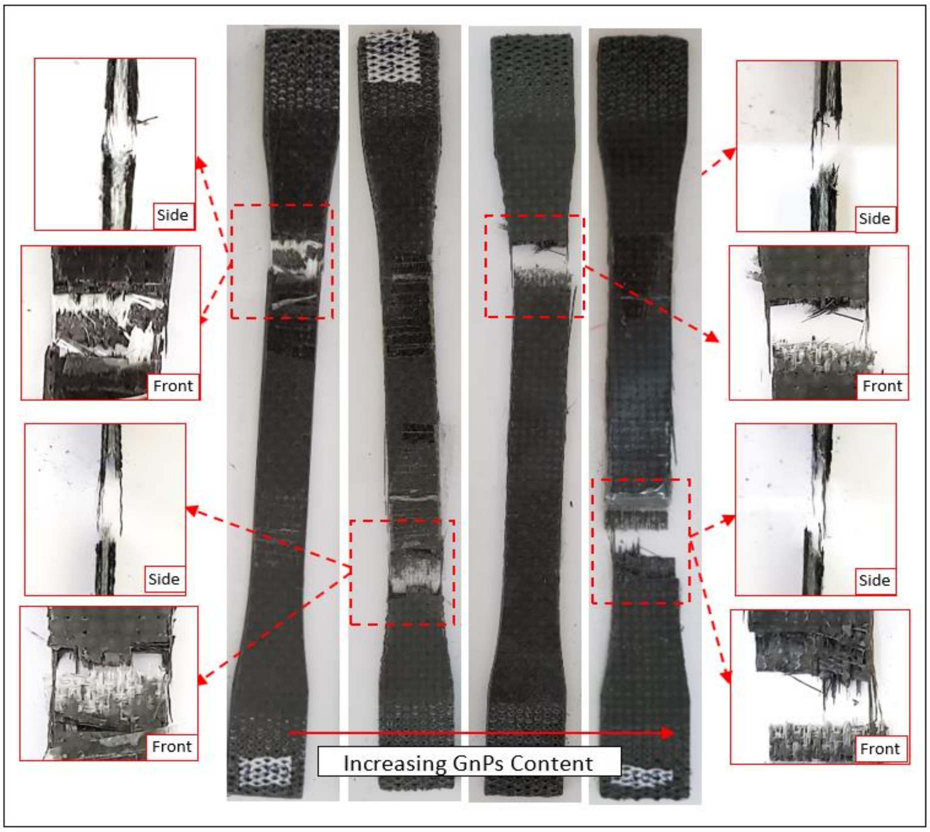

Figure 4.14 Tensile damage figures for CGFR samples with various GnPs content.

4.3 Flexural Test Results and Damage Characterization

Flexural behavior of fiber reinforced composite material is one of the important design parameters, and it can be described from the tension-compression of upper and lower layers. This behavior is mostly related to fiber properties and interaction between matrix and layers. Thus, it is possible to change this property of the composite material by fiber hybridization and matrix modification. For this reason, the flexural behaviors of the composite plates produced in the study were examined according to the fiber combinations used and the GnPs contribution rates and the following results were reached. To characterize the flexural behavior of test samples, force-displacement histories were recorded experimentally. In this perspective, the flexural behavior of the composite materials produced are presented below under two headings: effect of fiber hybridization and stacking configuration, effect of graphene nano platelets inclusion. In addition, the test results were interpreted by performing damage characterization of the test samples.

4.3.1 Effect of Fiber Hybridization and Stacking Sequence on the Flexural Behavior of Composite Laminates

Effect of stacking sequences of hybrid fiber reinforced unmodified epoxy composite laminates on the flexural strength and modulus will be presented in this section. Force-displacement histories of the unmodified hybrid/nonhybrid composite samples were illustrated in Figure 4.15. And, the flexural behavior of the composite laminates is given in Table 4.5.

The flexural strength and modulus values of the unmodified glass fiber reinforced epoxy composite sample (G0) were 602.90 MPa and 26.30 GPa. It can be seen from Table 4.5; maximum flexural strength value was recorded as 741.70 MPa in hybrid GC0 and minimum flexural strength value was recorded as 215.30 MPa in B0. Also, maximum flexural modulus value was recorded as 46.85 GPa in hybrid CG0 and minimum flexural modulus value was recorded as 15.98 GPa in B0.

Table 4.5 Flexural properties of unmodified composite samples with different stacking sequences.

Sample code	**Flexural strength (MPa)**	**Flexural modulus (GPa)**	**Flexural strain (mm/mm)**
G0	602.90	26.30	0.0218
A0	310.12	22.62	0.0283
B0	215.30	15.98	0.0220
C0	576.20	42.24	0.0131
GA0	429.26	20.93	0.0198
AG0	425.80	23.31	0.0343
GB0	522.70	21.50	0.0200
BG0	272.10	18.27	0.0190
GC0	741.70	36.31	0.0221
CG0	584.80	46.85	0.0122

(a)

(b)

(c)

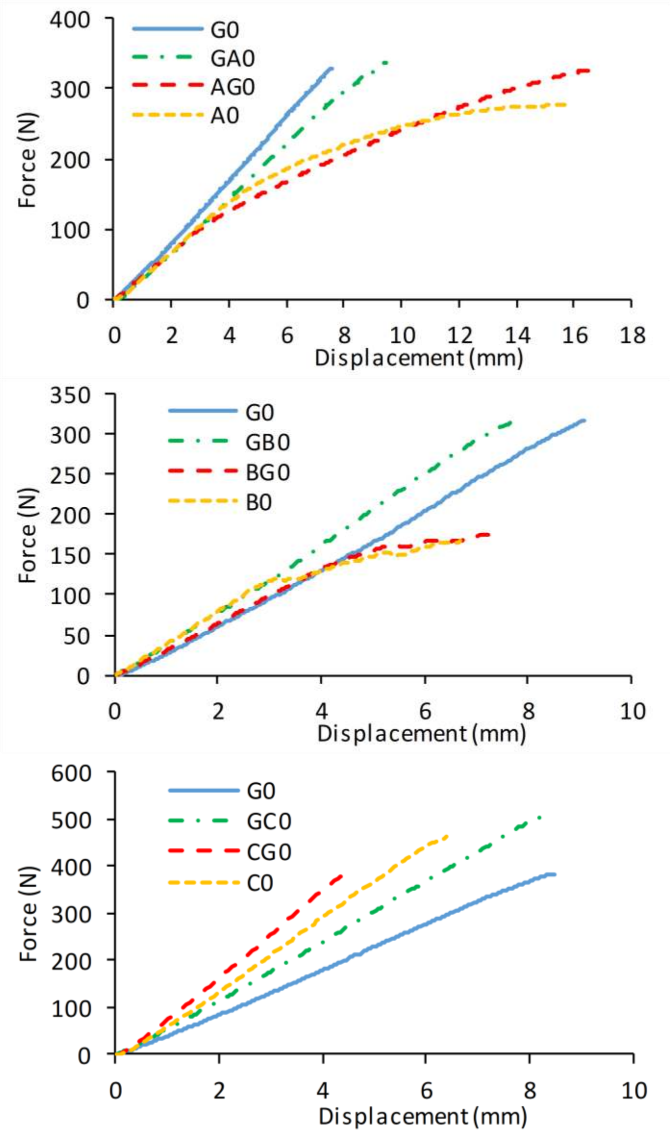

Figure 4.15 Force-displacement diagram of fiber reinforced composite samples with different stacking sequences.

4.3.1.1 Glass / Aramid Fiber Reinforced Composite

Flexural strength and modulus values of unmodified aramid fiber reinforced epoxy composite sample (A0) were recorded as 310.12 MPa and 22.62 GPa as given in Table 4.5. Glass fiber hybridization was resulted as improvement in flexural behavior of AFRP composite plate as seen in Figure 4.15(a) and Table 4.5. Improvement in flexural strength value of A0 sample was 38.42% for hybrid GA0 sample and 37.3% for hybrid AG0 composite sample. When glass fiber was placed at the outer skin, and aramid fiber was placed in the core, hybrid composite material with unmodified epoxy showed the better resistance to bending loading compared to the other hybrid configuration.

4.3.1.2 Glass / Basalt Fiber Reinforced Composite

Flexural strength and modulus values of unmodified basalt fiber reinforced composite samples (B0) were recorded as 215.3 MPa and 15.98 GPa as given in Table 4.5. Glass fiber hybridization contributed a positive effect on the basalt/glass hybrid composite structures in terms of flexural strength. When glass fiber was placed at the outer skin, and basalt fiber was in the core, hybrid composite laminates have shown higher flexural strength compared to other hybrid configuration due to higher flexural strength and modulus of glass fibers as compatible with the reference [104]. Furthermore, the flexural strength and modulus values of the hybrid composite samples were recorded as 522.7 MPa and 21.5 GPa in GB0, 272.1 MPa and 18.27 GPa in BG0 between the values of G0 and B0 samples. Improvement in flexural strength value of B0 sample was 142.7% for hybrid GB0 sample and 26.38% for hybrid BG0 composite sample.

4.3.1.3 Glass / Carbon Fiber Reinforced Composite

The effect of stacking sequence on flexural behavior of the unmodified glass/carbon fiber reinforced composite samples was illustrated in Figure 4.15(c) for the comparison of force-displacement histories. Also, flexural properties of the unmodified glass/carbon fiber reinforced composite samples were given in Table 4.5. As seen in Table 4.5, flexural strength and modulus values of unmodified carbon fiber reinforced composite samples (C0) were recorded as 576.2 MPa and 42.24 GPa. Glass fiber hybridization was revealed as improvement in flexural properties of carbon fiber reinforced composite plate and improvement in strength value was 28.72% for GC (glass fiber is placed at the outer skin, and carbon fiber is in the core), 1.49% for CG hybrid sample. It should also be noted that the fiber material on the outer surface is predominant on the flexural behavior of the hybrid composite samples. Considering the flexural test results, it can be interpreted that fiber hybridization is strikingly effective on flexural properties of fiber-reinforced composite materials.

4.3.2 Effect of Graphene Nano Platelets Inclusion on the Flexural Behavior of Composite Laminates

Effect of GnPs inclusion of hybrid/nonhybrid fiber reinforced composite laminates on the flexural strength and modulus will be investigate in this section. Force-displacement histories of the hybrid/nonhybrid composite samples were illustrated in Figure 4.17, 4.21, and 4.25. And, the flexural properties with varying content of GnPs of the composite laminates were given in Table 4.6-4.8.

The flexural strength and modulus values of the glass fiber reinforced composite sample used as common reinforcement composite sample in all productions were 602.9 MPa and 26.30 GPa. The flexural strength and modulus of glass fiber reinforced unmodified epoxy composites (G0) were clearly exhibited the highest value at GnPs content of 0.25 wt% with indicating 14% and 16% improvement, respectively. Further addition of GnPs content after the 0.25 wt% resulted in a reduction of flexural strength and modulus of the unmodified glass/epoxy samples, with indicating poor dispersion of GnPs particles in the epoxy resin.

Figure 4.16 presents the fractured specimens of glass fiber (G) reinforced composite samples with increasing GnPs content under flexural loading. It was observed that fiber rupture and fiber pull-out failures can be seen on the back side of the samples due to tensile loading. Delamination failure was also visible on back side of the samples. Kinking failure (fiber buckling) which is a compressive failure mode was seen on the front side of the composite sample with higher GnPs content.

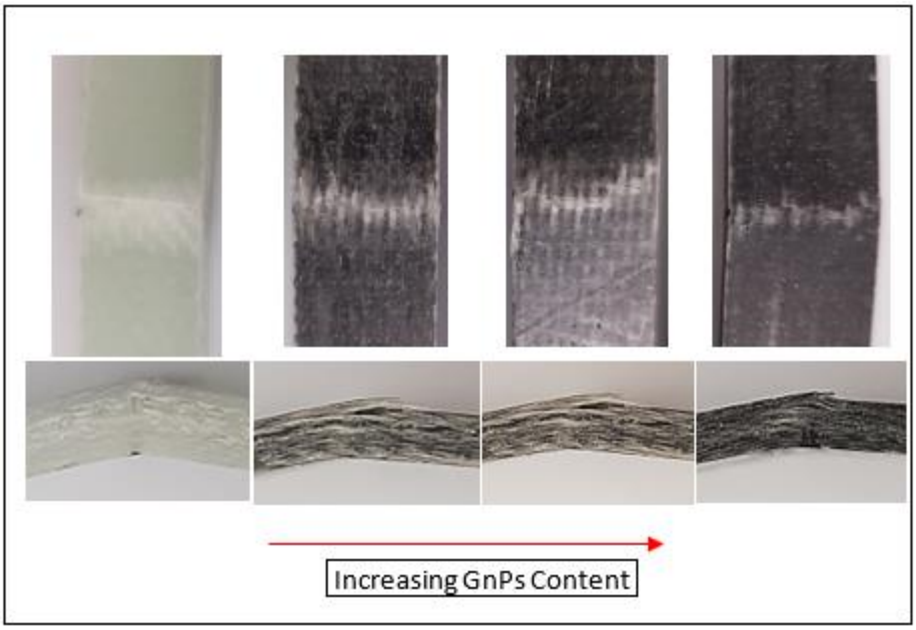

Figure 4.16 Flexural damage figures for GFR samples with various GnPs content.

4.3.2.1 Glass / Aramid Fiber Reinforced Composite

Three-point bending test results of the GnPs modified glass/aramid fiber reinforced composite samples were illustrated in Figure 4.17 for the comparison of force-displacement histories. And, flexural strength and modulus values were presented in Table 4.6. According to test results, GnPs modification can significantly improve the flexural strength of the material in GA hybrid configuration. On the other hand, the addition of GnPs particles to the epoxy matrix resulted in a reduction of the flexural strength of the aramid fiber (A) and AG hybrid fiber-reinforced composite material. Flexural strength values were recorded as 429.26, 425.80 and 310.12 MPa for unmodified samples of GA, AG and A configurations respectively. Flexural strength values were exhibited the highest value at GnPs content of 0.25 wt% with improvement of 14.56% for GA (when glass fiber is on skin and aramid fiber is in core). And the further increase of the GnP content results in a reduction of the flexural strength of the material, which indicates the irregular particle distribution and thus poor load transfer between the fabric layers. However, in case of A and AG (when glass fiber is in core and aramid fiber is in the skin), strength values were continuously decreased compared to unmodified samples and decreasing in these values were recorded as 31.8%, 5.14% in A and AG configurations for 0.5wt% GnPs content.

Table 4.6 Flexural properties of hybrid/non-hybrid glass/aramid fiber reinforced composite samples with various GnPs content.

Sample code	Flexural strength (MPa)	Flexural modulus (GPa)	Flexural strain (mm/mm)	Sample code	Flexural strength (MPa)	Flexural modulus (GPa)	Flexural strain (mm/mm)
G0	602.9	26.30	0.0218	**A0**	310.12	22.62	0.0283
G01	679.1	25.55	0.0251	**A01**	269.94	23.87	0.0260
G025	722.0	29.30	0.0228	**A025**	269.77	22.96	0.0243
G05	710.0	27.52	0.023	**A05**	211.28	16.79	0.0282
GA0	429.26	20.93	0.0198	**AG0**	425.80	23.31	0.0343
GA01	477.21	20.94	0.0227	**AG01**	407.26	18.74	0.0344
GA025	491.78	22.10	0.0215	**AG025**	410.62	23.15	0.0311
GA05	330.75	18.99	0.0190	**AG05**	403.89	19.90	0.0358

The fractured photographs of A, GA, and AG composite samples under flexural loading and with increasing GnPs content in the matrix was presented in figures from 4.18 to 4.20. Fiber rupture, matrix cracking and delamination type failures were observed in fractured samples. It can be seen fiber rupture and delamination failures in fractured surfaces. Increasing delaminated areas were observed in GnPs modified A and AG samples which resulted in decreased flexural strength values. Also, kinking was observed in compression side of GA samples.

(a)

(b)

(c)

(d)

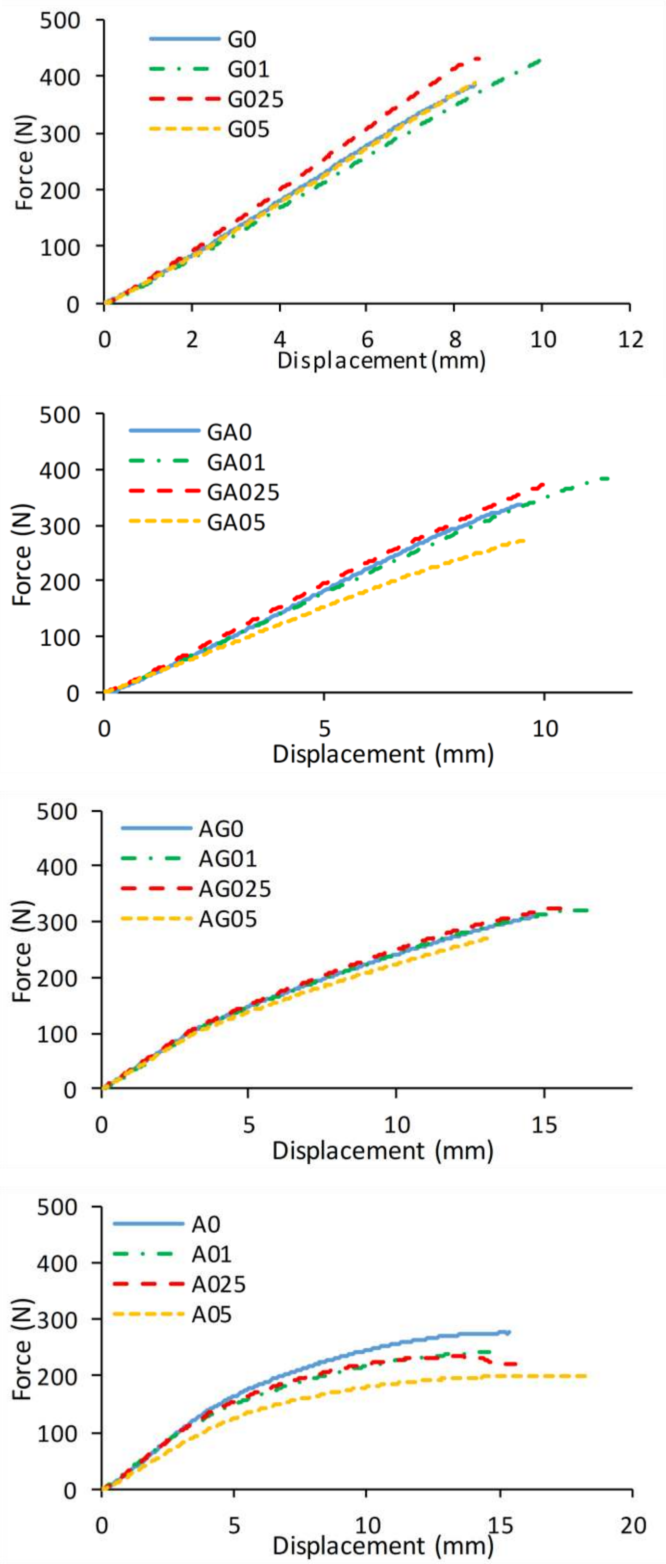

Figure 4.17 Force-displacement diagrams of hybrid/non-hybrid glass/aramid fiber reinforced composite samples with various GnPs content under bending.

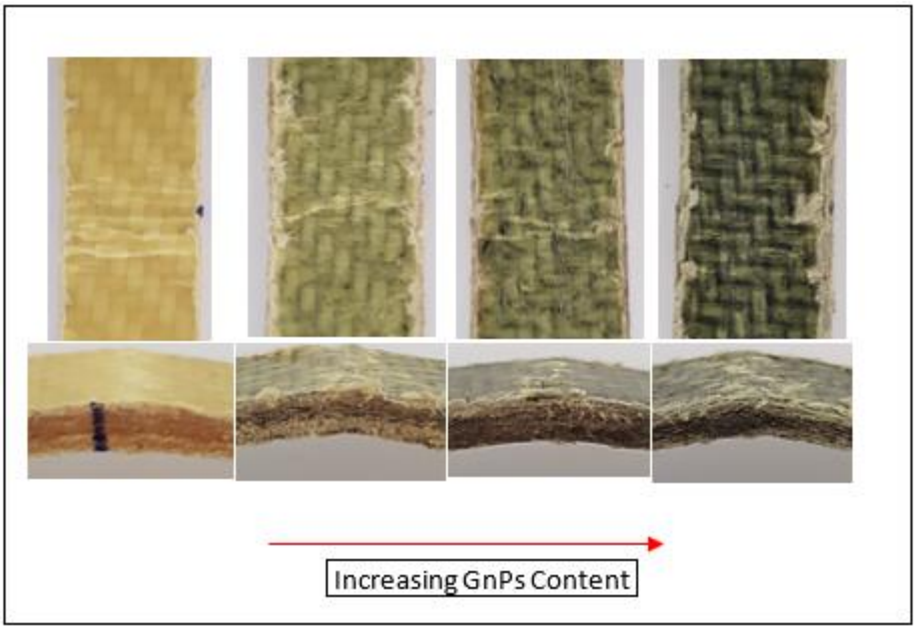

Figure 4.18 Flexural damage figures for AFR samples with various GnPs content.

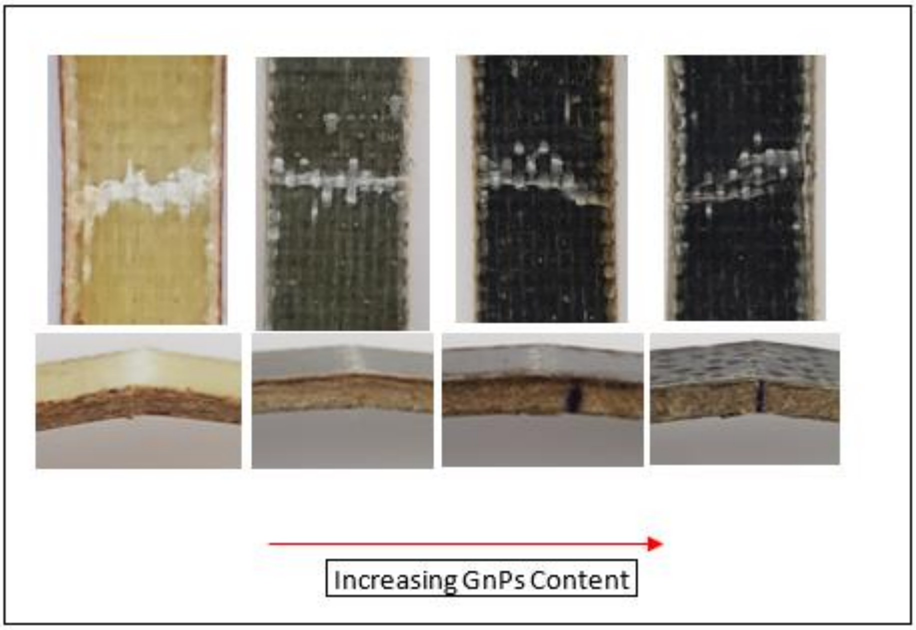

Figure 4.19 Flexural damage figures for GAFR samples with various GnPs content.

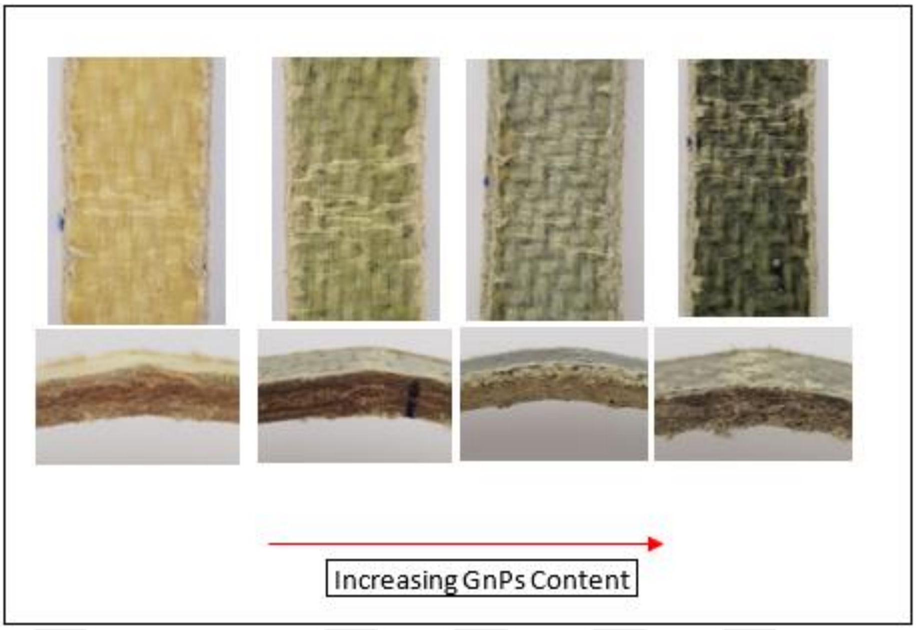

Figure 4.20 Flexural damage figures for AGFR samples with various GnPs content.

4.3.2.2 Glass / Basalt Fiber Reinforced Composite

Force-displacement history and flexural properties of glass/basalt reinforced composite samples were presented in Figure 4.21 and Table 4.7 with respect to stacking sequence and GnPs content. According to test results in Table 4.7, GnPs particle addition significantly improved the flexural strength and modulus of the samples, and flexural strength values were recorded as 522.7, 272.1 and 215.3 MPa for unmodified samples of GB, BG and B configurations, respectively. In particular, the presence of 0.1wt% of GnPs in the epoxy resin, flexural strength values were increased with the improvement of 20.1%, 63.06% and 45.84% for GB, BG and B fiber reinforced composite samples, respectively. Furthermore, given the increases in the hybrid composite samples produced, the bending behavior of the material in the outer layers appears to be dominant in the bending properties of the hybrid composite. It was also noted that flexural strain and modulus values of GB, BG, B designated samples were reached their maximum values with 0.1wt% GnPs filler, this could be attributed the better interfacial stress at fiber / matrix / GnPs particles, and these considerable improvements in flexural and tensile strength of composite samples filled with 0.1wt% GnPs suggests the improved interfacial bonding between fiber and matrix material mostly due to large surface area of GnPs particles. Thus, a certain amount of used GnP improved fiber/matrix interface bonding and significantly increased the transfer load between the fiber-GnPs particles-matrix, leading to the improvement of the mechanical properties of the composite samples. [99, 105].

Table 4.7 Flexural properties of hybrid/non-hybrid glass/basalt fiber reinforced composite samples with various GnPs content.

Sample code	**Flexural strength (MPa)**	**Flexural modulus (GPa)**	**Flexural strain (mm/mm)**	**Sample code**	**Flexural strength (MPa)**	**Flexural modulus (GPa)**	**Flexural strain (mm/mm)**
G0	602.9	26.30	0.0218	**B0**	215.3	15.98	0.022
G01	679.1	25.55	0.0251	**B01**	314.0	16.45	0.025
G025	722.0	29.30	0.0228	**B025**	185.9	13.45	0.014
G05	710.0	27.52	0.023	**B05**	193.9	11.52	0.016
GB0	522.7	21.50	0.020	**BG0**	272.1	18.27	0.019
GB01	627.9	22.53	0.024	**BG01**	443.7	21.11	0.030
GB025	324.7	17.28	0.015	**BG025**	214.8	14.33	0.018
GB05	346.9	19.71	0.017	**BG05**	254.3	15.63	0.021

Figures from 4.22 to 4.24 depict the fractured photographs of B, GB, and BG composite samples under flexural loading with increasing GnPs content in the matrix. Fiber rupture, pull-out and delamination failure modes have been mainly found in the fractured surfaces. In B and BG composite samples, fiber rupture and fiber pull-out were obvious on the back surface of the samples due to poor tensile strength of basalt fiber. In addition, highly localized kinking failure was clearly seen on compression side of these composite samples. It was also observed that the delaminated areas increased with the increased nanoparticle content. The reason for this situation is that the inhomogeneous distribution of the nanoparticles in the matrix and the weak load transfer between the fiber / matrix material can be concluded.

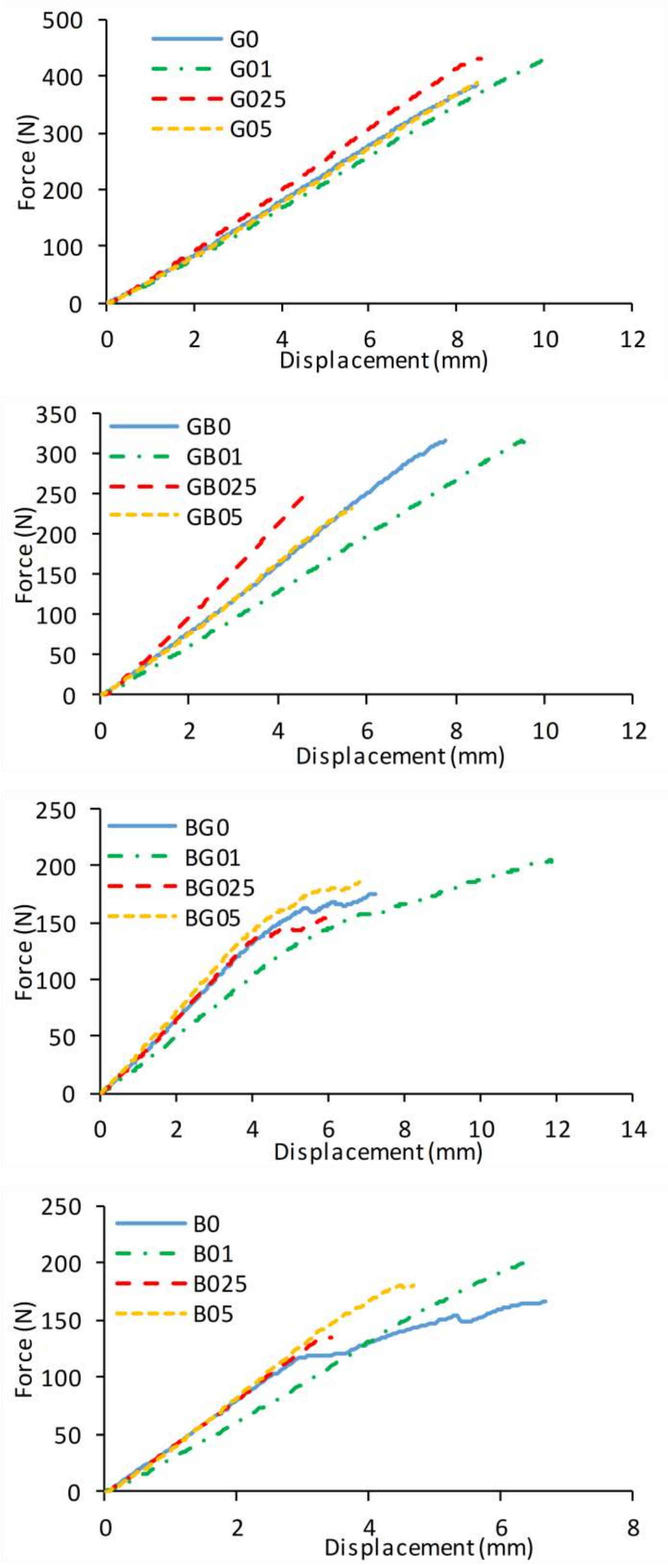

Figure 4.21 Force-displacement diagrams of hybrid/non-hybrid glass/basalt fiber reinforced composite samples with various GnPs addition under bending.

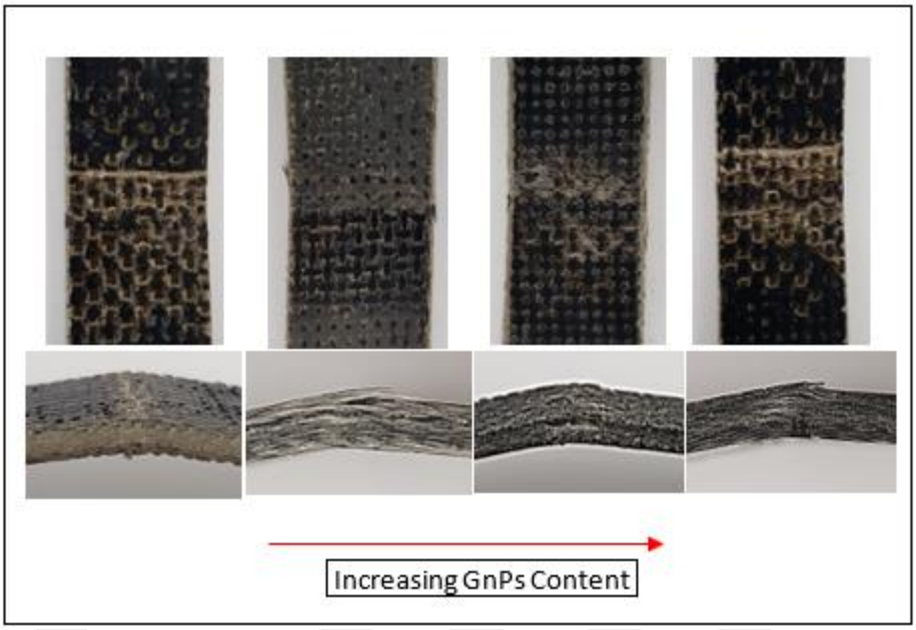

Figure 4.22 Flexural damage figures for BFR samples with various GnPs content.

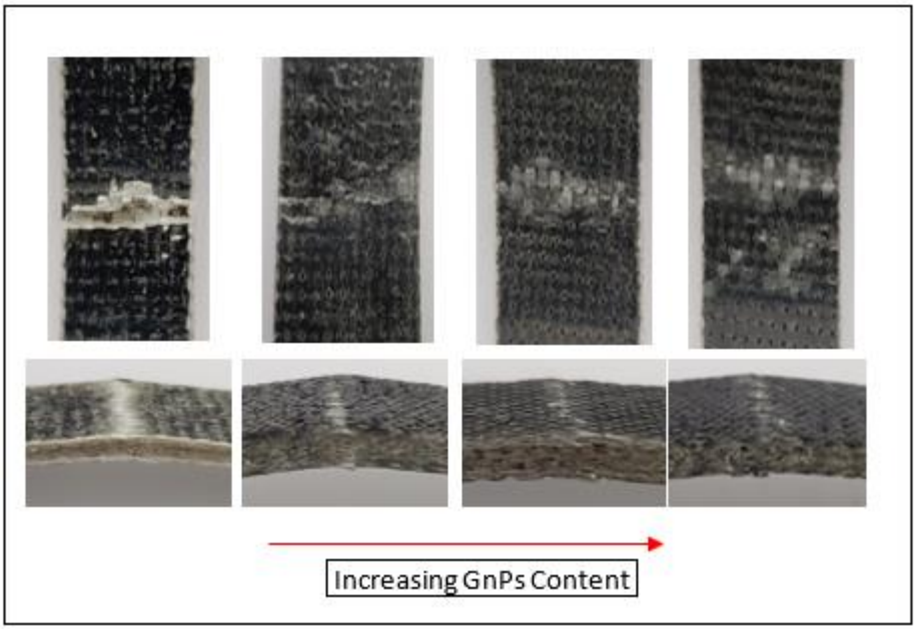

Figure 4.23 Flexural damage figures for GBFR samples with various GnPs content.

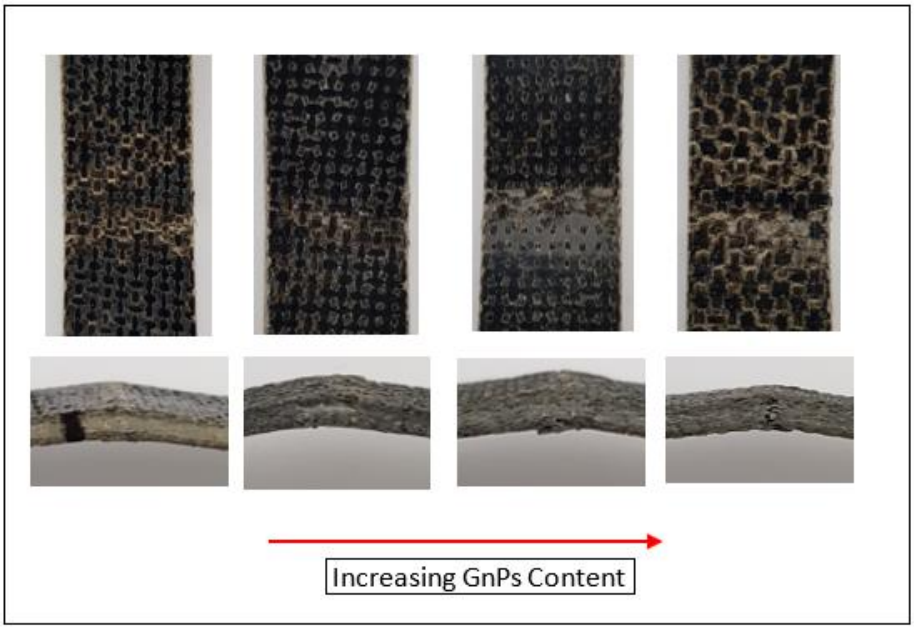

Figure 4.24 Flexural damage figures for BGFR samples with various GnPs content.

4.3.2.3 Glass / Carbon Fiber Reinforced Composite

Three-point bending test results of the GnPs modified glass / carbon fiber reinforced composite samples were illustrated in Figure 4.25 for the comparison of force-displacement histories. Their flexural strength and modulus values were presented in Table 4.8. For hybrid samples at which glass fabrics were at outer sides (GC samples), a little variation was observed by 2.9% of flexural strength at GnPs content of 0.25 wt% and fiber hybridization was more effective than GnPs particle functionalization. Similar results were observed for the hybrid samples at which carbon fabrics were at outer layers (CG), with indicating that only 13.5% and 15.2% improvements of flexural strength and modulus when modifying epoxy resin by GnPs particles, respectively. However, carbon fiber hybridization was mostly effective than GnPs particle functionalization for glass fiber reinforced composites. For the modified and unmodified carbon/epoxy samples, maximum flexural strength was recorded at the GnPs content of 0.1 wt% showing 18.1% improvement according to unmodified C0 samples. Further addition of GnPs particle content revealed the reduction of flexural strength with indicating that agglomeration effects of particles were occurred leading to poor interfacial adhesion between particles and matrix resin [106]. However, maximum flexural modulus was evaluated at GnPs content of 0.5 wt% indicating that brittle nature of the sample was increased.

Table 4.8 Flexural properties of hybrid/non-hybrid glass/carbon fiber reinforced composite samples with various GnPs content.

Sample code	Flexural strength (MPa)	Flexural modulus (GPa)	Flexural strain (mm/mm)	Sample code	Flexural strength (MPa)	Flexural modulus (GPa)	Flexural strain (mm/mm)
G0	602.9	26.30	0.0218	**C0**	576.2	42.24	0.0131
G01	679.1	25.55	0.0251	**C01**	704.9	41.5	0.0131
G025	722.0	29.30	0.0228	**C025**	641.7	44.15	0.013
G05	710.0	27.52	0.023	**C05**	663.7	47.25	0.0118
GC0	741.7	36.31	0.0221	**CG0**	584.8	46.85	0.0122
GC01	513.9	27.93	0.024	**CG01**	663.7	53.77	0.0153
GC025	763.4	31.82	0.02	**CG025**	619.7	39.32	0.0132
GC05	715.7	30.22	0.02	**CG05**	580.9	51.11	0.0122

The fractured photographs of C, GC, and CG composite samples under flexural loading and with increasing GnPs content in the matrix was presented in figures from 4.26 to 4.28. Fiber rupture, matrix cracking and delamination type failures were observed in fractured samples. In Figure 4.26 and 4.28; fiber pull out, rupture and kinking failures can be observed. These failure modes were more obvious in the samples with high GnPs content. And, this can be the result of increasing brittleness of the composite samples. And, obviously delaminated regions also increased with the increased GnPs content. These findings can be also seen in Figure 4.27.

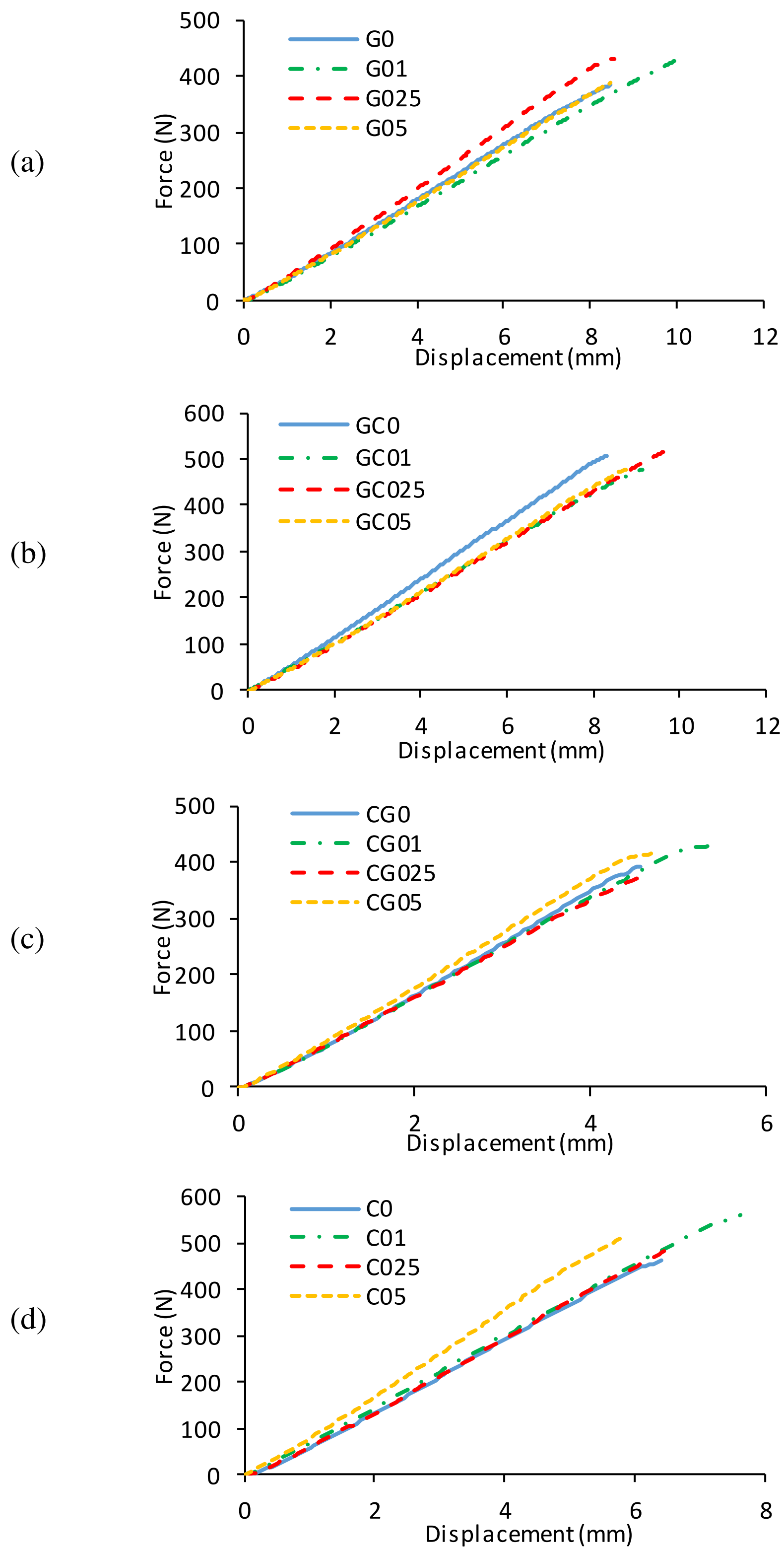

Figure 4.25 Force-displacement diagrams of hybrid/non-hybrid glass/carbon fiber reinforced composite samples with various GnPs addition under bending.

Figure 4.26 Flexural damage figures for CFR samples with various GnPs content.

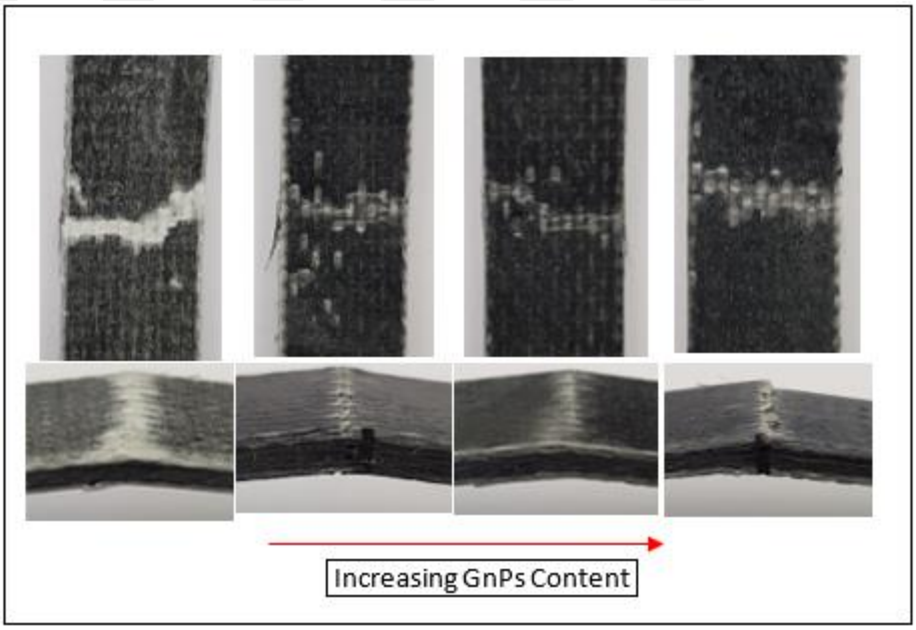

Figure 4.27 Flexural damage figures for GCFR samples with various GnPs content.

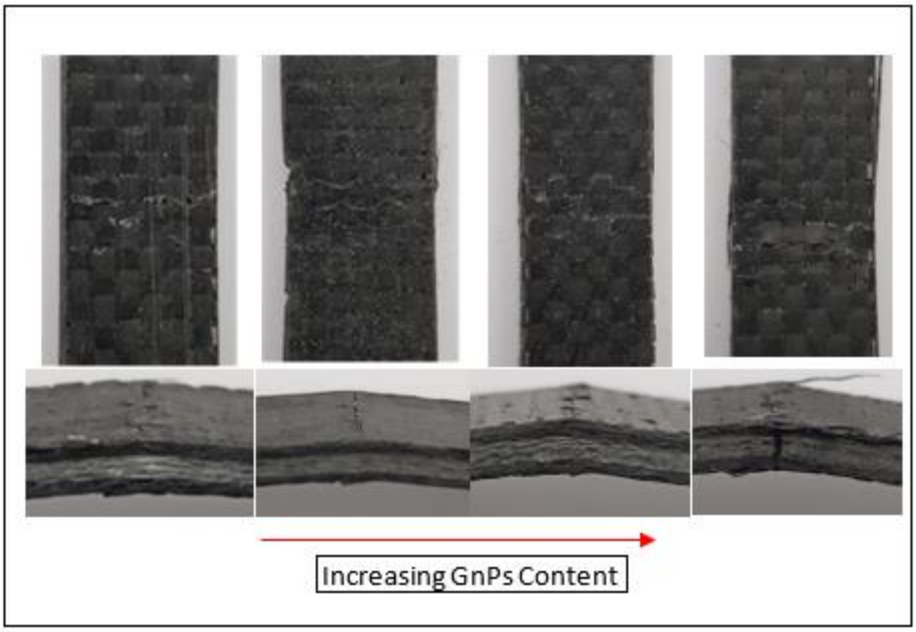

Figure 4.28 Flexural damage figures for CGFR samples with various GnPs content.

CHAPTER 5

LOW VELOCITY IMPACT BEHAVIOR OF COMPOSITE LAMINATES

5.1 Introduction

In this section, the results of the low velocity impact (LVI) tests which are conducted to the determination of the LVI properties of the produced composite plates are presented. The results of LVI tests are given according to fiber hybridization and matrix modification.

5.2 Low Velocity Impact Test Results

Drop weight test was conducted to determine the damage resistance of composite laminates under low velocity impact according to ASTM D7136. The effect of fiber hybridization and matrix modification on the low velocity impact behavior of composite plates was investigated in terms of absorbed energy (E_a) and peak load (F_{max}). The damage characteristics of composite materials is a complex phenomenon that is affected by various factors ranging from the content of composite material to lamina sequence, and they are associated with the energy absorption of the composite material, occurring in the whole of matrix cracking, fiber breakage and delamination. In this PhD study, the impact response of composite material varies with the fiber and matrix hybridization, and this makes the samples to become more complex with several variables in terms of impact properties (stacking sequence +filler incorporation + impact energy). To reduce this complexity, the impact response of each laminate in terms of force, energy and displacement was compared for different filler concentration under same impact energy of 30 J. The impactor is allowed to drop freely from a height of 61 cm, allowing the application of 30 J impact energy. The force histories were recorded along the impact tests, this can be considered as the resistance of material against penetration. Thus, a hard and tougher material must be expected to resist impact loading. Drop weight impact test results were presented under two headings: the effect of fiber hybridization and stacking sequence, and the effect of graphene nano platelets inclusion. In addition, the test results were interpreted by performing damage characterization of the test samples via damage photos and scanning electron microscopy (SEM) images.

5.2.1 Effect of Fiber Hybridization and Stacking Sequence on the Low velocity Impact Behavior of Composite Laminates

Figures 5.1 and 5.2 illustrate the force-time and force-displacement histories of the different stacking sequenced hybrid/non-hybrid fiber reinforced unmodified epoxy composite samples. Peak load, maximum displacement and absorbed energy values of the composite samples are presented in Table 5.1. In Figure 5.1, it is evident that force increases with fluctuations up to the maximum, then it generally follows a sudden load drops which indicating that modified and unmodified samples behave as brittle nature. The sudden load drops in contact force after the first peak in the force-time curve indicate the formation of delamination or cracking damages as reported by many researchers [47, 109]. In addition, the fluctuating force-time and force-displacement schemes have been associated with the elastic wave caused by rapid vibration after the impact event [110].

The peak load and absorbed energy values of the glass fiber reinforced having unmodified epoxy composite sample (G0) were recorded as 3.25 MPa and 19.57 J as given in Table 5.1. The highest peak load and absorbed energy values were found as 4.46 kN and 28.36 J in carbon fiber reinforced having unmodified epoxy composite sample (C0) as seen in Figure 5.3. On the other hand, the highest maximum displacement value was 35.71 mm in aramid fiber reinforced unmodified epoxy composite sample (A0).

(a)

(b)

(c)

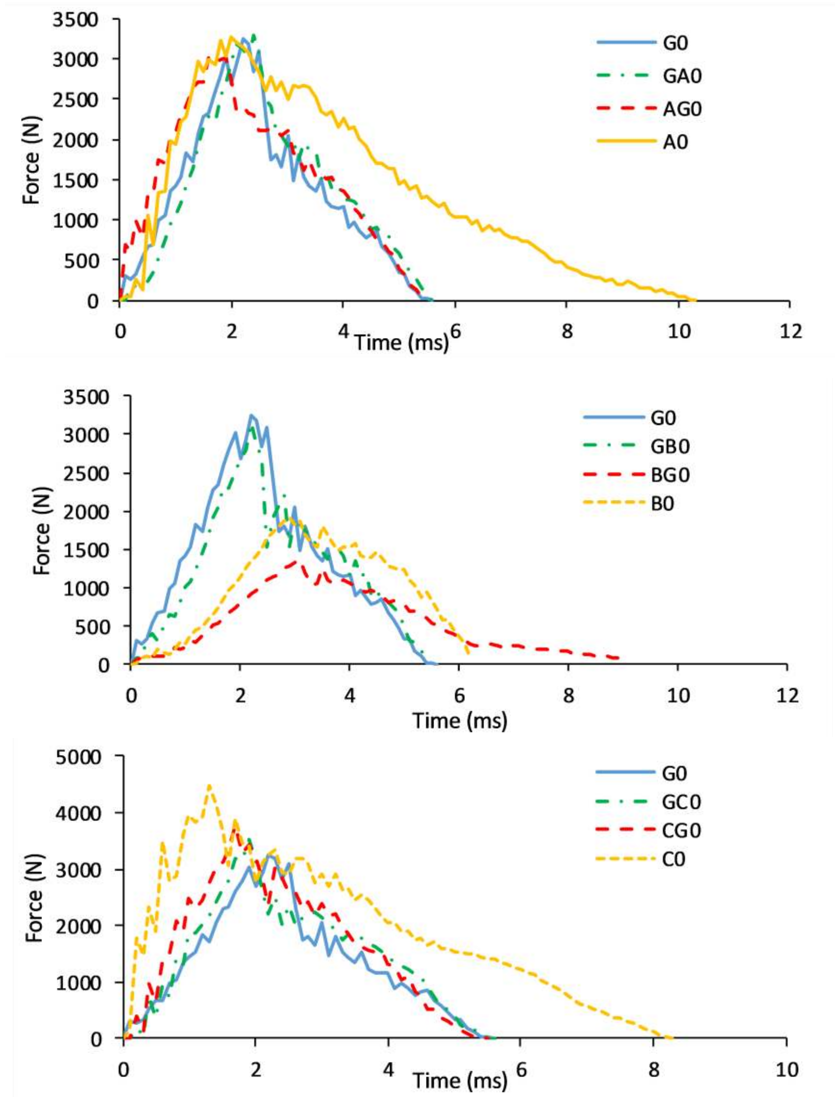

Figure 5.1 Force-time histories of fiber hybridized composite samples without GnPs addition.

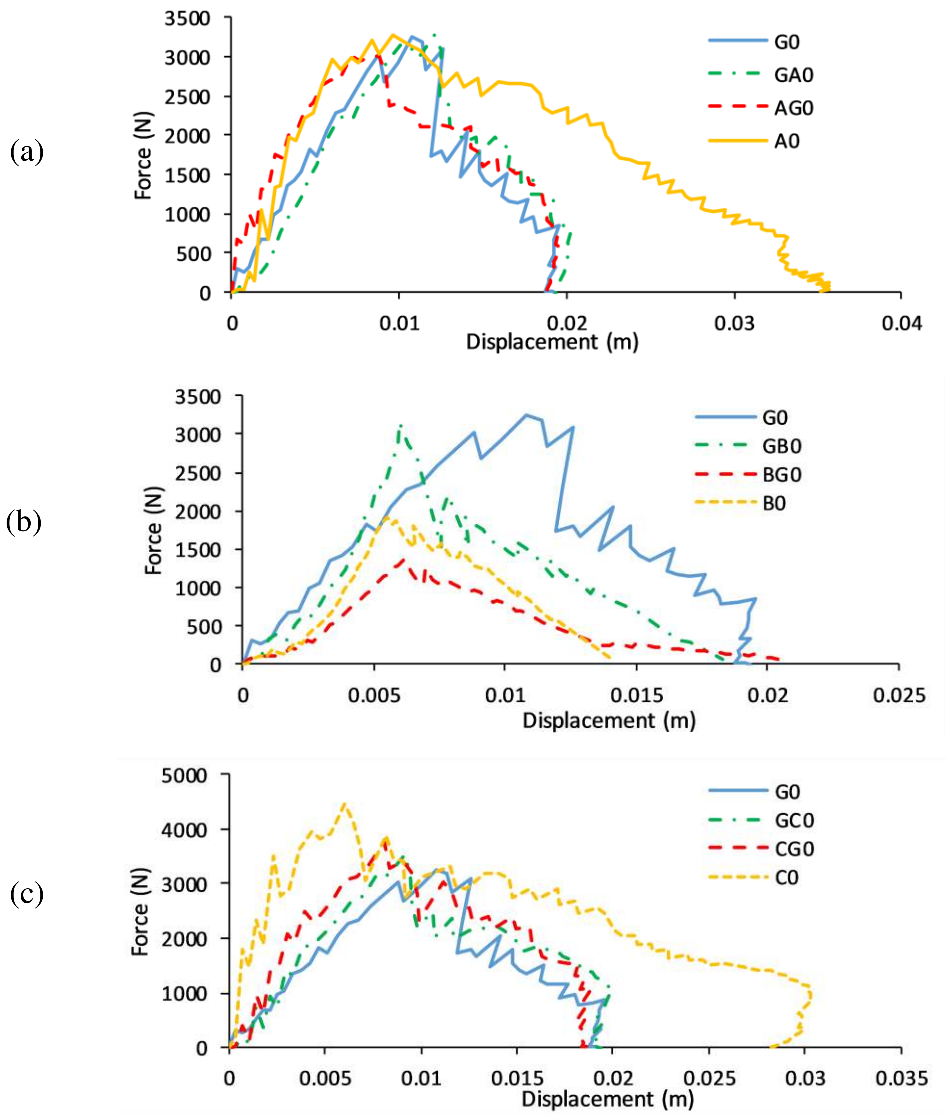

Figure 5.2 Force-displacement diagrams of fiber hybridized composite samples without GnPs addition.

Table 5.1 LVI properties of unmodified composite samples with different stacking sequences.

Sample code	Peak load (kN)	Maximum displacement (mm)	Absorbed energy (J)
G0	3.25±0.01	19.57±1.0	19.32±0.1
A0	3.27±0.02	35.71±0.4	26.91±0.3
B0	1.91±0.02	10.47±0.2	17.36±0.3
C0	4.46±0.02	30.35±1.0	28.36±0.2
GA0	3.28±0.01	20.28±0.3	19.77±0.4
AG0	3.01±0.02	19.62±1.0	21.36±0.4
GB0	3.15±0.01	18.65±0.3	22.70±0.4
BG0	1.36±0.02	18.65±0.8	16.80±0.4
GC0	3.52±0.02	20.02±0.4	20.74±0.2
CG0	3.42±0.10	18.99±0.3	22.16±0.2

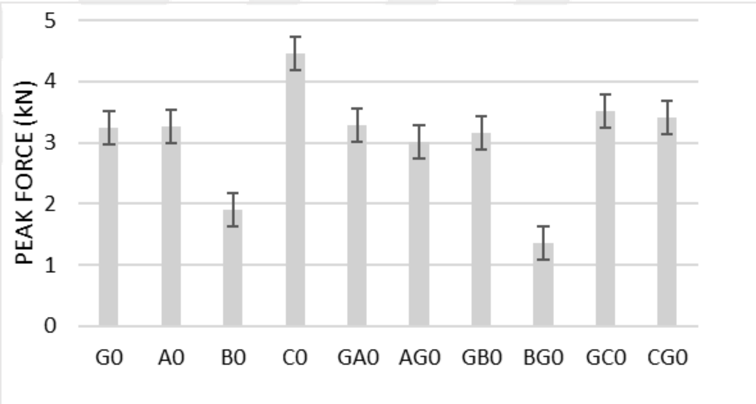

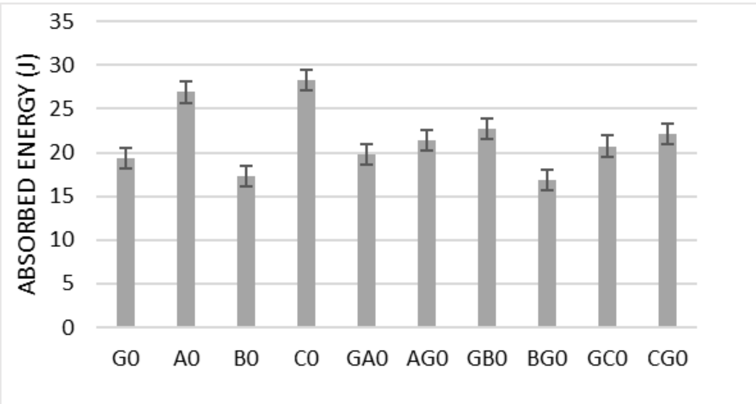

Figure 5.3 Comparison of the key characteristics of hybrid/non-hybrid fiber reinforced unmodified epoxy composites subjected to drop-weight impact test.

5.2.1.1 Glass / Aramid Fiber Reinforced Composite

Peak load and absorbed energy values of aramid fiber reinforced unmodified epoxy composite sample (A0) were recorded as 3.27 kN and 26.91 J as given in Table 5.1. A0 composite sample was performed better compared to G0 composite in terms of peak load and absorbed energy sample as expected. This is due to superior impact resistance of aramid fiber than glass fiber [107]. The force-time diagram can be analyzed into two part: damage initiation and damage propagation part. In the first part, there is an increasing linear curve showing the elastic response of the structure to the peak load. It is expected that no damage occurs if the loading interrupted at this stage. If the fluctuations are observed at this part, it shows that the damage initiation occurs in different moments. Second part of the curve is mainly related with the damage propagation. Sudden drops of the curve indicate major fractures such as fiber pull-out and complete perforations [67, 115, 116].

The slope of Figure 5.1(a) is greater for G0 composite sample than that of A0 composite sample due to higher flexural modulus of glass fiber than aramid fiber. As a known fact that the initial stage of the LVI response depends on the flexural modulus of the composite [37]. After peak load, smoother drop and longer impact duration can be observed in the force-time diagram of A0 sample which indicates the fiber/matrix debonding and fiber pull-out. This progressive load drop shows the higher and continuing energy absorption of the composite sample.

As given in Table 5.1, aramid fiber hybridization resulted as an improvement in the absorbed energy and displacement values of the glass fiber reinforced composites which indicates that the increased ductility of composite samples. Enhancement in absorbed energy values were calculated as 2.3% in GA0 and 10.5% in AG0 compared to G0 composite sample. Thus, AG (when aramid fiber is on the skin, glass is in the core) sequenced composite laminate had better impact resistance than that of GA sequenced hybrid composite laminate which is consistent with the study in [37].

5.2.1.2 Glass / Basalt Fiber Reinforced Composite

In Table 5.1, the peak load and absorbed energy values of basalt reinforced unmodified epoxy composite sample (B0) is given as 1.91 kN and 17.36 J. B0 composite sample was showed worse impact performance than G0 composite sample as predicted. When the test results given in the previous section are examined, the fact that basalt fibers have lower tensile and flexural modulus than glass fibers explain the low impact strength of basalt fibers. As can be seen in Figures 5.1 (b) and 5.2 (b), the B0 composite sample has a lower impact response time and displacement values, which indicates a sudden perforation damage in the sample.

Glass fiber hybridization improved the peak load and absorbed energy values of the basalt fiber reinforced unmodified epoxy composite. Besides that, the peak load and absorbed energy values of the hybrid sample BG0 were lower than B0 composite sample. In this hybrid sequence, basalt fiber which had low flexural modulus and strength was on the skin layer of the composite laminate so that the lowest peak load and also lower absorbed energy value (compared to the other hybrid composite sample) were recorded. Enhancement in absorbed energy and peak load values were calculated as 30.8% and 64.9% in GB0; -3.2% and -28.8% in BG0 compared to B0 composite sample.

5.2.1.3 Glass / Carbon Fiber Reinforced Composite

The highest peak load and absorbed energy values were found as 4.46 kN and 28.36 J in carbon fiber reinforced unmodified epoxy composite sample (C0) as seen in Table 5.1. The slope of Figure 5.1(c) is greater in C0 composite sample than G0 composite sample which verifies higher flexural modulus of carbon fiber reinforced composite sample. Also, C0 composite sample shows longer impact duration than G0 which indicates the impact response of C0 sample in the mode of delamination and fiber pull-out. Thus, higher energy absorption value was recorded in the C0 sample compared to G0 sample.

Carbon fiber hybridization improved the LVI response of glass fiber reinforced composite in terms of peak load and absorbed energy values. Enhancement in absorbed energy and peak load values were calculated as 7.3% and 8.3% in GC0; 14.7% and 12.8% in CG0 compared to G0 composite sample. The peak load was higher when carbon fabric was on outer layers and glass fabric was inside. These results are also in line with the results given in [38, 114]. All hybrid configurations of glass/carbon fiber composites have shown similar impact duration even though force values vary with high oscillations after the maximum load. In addition, it has been found to have similar impact behavior in both hybrid configurations.

5.2.2 Effect of Graphene Nano Platelets Inclusion on the LVI Behavior of Composite Laminates

The mechanical properties of composite material are highly dependent on the fiber material and the bonding strength between the fiber and matrix materials. As mentioned in previous chapters, the reinforcement material (fiber) is the main load-bearing structure of the composite body and the bonding strength between reinforcement and matrix phase is extremely important to load transfer between reinforcement materials. Besides, the fiber/matrix interfacial bonding strength has importance in LVI damage modes of composite material. Thus, a functional load transfer in the fiber/matrix interface will directly affect the mechanical and impact characteristics of the composite structure [111-113]. In this section, the LVI behavior of hybrid/non-hybrid fiber reinforced composite plates was discussed according to various GnPs filler content. The force histories which can be considered as the resistance of a material against penetration were recorded along with the impact tests. The force histories of composite samples with varying content of GnPs are presented under three headings according to reinforcement types.

First, it can be stated that the GnPs additive significantly affects the impact behavior of the composite plates. The peak load and absorbed energy values of the glass fiber reinforced composite sample used as common composite sample in all productions were 3.25 kN and 19.32 J as given in Table 5.2. The peak load and absorbed energy of glass fiber reinforced unmodified epoxy composites (G0) were clearly exhibited the highest value at GnPs content of 0.25 wt% with indicating 3.4% and 9.21% improvement, respectively. Further addition of GnPs content after the 0.25 wt% resulted in a reduction of peak load and absorbed energy values which could resulted from debonding between matrix and GnPs particles. All glass fiber reinforced composite samples have similar impact duration. However, the slope of force-time curve in Figure 5.5(a) was increased with increasing filler content which shows the increasing flexural modulus of composite samples. Also, the higher area under force-time curves of GnP modified samples suggest better energy absorption capacity of composite samples. In addition, unmodified/modified glass fiber reinforced epoxy samples did not withstand the impact load of 30J showing the characteristics of penetration and perforation as seen in force histories in Figures 5.5(a) and 5.6(a).

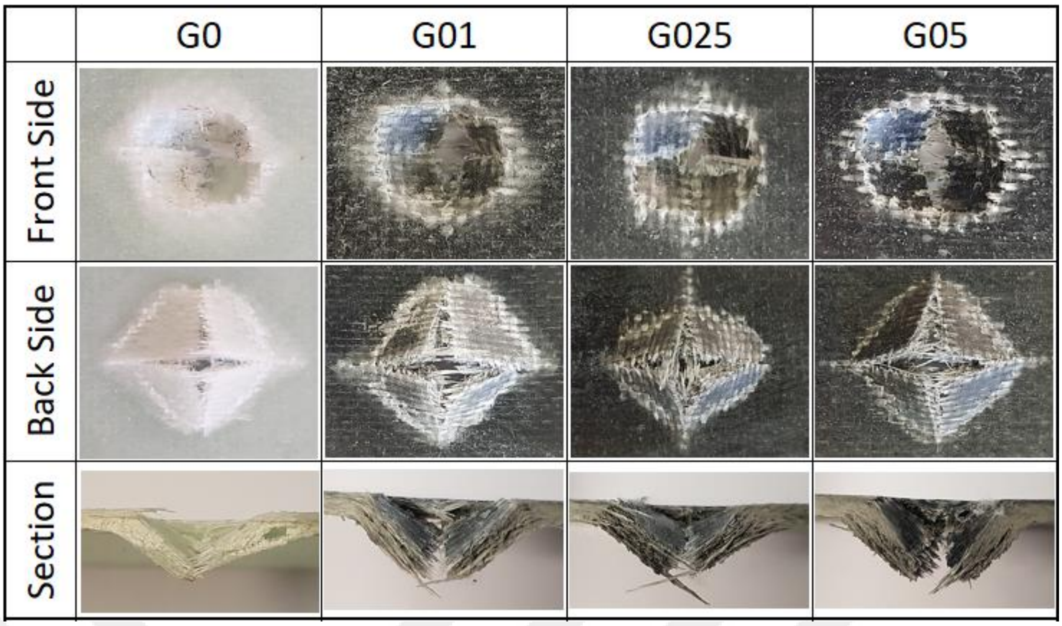

Figure 5.4 Photos of glass fiber reinforced composite samples with various GnPs content after drop weight impact.

5.2.2.1 Glass / Aramid Fiber Reinforced Composite

The impact test results for unmodified/modified glass/aramid fiber reinforced composite samples are presented in Figures 5.5-5.6 and Table 5.2. Peak load and absorbed energy values were recorded as 3.28 kN and 19.77 J in GA0, 3.01 kN and 21.36 J in AG0, 3.27 kN and 29.91 J in A0 unmodified composite samples. Decreasing absorbed energy values were seen in aramid fiber reinforced composite samples with increasing GnPs content similar to the flexural behavior of GnPs modified aramid composite samples. On the other hand, enhanced absorbed energy value were recorded in modified hybrid fiber composite samples. In the presence of 0.25 wt% GnPs, hybrid composites GA025 and AG025 showed the highest peak load and absorbed energy values as 3.48 kN and 23.62 J, 3.31 kN and 22.24 J respectively. With further GnPs addition after 0.25 wt% of GnPs, a decreasing trend was observed for impact strength values. This may be due to the agglomeration of nanoparticles in the epoxy matrix and the behavior of these areas as crack initiation/progression points. Also, it is expected that, the poor fiber- matrix interfacial bonding leads to a low peak load which indicates the damage initiation energy [67]. In contrast to the AG025 sample, the GA025 sample showed a longer impact duration. This progressive load drop and longer impact duration show the higher and continuing energy absorption of the composite sample.

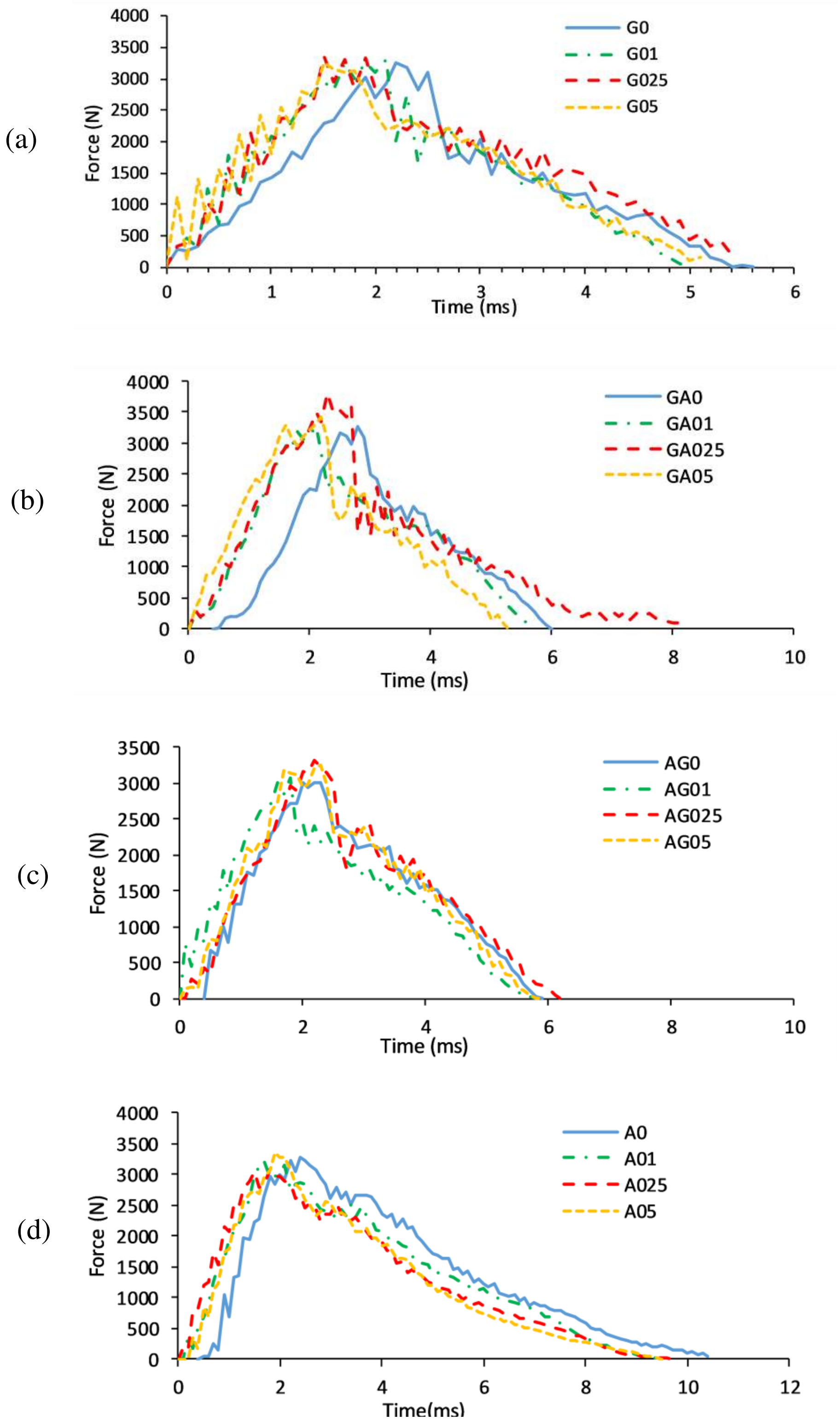

Figure 5.5 Force-time history of hybrid/non-hybrid glass/aramid fiber reinforced composite samples with various GnPs addition.

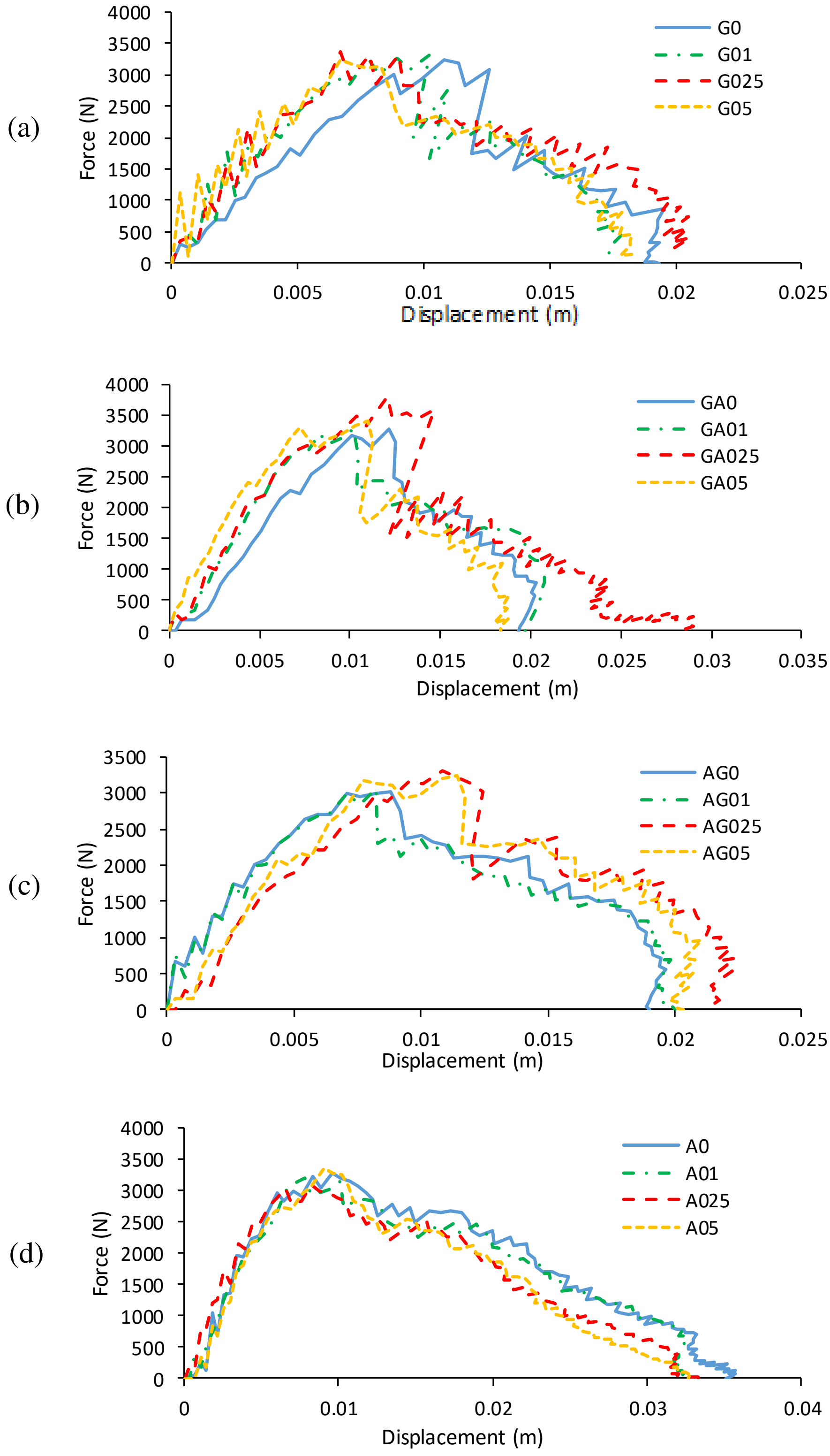

Figure 5.6 Force-displacement history of hybrid/non-hybrid glass/aramid fiber reinforced composite samples with various GnPs addition.

Table 5.2 Key characteristics of different composite configurations under LVI loading.

Sample code	Peak load (kN)	Maximum displacement (mm)	Absorbed energy (J)
G0	3.25±0.01	19.57±1.0	19.32±0.1
G01	3.31±0.03	17.87±0.2	19.90±0.5
G025	3.36±0.02	20.61±1.0	21.10±0.4
G05	3.24±0.03	18.43±1.0	20.50±0.2
GA0	3.28±0.01	20.28±0.3	19.77±0.4
GA01	3.28±0.03	21.00±0.4	21.45±0.4
GA025	3.48±0.02	29.00±0.2	23.62±0.3
GA05	3.42±0.04	18.80±0.5	21.09±0.6
AG0	3.01±0.02	19.62±1.0	21.36±0.4
AG01	3.07±0.01	20.02±0.6	20.80±0.5
AG025	3.31±0.02	22.38±0.8	22.24±0.3
AG05	3.25±0.04	21.08±0.5	22.03±0.6
A0	3.27±0.02	35.71±0.4	26.91±0.3
A01	3.21±0.04	32.95±0.4	26.45±0.3
A025	3.08±0.03	33.30±0.5	25.73±0.4
A05	3.35±0.05	32.95±0.3	25.06±0.6

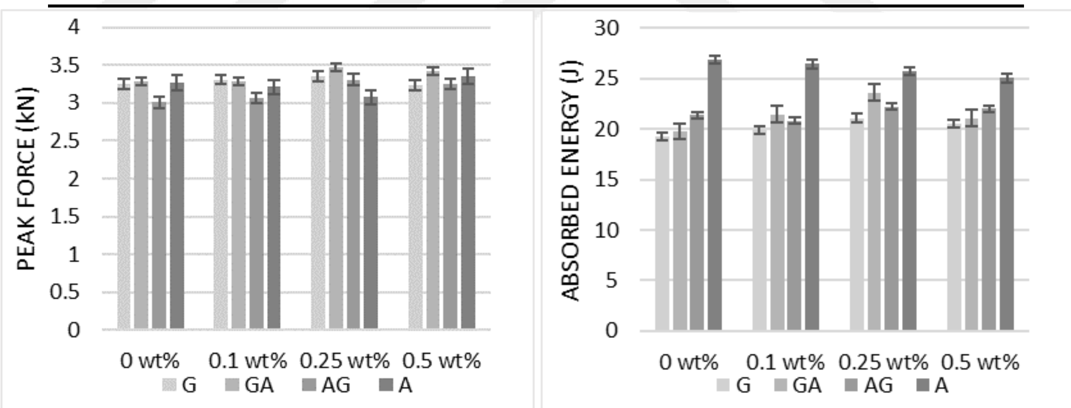

Figure 5.7 Comparison of key characteristics of glass/aramid fiber reinforced composites subjected to drop-weight impact test.

Figure 5.8 illustrates the results of the damaged sections of the modified/unmodified composite samples with subjecting a constant impact energy of 30J. It was found that addition of GnPs into the glass/aramid composite samples resulted in irregular damage modes in the form of back surface splitting, and the decrease in the depth of the dent was observed at the rate of GnPs addition at maximum force values. According to Aktaş et al. [51] fiber rupture and delamination failures are the main energy absorption mechanisms of the glass and aramid fiber reinforced composites.

In accordance with this suggestion, it can clearly be seen the fiber rupture on the impacted as well as the non-impacted sides of the laminates. On the other hand, delamination failure was visible on the A and hybrid samples with low GnPs contents (0 and 0.1 wt%). But delamination can be clearly seen on the interior layer in the sectional photos of composite samples. In the modified and unmodified G and hybrid samples, splitting between fiber/matrix and fiber ruptures on non-impacted side was observed. Despite the high impact strength of aramid fibers, a permanent indentation was also observed in A sample. In addition, it was observed that the damage observed in samples G025, GA025, AG025, where the absorbed energy increased, was in a smaller area than the damage observed in the impacted side of samples produced at the other GnPs concentration. This is an indication that the ability of GnPs to absorb and dissipate impact energy through thickness of the laminates. It is also an indication that GnPs improves the fiber / matrix interface bond in the composite sample.

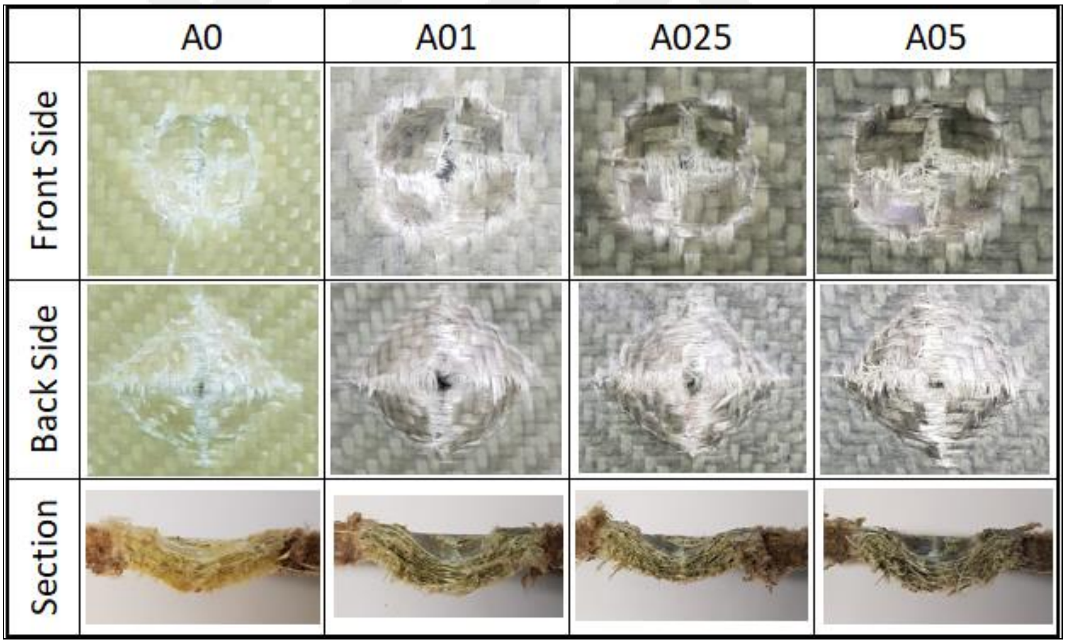

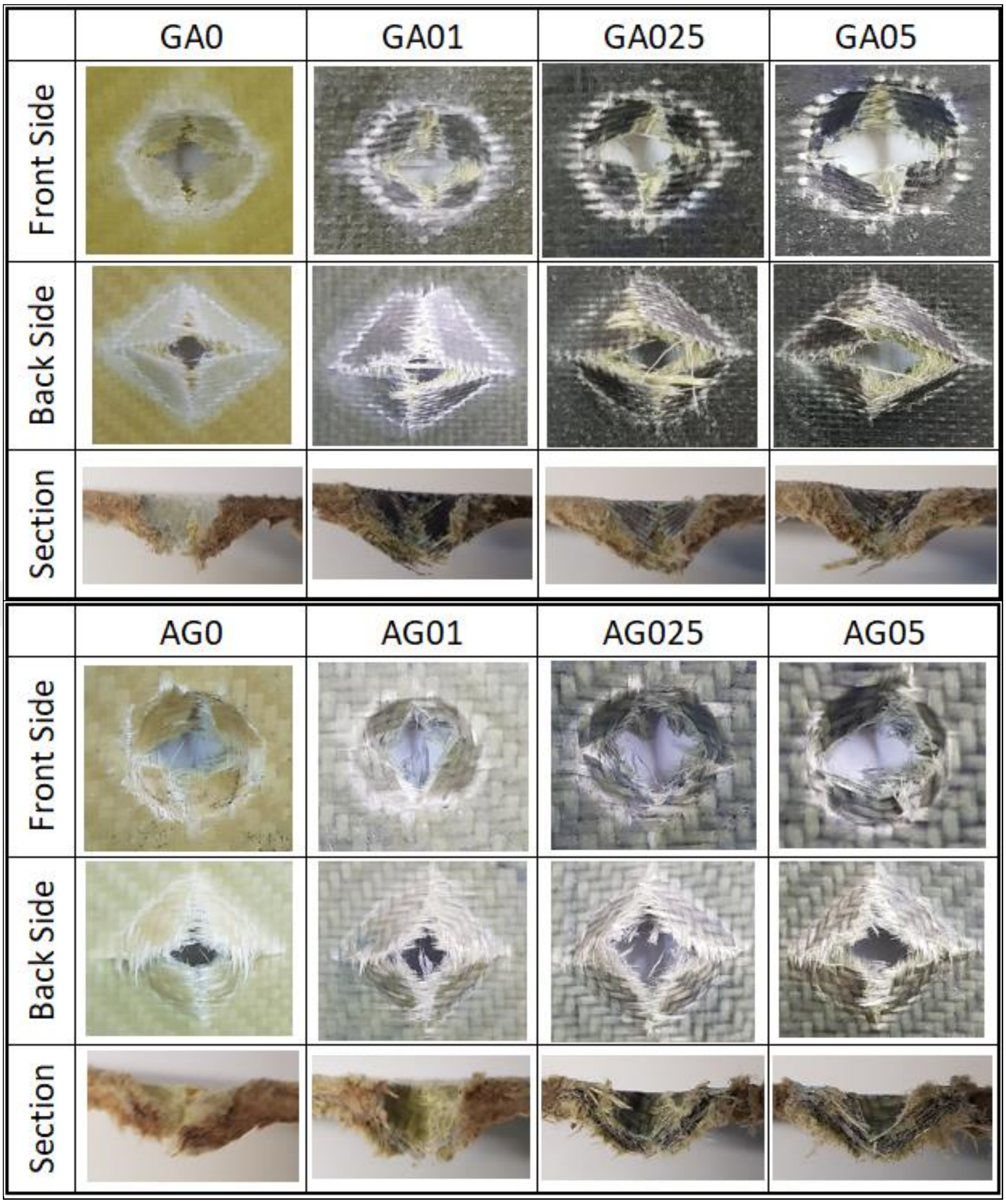

Figure 5.8 Photos of glass/aramid fiber reinforced composite samples with various GnPs content after drop weight impact.

5.2.2.2 Glass / Basalt Fiber Reinforced Composite

Peak load, absorbed energy and maximum displacement values were summarized in Table 5.3. Figures 5.9-5.10 illustrate the force-time and force-displacement histories of different stacking sequenced glass (G), basalt (B) non-hybrid/hybrid fiber reinforced composites with respect to GnPs filler content at 30 J. Peak load and absorbed energy values fiber reinforced unmodified epoxy composites were recorded as 3.15 kN and 22.7 J in GB0, 1.36 kN and 16.8 J in BG0, 1.91 kN and 17.36 J in B0 unmodified composite samples. Increasing peak load and absorbed energy values were recorded with the addition of GnPs until 0.25wt% in GB hybrid sample and 0.1wt% in BG and B composite samples. These results indicate that the fiber type on the outer surfaces of the hybrid composite samples predominates in the impact strength of the material. Thus, GnP filled hybrid samples with maximum impact strength, similar to G025 and B01 samples, were GB025 and BG01 samples compared to the same hybrid configurations. The percentage improvement in peak load and absorbed energy values were recorded as 15.87% and 10.57% in GB025, 13.97% and 20.9% in BG01, 11.0% and 11.17% in B specimens. With further GnPs addition after 0.1 wt % of GnPs, a decreasing trend was seen for impact strength values due to the agglomeration of nanoparticles in the epoxy matrix.

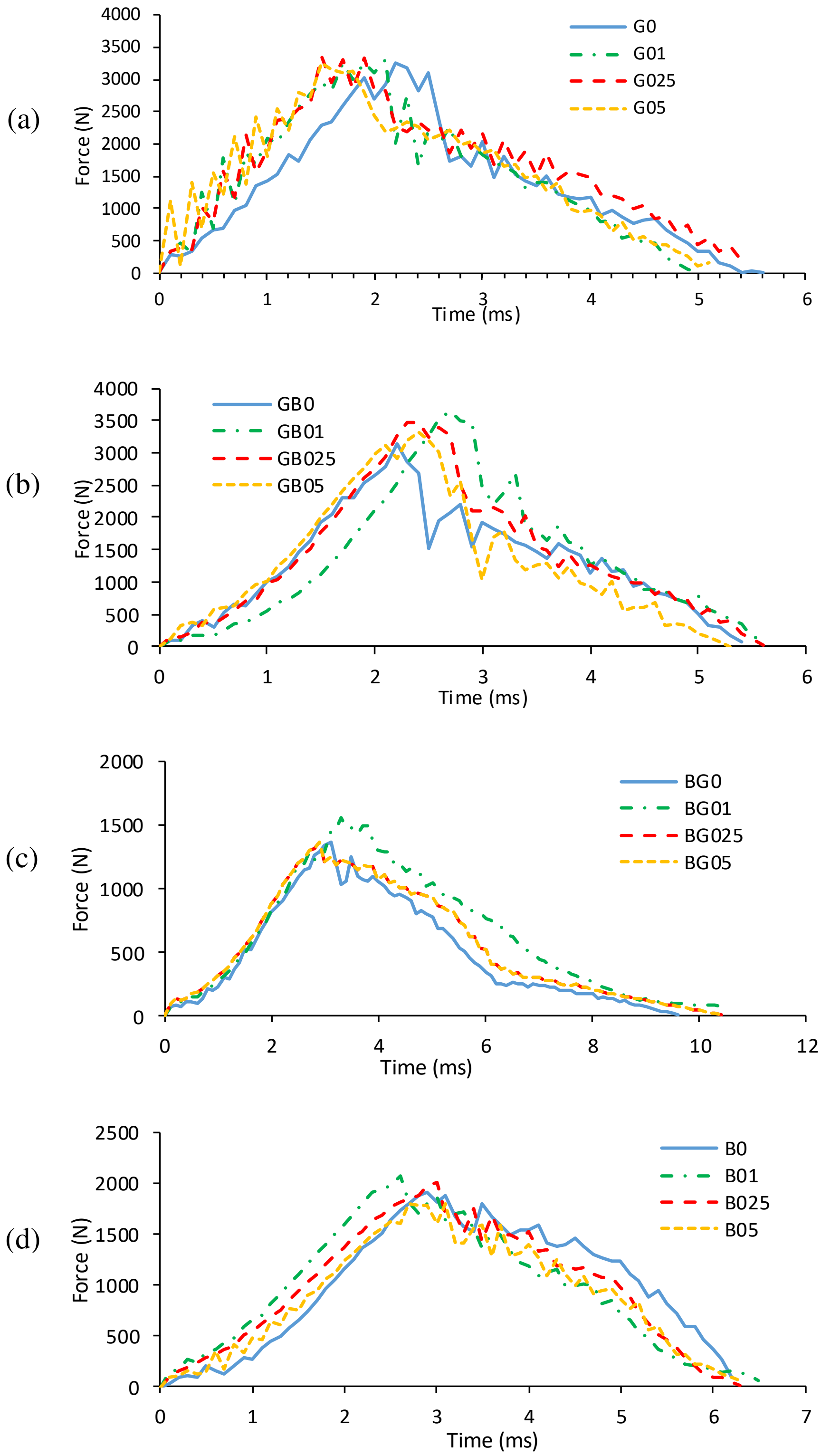

Figure 5.9 Force-time history of hybrid/non-hybrid glass/basalt fiber reinforced composite samples with various GnPs addition.

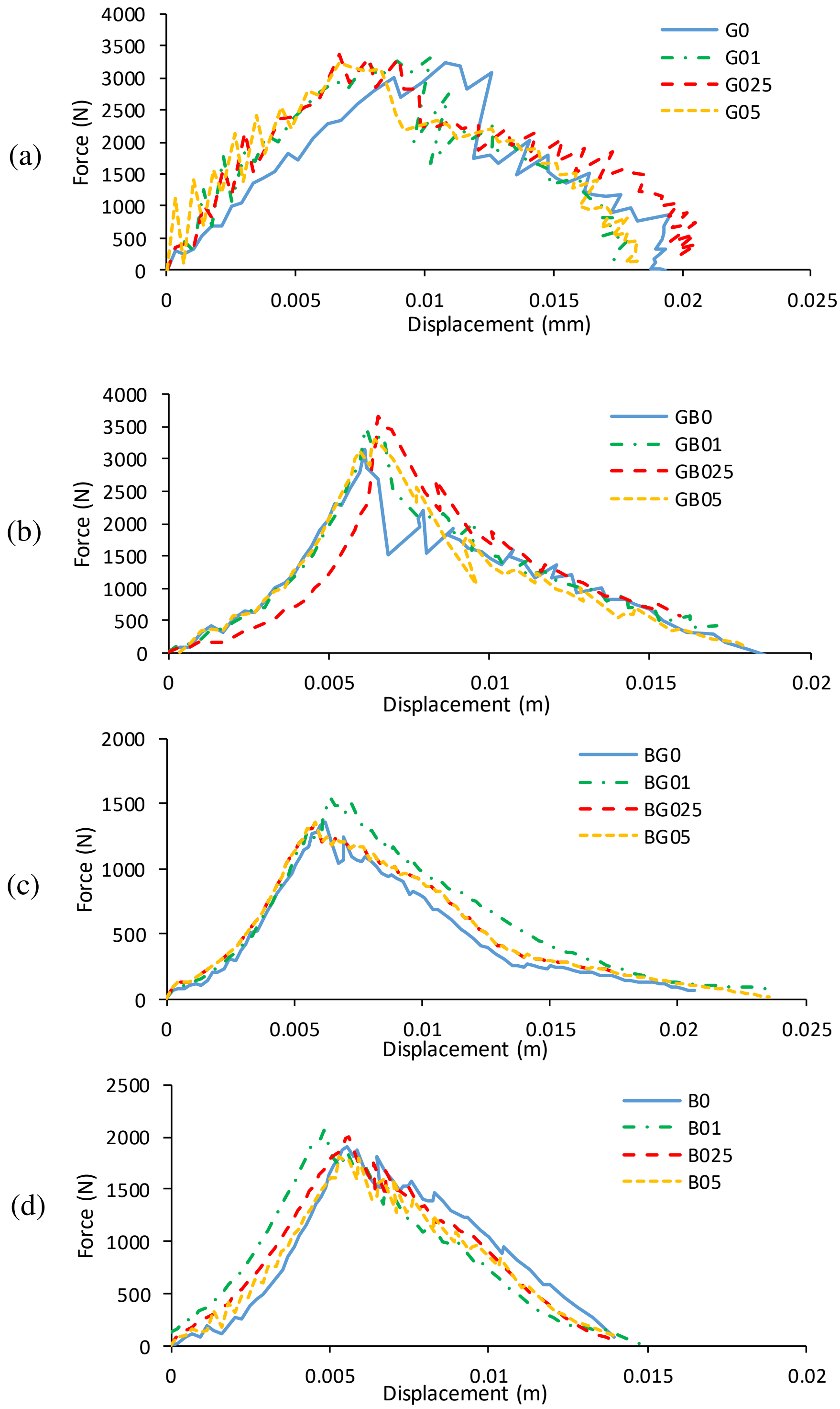

Figure 5.10 Force-displacement history of hybrid/non-hybrid glass/basalt fiber reinforced composite samples with various GnPs addition.

Table 5.3 Key characteristics of different composite configurations under LVI loading.

Sample code	Peak load (kN)	Maximum displacement (mm)	Absorbed energy (J)
G0	3.25±0.01	19.57±1.0	19.32±0.1
G01	3.31±0.03	17.87±0.2	19.90±0.5
G025	3.36±0.02	20.61±1.0	21.10±0.4
G05	3.24±0.03	18.43±1.0	20.50±0.2
GB0	3.15±0.01	18.65±0.3	22.7±0.4
GB01	3.48±0.02	19.38±0.4	23.7±0.3
GB025	3.65±0.03	19.43±0.3	25.1±0.4
GB05	3.31±0.04	18.02±0.2	22.6±0.6
BG0	1.36±0.02	18.65±0.8	16.8±0.4
BG01	1.55±0.01	20.02±0.6	20.3±0.5
BG025	1.48±0.02	22.38±0.8	17.3±0.3
BG05	1.36±0.04	21.08±0.5	17.28±0.6
B0	1.91±0.02	10.47±0.2	17.36±0.3
B01	2.12±0.04	11.15±0.4	19.3±0.3
B025	2.07±0.03	10.61±0.3	19.1±0.4
B05	1.63±0.05	10.52±0.5	16.8±0.6

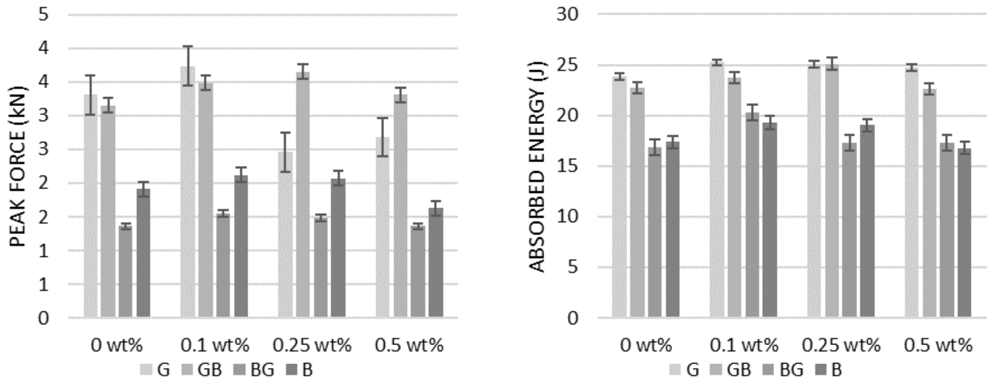

Figure 5.11 Comparison of key characteristics of glass/basalt fiber reinforced composites subjected to drop-weight impact test.

Figure 5.12 illustrates damaged sections of the modified/unmodified glass/basalt composite samples with subjecting a constant impact energy of 30J. Various damage modes were observed by means of delamination, matrix cracking and fiber rupture type. All laminates were perforated locally around the impactor revealing the several of damage modes over the front and back surfaces such as penetration, back surface splitting, fiber pull outs, delamination of layers. Visual observations show that on the impacted surface of BFR samples cross-shaped cracks are formed through warp-weft directions. It can be seen from photos in Figure 5.12 that BFR samples has shown direct perforation until with the 30 J impact energy. Hybrid laminates were exhibited the damage modes as the combination of G and B fiber reinforced composite samples. In addition, the fibers on the outer surfaces played a dominant role on the impact behavior of hybrid composites. Additionally, it was also observed that the damaged area was increased after the 0.1wt% and 0.25wt% of GnPs, and this could be attributed to the facts of reduction in fiber / matrix interfacial bonding for which impact damage of composite materials was directly depended on fiber/matrix and filler/matrix bonding [16, 81].

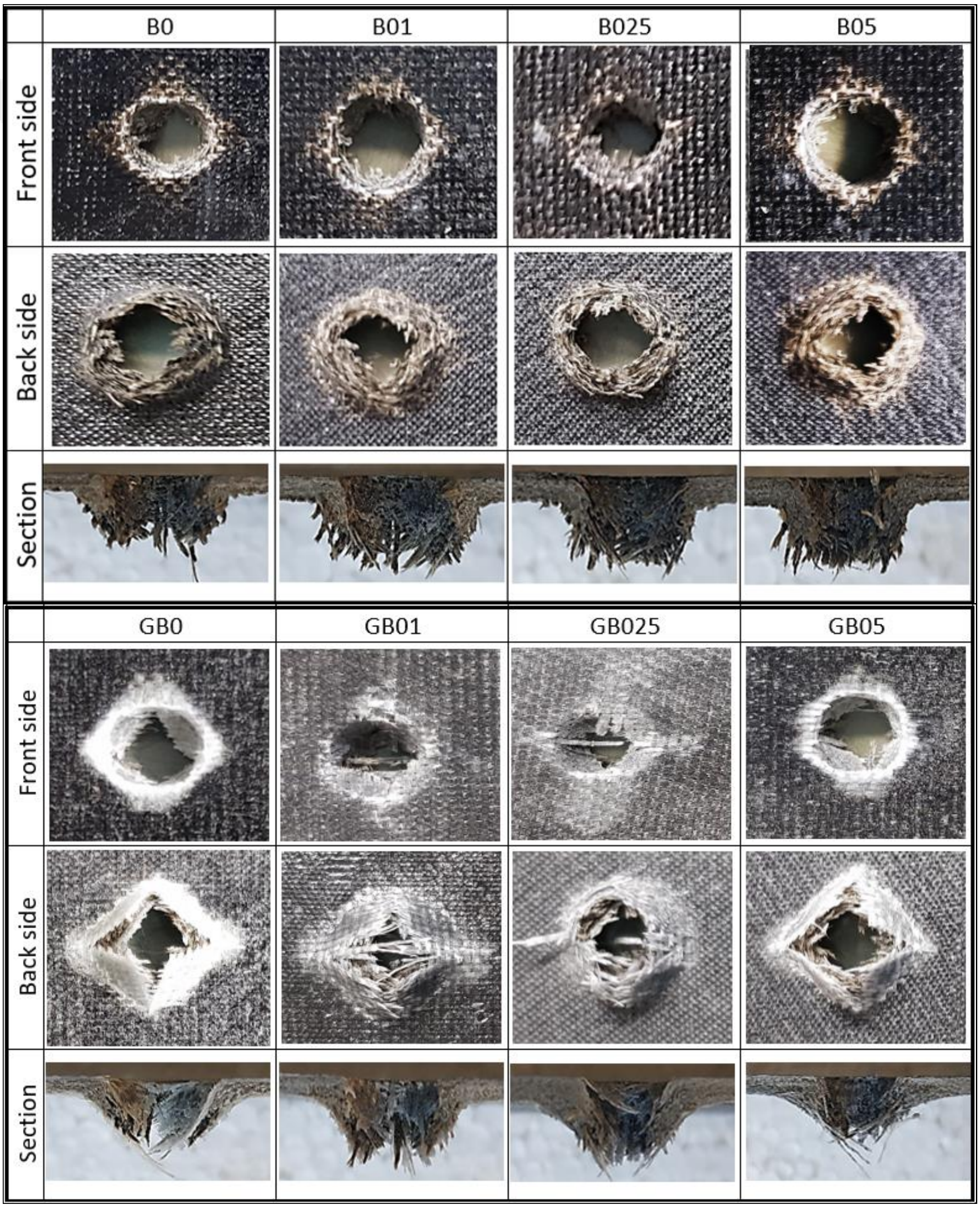

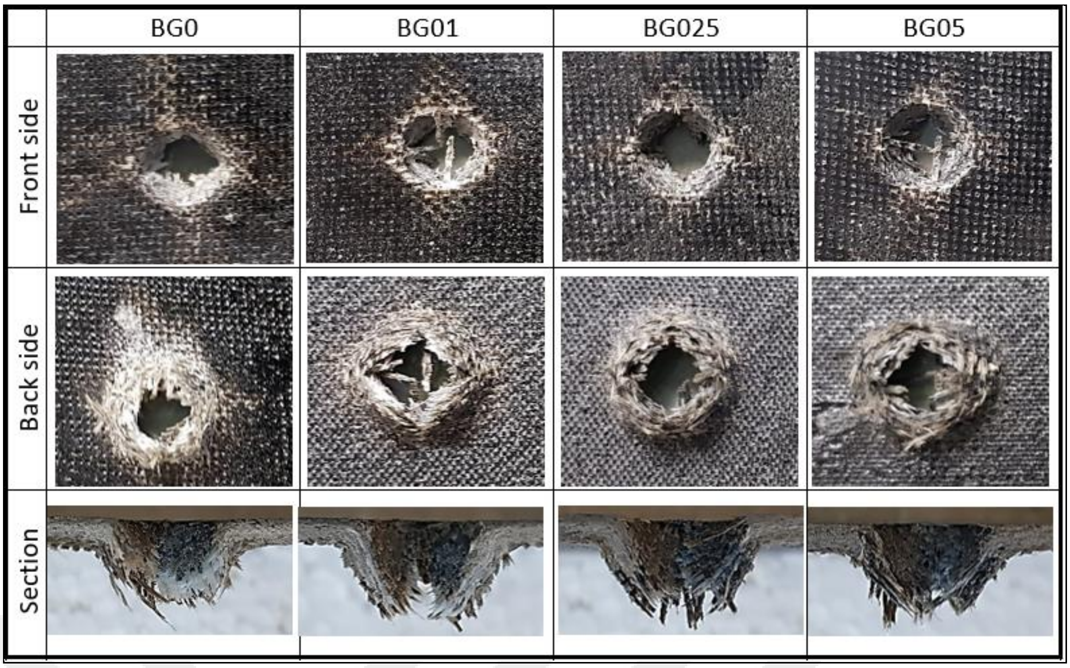

Figure 5.12 Photos of glass/basalt hybrid fiber reinforced composite samples with various GnPs content after drop weight impact.

5.2.2.3 Glass / Carbon Fiber Reinforced Composite

Addition of GnPs significantly influenced force-time histories especially for hybrid samples (CG configurations). C01 composite sample showed the highest peak load compared with other samples indicating that GnPs content of 0.1 wt % was the optimum value for better impact resistance of unmodified carbon/epoxy composites. For the hybrid samples when carbon fabrics were at outer layers (CG), an addition of GnPs content into the epoxy resin increased the overall impact duration, and maximum impact duration was recorded at the hybrid sample of CG01. However, further increasing of GnPs content to the 0.5 wt. % reduced the impact duration implying the poor interfacial strength of GnPs particles and epoxy matrix.

Force-displacement histories of the GnPs modified and unmodified samples were illustrated in Figure 5.14, and their maximum forces with absorbed energy values were comparatively shown in Figure 5.13 and Table 5.4. It was recorded that incorporation of GnPs into the hybrid samples significantly increased the impact resistance of the samples with increasing energy absorption capacity. Unmodified/modified glass/epoxy and hybrid samples did not withstand the impact load of 30J showing the characteristics of penetration and perforation, while unmodified and modified carbon/epoxy samples showed a small rebound after the impact revealing with penetration of the impactor into the sample. Additionally, it can be stated that the degree of recovery during the load release after the maximum load was the highest for the sample of C05 indicating the better impact resistance compared with other samples in this configuration.

It is clear from Figure 5.13 and Table 5.4 that GnPs addition significantly affects the force variation and absorbed energy values. Incorporation of GnPs particle at 0.1 wt % into the carbon/epoxy samples contributed the highest peak load and absorbed energy, with 14.5% and 1.06 % improvements, respectively. For carbon/epoxy samples, absorbed energy values were decreased after a slight improvement with addition of GnPs into the epoxy indicating reduction of impact resistance, and this can be attributed the poor load transfer between particles and matrix as a result of particle agglomeration. For hybrid samples, sample of GC05 showed the highest peak load while sample of CG025 showed the highest absorbed energy indicating a better functionalization of GnPs particles with epoxy resin and fibers.

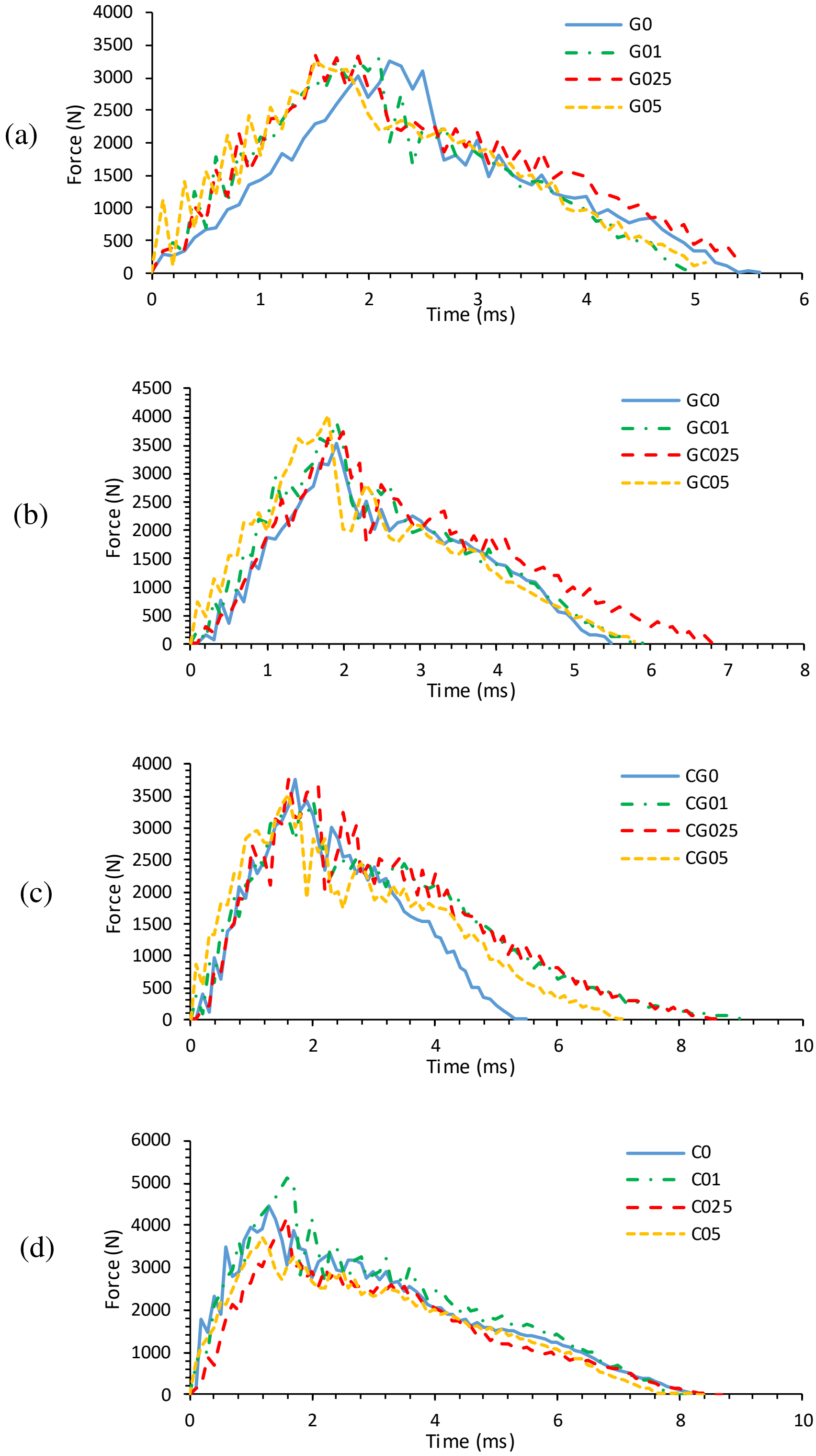

Figure 5.13 Force-time history of hybrid/non-hybrid glass/carbon fiber reinforced composite samples with various GnPs addition.

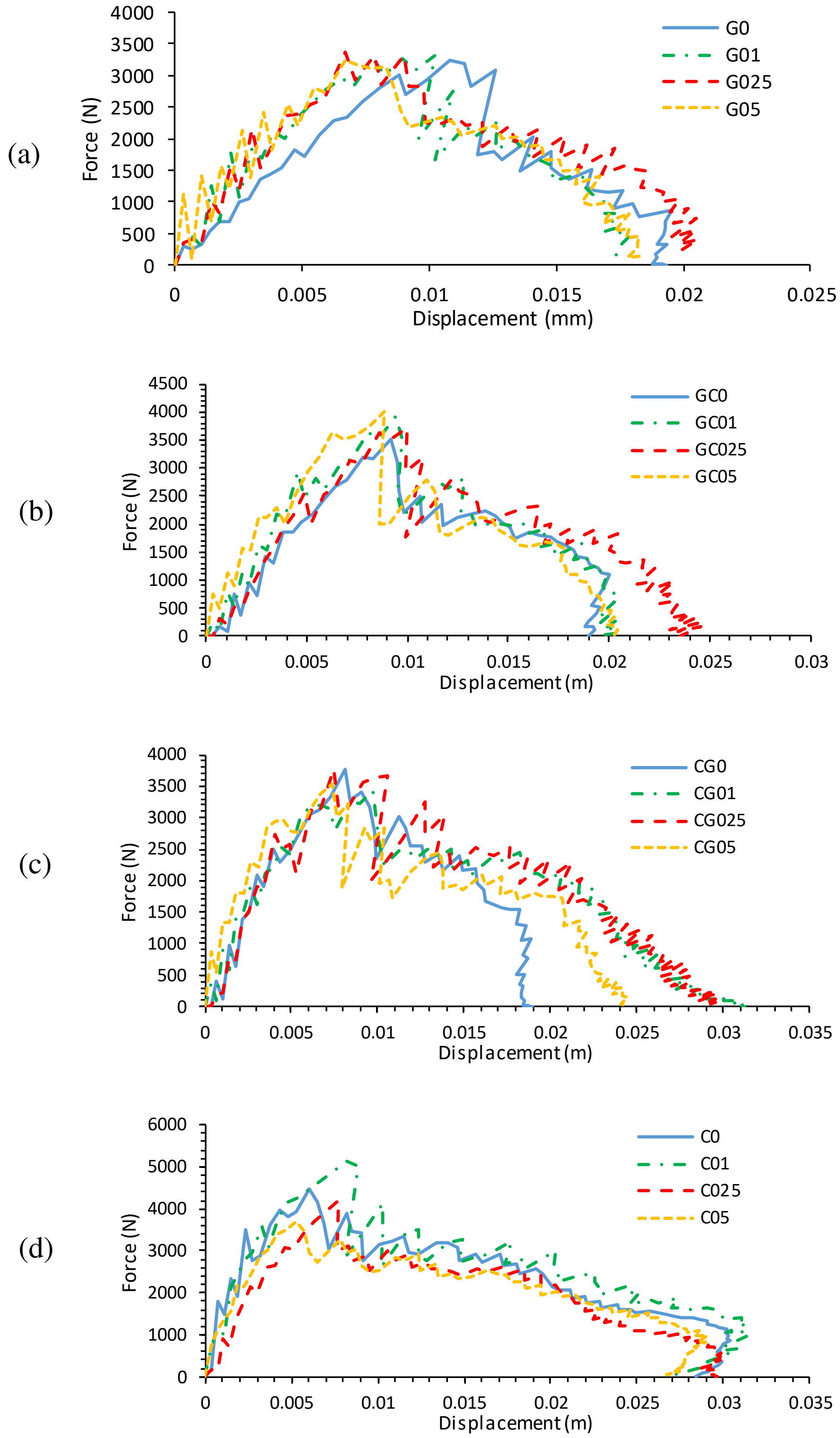

Figure 5.14 Force-displacement history of hybrid/non-hybrid glass/carbon fiber reinforced composite samples with various GnPs addition.

Table 5.4 Key characteristics of hybrid/non-hybrid glass/carbon fiber reinforced composite samples with various GnPs content.

Sample code	Peak load (kN)	Maximum displacement (mm)	Absorbed energy (J)
G0	3.25±0.01	19.57±1.0	19.32±0.2
G01	3.31±0.03	17.87±0.2	19.90±0.2
G025	3.36±0.02	20.60±1.0	21.10±0.2
G05	3.24±0.03	18.43±1.0	20.50±0.2
GC0	3.52±0.02	20.02±0.4	20.74±0.2
GC01	3.90±0.03	20.70±0.5	22.52±0.2
GC025	3.73±0.02	24.57±1.0	23.38±0.2
GC05	4.02±0.03	20.44±0.6	22.53±0.2
CG0	3.42±0.10	18.99±0.3	22.16±0.2
CG01	3.43±0.02	31.30±0.8	25.62±0.2
CG025	3.75±0.03	29.63±1.0	25.91±0.2
CG05	3.53±0.02	24.49±1.0	24.38±0.2
C0	4.46±0.02	30.35±1.0	28.36±0.2
C01	5.11±0.02	31.46±0.6	28.67±0.2
C025	4.19±0.01	30.03±0.5	26.85±0.2
C05	3.70±0.03	29.05±0.5	27.25±0.2

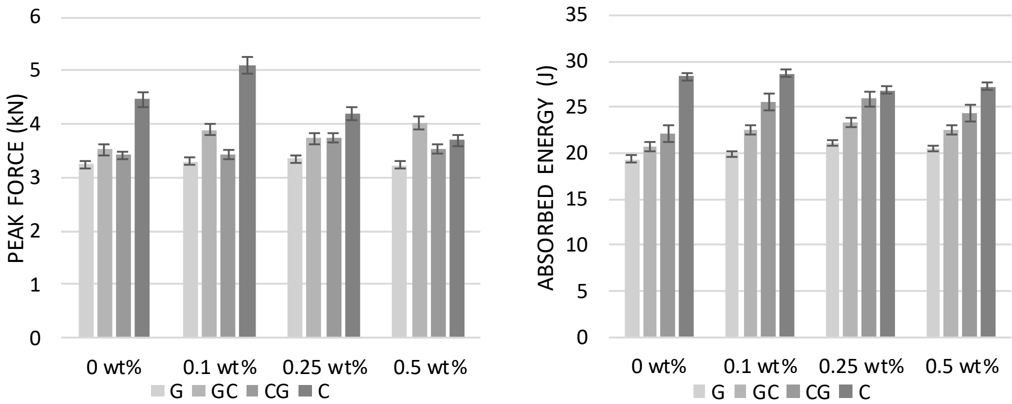

Figure 5.15 Comparison of key characteristics of glass/carbon fiber reinforced composites subjected to drop-weight impact test.

Figure 5.16 illustrates the results of the damaged sections of the GnPs modified/unmodified composite samples with subjecting a constant impact energy of 30J. It was found that addition of GnPs into the composite samples resulted in irregular damage modes in the form of butterfly-type, and depth of the dent was decreased with inclusion of GnPs at 0.1 wt%. Several samples showed the elliptical damage forms around the impacted region such as G01, G025, G05 and CG25. However, modified and unmodified carbon/epoxy samples showed a circular damage with high amount of penetration and indentation without perforation. In addition, fiber ruptures and depth of the dent were decreased with incorporation of GnPs particles at 0.1 wt. % even though delamination between layers were much more than other GnPs particle loadings, with implying that the amount of energy dissipated along the in-plane shear directions was increased. Damage modes around the impacted surfaces of the hybrid samples showed that position of carbon and glass fabrics was highly effective on damaged areas as well as impact resistance. In the case of carbon fabrics were stacked at the outer layers, only sample of CG01 samples showed the perforation, and other samples behaved the better impact resistance without perforation evenly occurring indentation and penetration [81]. For the sample of GC01, fiber ruptures were much more than other hybrid samples indicating more dissipation of impact energy along the in-plane and impact directions, and similar behavior was seen at the samples of CG01 sample.

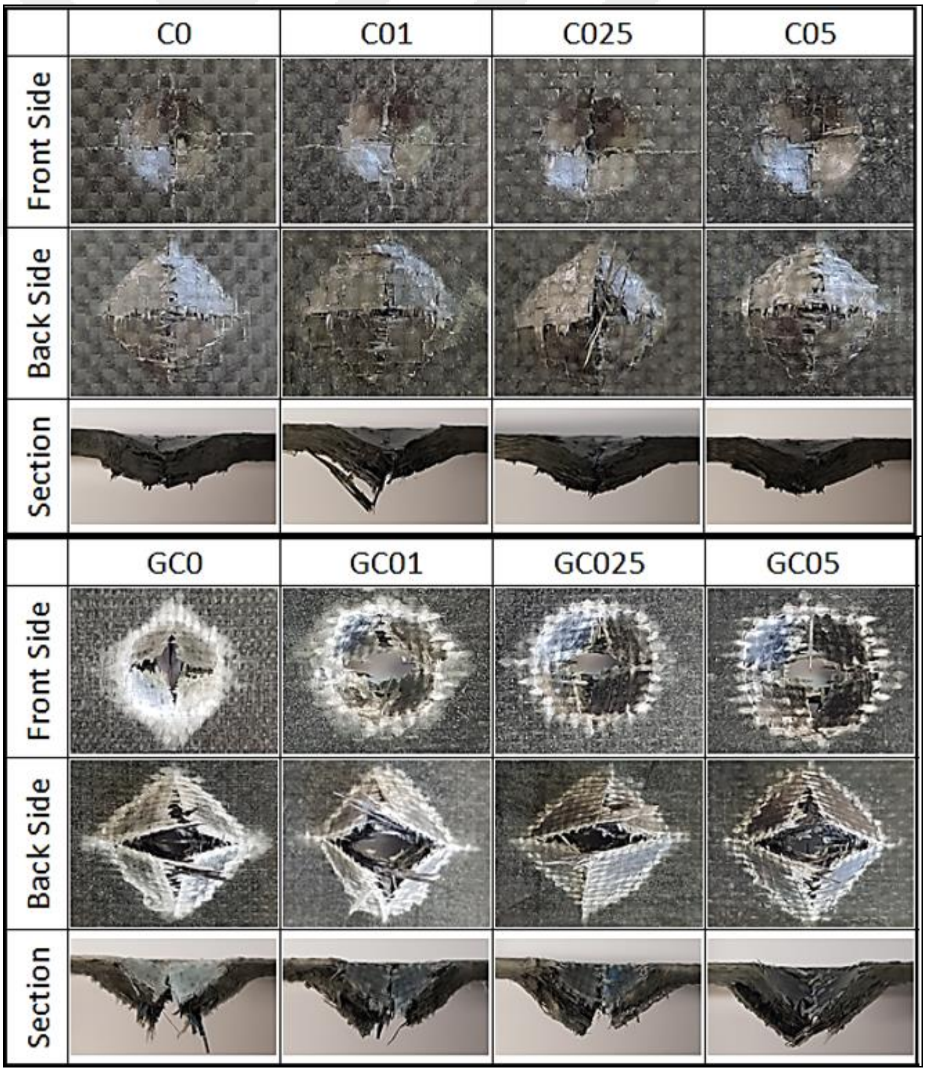

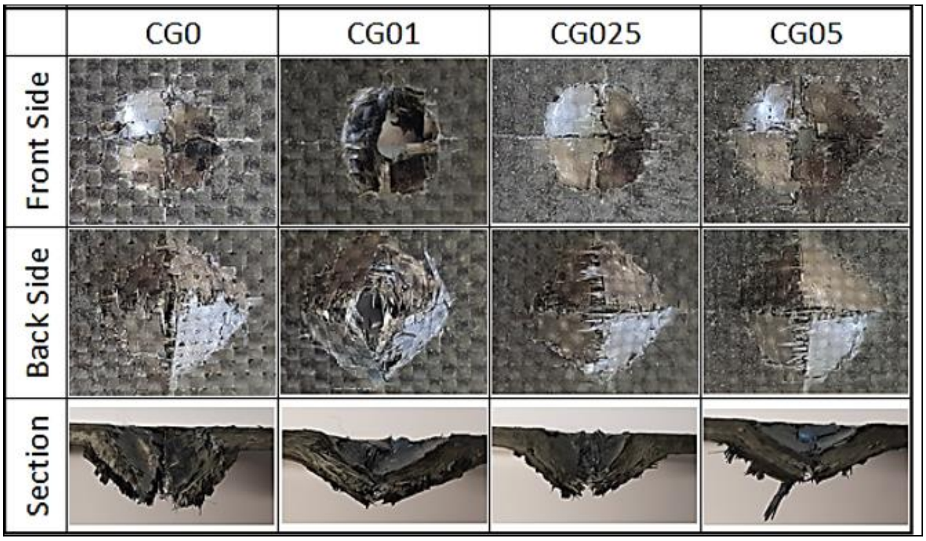

Figure 5.16 Photos of glass/carbon fiber reinforced composite samples with various GnPs content after drop weight impact.

5.3 Damage Characterization by Scanning Electron Microscopy

In order to examine the micro-mechanical properties of GnPs addition of composite samples, impacted surfaces were observed by SEM imaging technique.

In Figures 5.17-5.19, fracture photographs of GnPs modified/unmodified composite samples are given for all fiber configurations. As can be seen from the photographs, it has been found that GnPs additive directly affects the fiber / matrix interface bonding and also the load transfer between the phases. When the photographs of the composite plates produced with pure epoxy are examined, it is seen that the fibers are easily separated from matrix with a clear interfacial rupture, and this is thought to be caused by poor fiber / matrix interfacial bonding. It is also understood that the fibers are easily separated from the matrix due to the weak fiber / matrix bond [110]. On the other hand, in GnPs modified samples, the fibers are hardly removed from the epoxy matrix during plate damage and have large amounts of epoxy matrix residues on them.

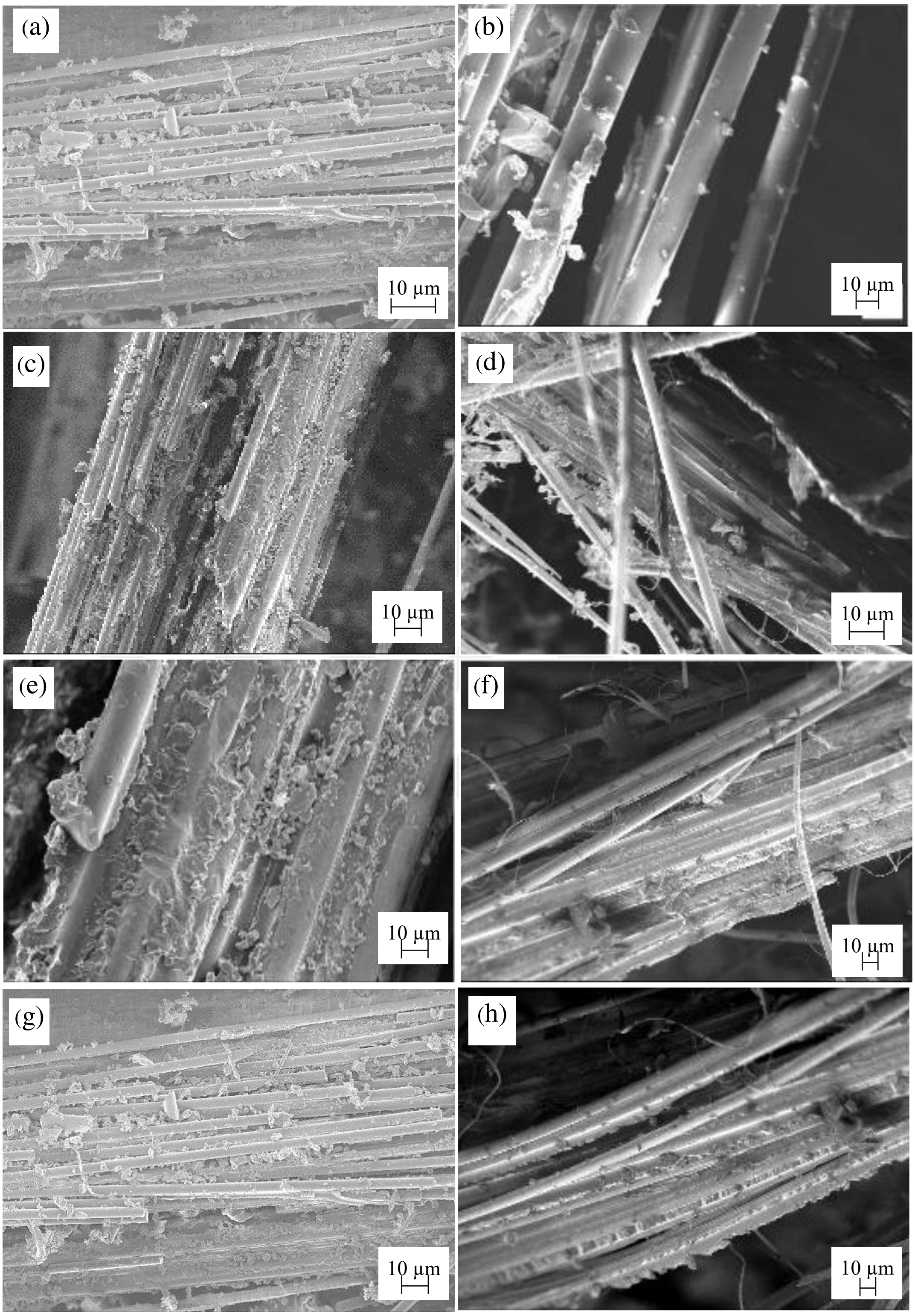

Figure 5.17 SEM micrograph of glass / aramid reinforced hybrid / non-hybrid composite samples; (a)G0, (b)G025, (c)GA0, (d) GA025, (e)AG0, (f)AG025, (g)A0, (h)A05.

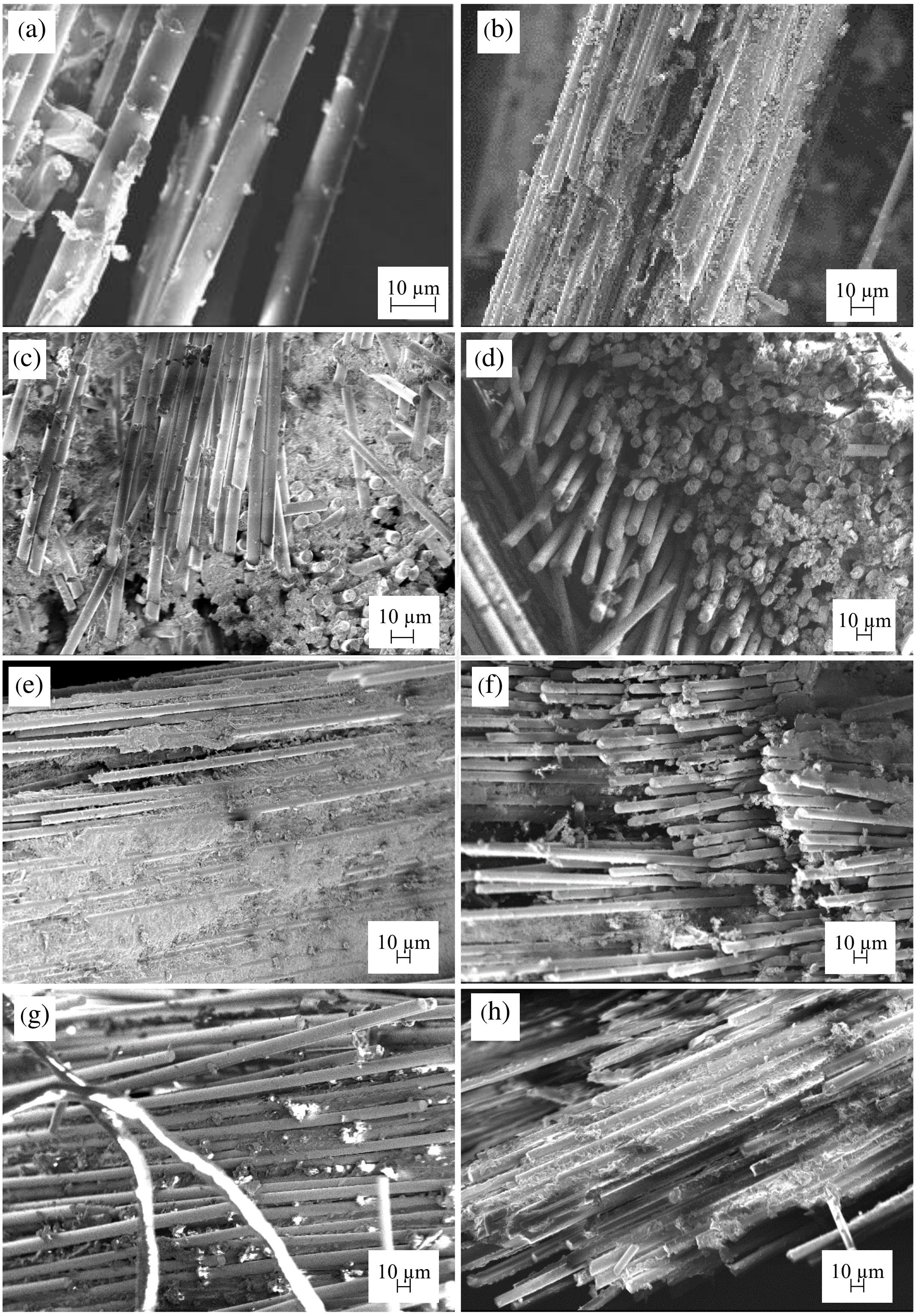

Figure 5.18 SEM micrograph of glass / basalt reinforced hybrid / non-hybrid composite samples; (a)G0, (b)G025, (c)GB0, (d) GB025, (e)BG0, (f)BG01, (g)B0, (h)B01.

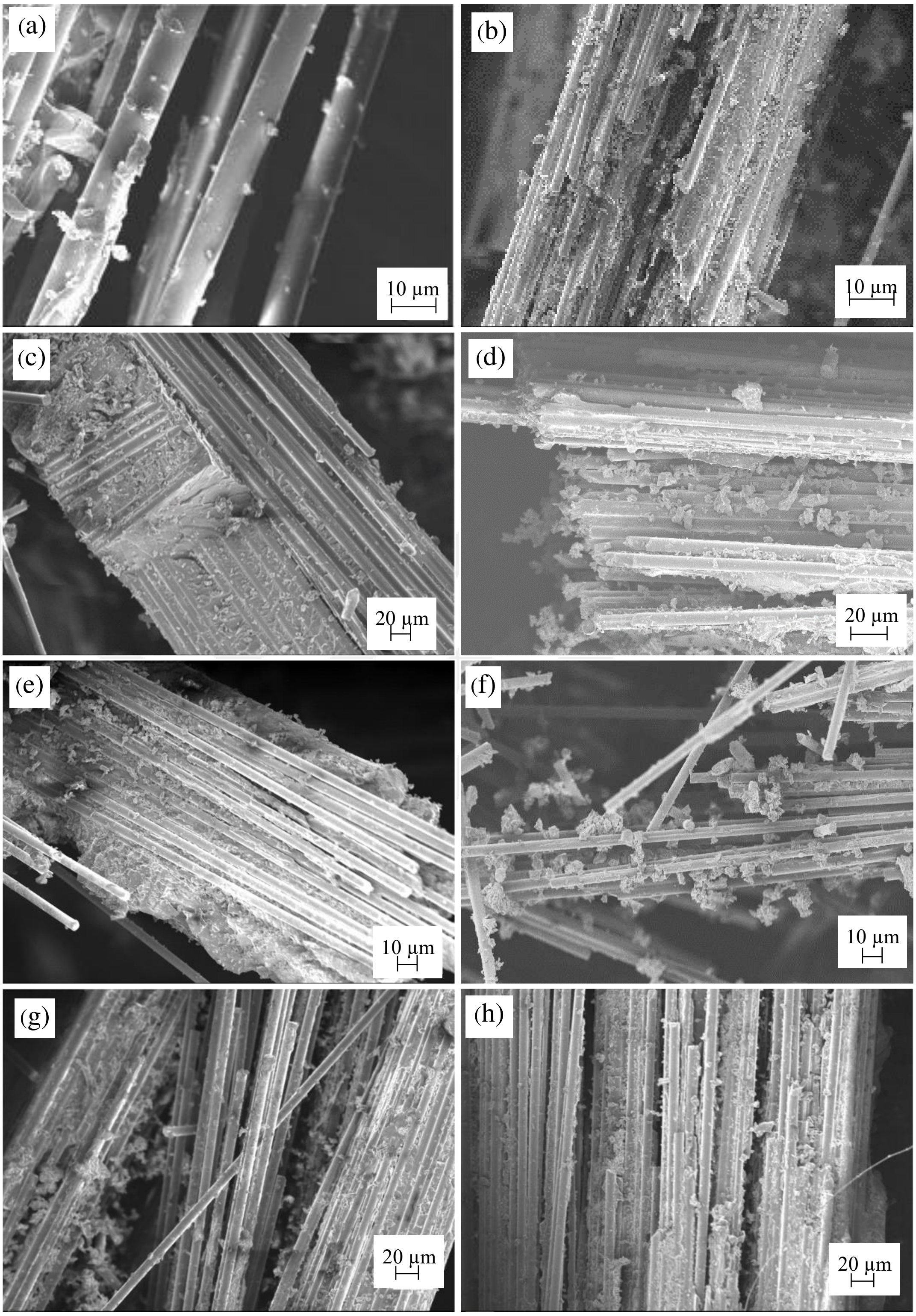

Figure 5.19 SEM micrograph of glass / carbon reinforced hybrid / non-hybrid composite samples; (a)G0, (b)G025, (c)GC0, (d) GC025, (e)CG0, (f)CG025, (g)C0, (h)C01.

CHAPTER 6

CONCLUSIONS

Low velocity impact and mechanical behavior of fiber reinforced polymer composites were investigated under the effects of fiber hybridization and nano particle addition. Hybrid / non-hybrid fiber-reinforced composite plates were designed and fabricated by adding various weight content of GnPs to the epoxy polymer matrix. LVI, tensile and flexural behaviors of the composite laminates were investigated according to the effect of fiber hybridization and matrix modification. Based on the experimental results of the current study, following conclusions can be summarized:

- Fiber hybridization directly affects the tensile properties of the fiber reinforced composites. According to the tensile test results, hybrid fiber reinforced composite plates have tensile strength values between the values of the single fiber reinforced composite plates that form the hybrid structure.
- It can be said that the fabric stacking sequence of the composite plates affects the tensile strength of the hybrid composite structure, and when the high tensile strength fabric was placed on the outer surface, high tensile strength can be achieved in the hybrid structure.
- Maximum improvements in tensile strength of hybrid fiber reinforced unmodified composite plates were obtained with AG, GB and, GC samples with 9.97%, 17.56% and, 67.7%, respectively.
- When the effect of GnPs addition on the tensile properties of composite material is examined, it is observed that the small amount of GnPs additive significantly affects the tensile strength of the produced composite materials. However, excessive GnPs loading creates a reverse effect on the tensile strength and modulus with a decreasing trend.
- It is concluded from results that the 0.1 wt% content of GnPs slightly increases the tensile strength by 6.1% in glass fiber (G), 6.5% in aramid fiber

- (A) and 1.67% in basalt fiber (B) reinforced composite samples. On the other hand, the tensile strength of carbon fiber (C) reinforced composite plates was increased with the increased GnPs filler content and 10.2% improvement was achieved with 0.5wt% GnPs.
- It was seen that 0.1 wt% GnPs content causes an increase in tensile strengths of GA and AG hybrid composites with 6.5% and 5.3%. Also, the tensile strength values were increased by 10% in GB and 24.36% in BG with 0.1 wt% GnPs addition.
- Additionally, improvement in tensile strength values of hybrid glass/carbon composites were reached with different filler contents. Maximum improvement was recorded as 3.63% in CG with 0.1 wt% and 1.5% in GC with 0.5 wt% of GnPs content.
- Based on flexural test results, the flexural strength and modulus values were found as the highest in the carbon fiber (C) and the lowest in basalt fiber (B) reinforced unmodified composite plates.
- It was found that fiber hybridization directly affects the flexural properties of the fiber reinforced composites. When higher flexural strength fabric was placed on the outer surface, hybrid composite structure was reached higher flexural strength.
- Maximum improvements in flexural strength of hybrid fiber reinforced unmodified composite plates were reached in GA, GB and, GC samples with 38.42% compared to A, 142.7% compared to B and, 28.72% compared to G, respectively.
- When the effect of GnPs addition on the flexural properties of composite material is examined, it was observed that GnPs additive significantly affects the flexural strength of the produced composite materials. However, excessive GnPs loading created a reverse effect on the flexural strength and modulus with a decreasing trend likewise in tensile properties.
- The flexural strength and modulus of glass fiber reinforced unmodified epoxy composites (G0) were clearly exhibited the highest value at GnPs content of 0.25 wt% with indicating 14% and 16% improvement, respectively.

- The flexural strength and modulus of basalt fiber reinforced unmodified epoxy composites (B0) were increased with the content of 0.1 wt% GnPs by 45.84% and 2.94%, respectively.
- In the GnPs content of 0.1wt%, carbon fiber (C) reinforced epoxy composites were exhibited the maximum value of flexural strength and percentage improvement was 18.1%. However, maximum flexural modulus was evaluated at GnPs content of 0.5 wt% indicating that brittleness of the composite sample was increased.
- On the other hand, flexural strength of the aramid fiber (A) reinforced epoxy composite were reduced continuously with the inclusion of GnPs.
- In addition, flexural strength and modulus of hybrid composite GA were reached their maximum values with 0.25 wt% of GnPs like G composite sample. The percentage improvement in flexural strength and modulus was 14.56% and 5.6% compared to pure GA0. Besides, flexural strength and modulus of hybrid composite AG was continuously decreased with the GnPs inclusion.
- According to test results, GnPs particle addition significantly improved the flexural strength and modulus of GB, BG and B composite samples. In particular, the content of 0.1wt% of GnPs in the epoxy resin, flexural strength values were increased with the improvement of 20.1%, 63.06% and 45.84% for GB, BG and B fiber reinforced composite samples, respectively.
- For the hybrid samples of GC and CG, GnPs filler addition resulted as improvement in flexural strength values. The percentage improvement of these values was 2.92% in GC sample with 0.25wt% GnPs and 13.49% in CG sample with 0.1wt%.
- According to drop weight impact test results, the fiber hybridization and fabric stacking sequence directly affect the LVI characteristics of composite samples in terms of peak load and absorbed energy. When higher capacity of absorbed energy fabric was placed on the outer surface, hybrid composite structure was reached higher capacity of absorbed energy.
- The highest peak load and absorbed energy values were found as 4.46 kN and 28.36 J in carbon fiber reinforced having unmodified epoxy composite sample (C0). On the other hand, the highest maximum displacement value was 35.71 mm in aramid fiber reinforced unmodified epoxy composite sample (A0).

- Aramid fiber hybridization resulted as an improvement in the absorbed energy and displacement values of the glass fiber reinforced composites which indicates that the increased ductility of composite samples. Enhancement in absorbed energy values were calculated as 2.3% in GA0 and 10.5% in AG0 compared to G0 composite sample.
- Glass fiber hybridization improved the peak load and absorbed energy values of the basalt fiber reinforced unmodified epoxy composite when glass fiber was placed on the outer surface. Enhancement in absorbed energy and peak load values were calculated as 30.8% and 64.9% in GB0. However, reduction in these values were recorded in the other hybrid configuration as -3.2% and -8.8% in BG0 compared to B0 composite sample.
- Carbon fiber hybridization improved the LVI response of glass fiber reinforced composite in terms of peak load and absorbed energy values. Enhancement in absorbed energy and peak load values were calculated as 7.3% and 8.3% in GC0; 14.7% and 12.8% in CG0 compared to G0 composite sample.
- As mentioned in previous chapters, the reinforcement material (fiber) is the main load-bearing structure of the composite body and the bonding strength between reinforcement and matrix phase is extremely important to load transfer between reinforcement materials. Thus, GnPs additive significantly affects the impact behavior of the composite plates.
- The peak load and absorbed energy of glass fiber reinforced unmodified epoxy composites (G0) were clearly exhibited the highest value at GnPs content of 0.25 wt% with indicating 3.4% and 9.21% improvement, respectively. Further addition of GnPs content after the 0.25 wt% resulted in a reduction of peak load and absorbed energy values which could resulted from debonding between matrix and GnPs particles.
- Decreasing absorbed energy values were seen in aramid fiber reinforced composite samples with increasing GnPs content like the flexural behavior of GnPs modified aramid composite samples.
- The percentage improvement in peak load and absorbed energy values of basalt reinforced composite samples were recorded as 11.0% and 11.17%. With further GnPs addition after 0.1 wt % of GnPs, a decreasing trend was seen for impact strength values.

- As in basalt reinforced composite samples, carbon fiber reinforced composite samples were reached their highest peak load and absorbed energy values with 0.1wt% GnPs addition. The improvement in these values were 14.5% and 1.06% compared to pure carbon/epoxy sample (C0).
- Improved absorbed energy value were recorded in modified glass/aramid hybrid fiber composite samples. In the presence of 0.25 wt% GnPs, hybrid composites GA025 and AG025 showed the highest peak load and absorbed energy values. The percentage improvement in peak load and absorbed energy values were 6.1% and 19.47% in GA; 9.96% and 4.12% in AG hybrid composite sample.
- Increasing peak load and absorbed energy values were recorded with the addition of GnPs until 0.25wt% in GB and 0.1wt% in BG hybrid sample. These results indicate that the fiber type on the outer surfaces of the hybrid composite samples predominates in the impact strength of the material. The percentage improvement in peak load and absorbed energy values were recorded as 15.87% and 10.57% in GB, 13.97% and 20.9% in BG.
- Increasing absorbed energy values were recorded with the addition of GnPs until 0.25wt% in GC and CG hybrid samples. The percentage improvement in absorbed energy values were recorded as 12.73% in GC, 16.9% in CG.
- Impacted surfaces were observed by SEM imaging technique to examine the micro-mechanical properties of GnPs addition of composite samples. it has been found that GnPs additive directly affects the fiber / matrix interface bonding and thus affects the load transfer between the phases.
- It was seen that the fibers were easily separated from matrix with a clear interfacial rupture in composite samples with pure epoxy matrix and this is thought to be caused by poor fiber / matrix interfacial bonding. On the other hand, GnPs modified samples show that the fibers were hardly removed from the epoxy matrix during plate damage and have large amounts of epoxy matrix residues on them which indicates that the improved fiber / matrix interfacial bonding.

CHAPTER 7

FUTURE WORKS

This experimental study and its results provide the basis for future research and pave the way for possible studies. Some of the possible studies may include:

- Mechanical and impact behavior of hybrid fiber reinforced composites can be studied by using different nano particles (such as carbon nanotube, nano boron) and different fiber combinations (with metal reinforcements or natural fibers),
- Thermal, electrical behavior of nanoparticle filled hybrid/non-hybrid fiber reinforced composites can be studied,
- Thermal and water aging effects on the mechanical, LVI properties can also be studied.

REFERENCES

[1] Kaw, A. K. (2005). Mechanics of composite materials. CRC press.

[2] Chawla, K. K. (2012). Composite materials: science and engineering. Springer Science & Business Media.

[3] Bunsell, A. R., & Renard, J. (2005). Fundamentals of fibre reinforced composite materials. CRC Press.

[4] D. Hull and T. W. Clyne, An Introduction to Composite Materials, Cambridge University Press, 1996.

[5] Rajisha, K. R., Deepa, B., Pothan, L. A., & Thomas, S. (2011). Thermomechanical and spectroscopic characterization of natural fibre composites. In Interface Engineering of Natural Fibre Composites for Maximum Performance (pp. 241-274). Woodhead Publishing.

[6] Vasiliev, V. V., & Morozov, E. V. (2001). Mechanics and analysis of composite materials. Elsevier.

[7] Reid, S. R., & Zhou, G. (Eds.). (2000). Impact behaviour of fibre-reinforced composite materials and structures. Elsevier.

[8] S. Abrate, Impact on Composite Structures, Cambridge University Press, 1998.

[9] Starratt D., Sanders, T., Cepus, E., Porsartip, A. Vaziri, R. (2000). An efficient method for continous measurment of projectile motion in ballistic impact experiments, *Elsevier International Journal of Impact Eng.,* **24**, 155-170.

[10] Razali, N., Sultan, M. T. H., Mustapha, F., Yidris, N., & Ishak, M. R. (2014). Impact damage on composite structures–a review, The International Journal of Engineering and Science, **3**, 7.

[11] Abrate, S. (1991). Impact on laminated composite materials, Applied mechanics reviews, **44(4)**, 155-190.

[12] Robinson, P., & Davies, G. A. O. (1992). Impactor mass and specimen geometry effects in low velocity impact of laminated composites, International Journal of Impact Engineering, **12(2)**, 189-

207.Abrate, S. (Ed.). (2011). Impact engineering of composite structures (Vol. 526). Springer Science & Business Media.

[13] KEVLAR Technical Guide. dupont.com, 01.04.2019.

[14] Sevkat E, Liaw B, Delale F, Raju BB (2009). Drop-weight impact of plain-woven hybrid glass–graphite/toughened epoxy composites, *Compos Part A Appl Sci Manuf,* **40**:1090–110.

[15] Bunea M, Cîrciumaru A, Buciumeanu M, Bîrsan IG, Silva FS. (2019). Low velocity impact response of fabric reinforced hybrid composites with stratified filled epoxy matrix, *Compos Sci Technol,* **169**:242–8.

[16] Bulut M, Erkliğ A, Yeter E. (2016). Hybridization effects on quasi-static penetration resistance in fiber reinforced hybrid composite laminates, *Compos Part B Eng*, **98**:9–22. doi: 10.1016 /J. COMPOSITESB.2016.05.025.

[17] Alsaadi M, Erkliğ A, Alrawi H. (2017) Effect of S-glass fabric on the mechanical characteristics of a hybrid carbon/aramid fabric reinforced epoxy composites, *Mater. Res. Express*, **4**:055304. doi:10.1088/2053-1591/aa6bab.

[18] Šupová M, Martynková GS, Barabaszová K. (2011). Effect of nanofillers dispersion in polymer matrices: a review, *Sci Adv Mater*, **3**:1–25.

[19] Hussain, F., Hojjati, M., Okamoto, M., & Gorga, R. E. (2006). Polymer-matrix nanocomposites, processing, manufacturing, and application: an overview, *Journal of composite materials*, **40(17)**, 1511-1575.

[20] Hanemann, T., & Szabó, D. V. (2010). Polymer-nanoparticle composites: from synthesis to modern applications, *Materials*, **3(6)**, 3468-3517.

[21] Davies, G. A. O., & Zhang, X. (1995). Impact damage prediction in carbon composite structures, *International Journal of Impact Engineering*, **16(1)**, 149-170.

[22] Richardson, M. O. W., & Wisheart, M. J. (1996). Review of low-velocity impact properties of composite materials, *Composites Part A: Applied Science and Manufacturing*, **27(12)**, 1123-1131.

[23] Sapuan, S. M., & Maleque, M. A. (2005). Design and fabrication of natural woven fabric reinforced epoxy composite for household telephone stand, *Materials & design*, **26(1)**, 65-71.

[24] Campbell, F. C. (2010). Structural composite materials. ASM international.

[25] Elanchezhian, C., Ramnath, B. V., & Hemalatha, J. (2014). Mechanical behaviour of glass and carbon fibre reinforced composites at varying strain rates and temperatures, *Procedia materials science*, **6**, 1405-1418.

[26] Shokrieh, M. M., Saeedi, A., & Chitsazzadeh, M. (2013). Mechanical properties of multi-walled carbon nanotube/polyester nanocomposites, *Journal of Nanostructure in Chemistry*, **3(1)**, 20.

[27] Coleman, J. N., Khan, U., Blau, W. J., & Gun'ko, Y. K. (2006). Small but strong: a review of the mechanical properties of carbon nanotube–polymer composites, *Carbon*, **44(9)**, 1624-1652.

[28] Gojny, F. H., Wichmann, M. H., Fiedler, B., Bauhofer, W., & Schulte, K. (2005). Influence of nano-modification on the mechanical and electrical properties of conventional fibre-reinforced composites, *Composites Part A: Applied Science and Manufacturing*, **36(11)**, 1525-1535.

[29] Olsson, R. (2000). Mass criterion for wave controlled impact response of composite plates, *Composites Part A: Applied Science and Manufacturing*, **31(8)**, 879-887.

[30] Olsson, R. (2001). Analytical prediction of large mass impact damage in composite laminates, *Composites Part A: Applied Science and Manufacturing*, **32(9)**, 1207-1215.

[31] Hasan, K. F., Islam, M., Morshed, M. N., Iqbal, M. I. I., & Wu, J. H. W. (2016). Dynamic mechanical behavior & analysis of the jute-glass fiber reinforced polyester hybrid composites, *Am. J. Appl. Phys*, **1(1)**, 1-12.

[32] Behnia, S., Daghigh, V., Nikbin, K., Fereidoon, A., & Ghorbani, J. (2016). Influence of stacking sequence and notch angle on the Charpy impact behavior of hybrid composites, *Mechanics of Composite Materials*, **52(4)**, 489-496.

[33] Lee, Y. S., Kang, K. H., & Park, O. (1997). Response of hybrid laminated composite plates under low-velocity impact, *Computers & structures*, **65(6)**, 965-974.

[34] Agarwal, G., Patnaik, A., Kumar SHARMA, R., & Agarwal, J. (2014). Effect of stacking sequence on physical, mechanical and tribological properties of glass-carbon hybrid composites, *Friction*, **2(4)**, 354-364.

[35] Park, R., & Jang, J. (2001). Impact behavior of aramid fiber/glass fiber hybrid composite: Evaluation of four-layer hybrid composites, *Journal of materials science*, **36(9)**, 2359-2367.

[36] Park, R., & Jang, J. (2001). Impact behavior of aramid fiber/glass fiber hybrid composites: the effect of stacking sequence, *Polymer composites*, **22(1)**, 80-89.

[37] Naik, N. K., Ramasimha, R., Arya, H. E. M. E. N. D. R. A., Prabhu, S. V., & ShamaRao, N. (2001). Impact response and damage tolerance characteristics of glass–carbon/epoxy hybrid composite plates, *Composites Part B: Engineering*, **32(7)**, 565-574.

[38] Hosur, M. V., Adbullah, M., & Jeelani, S. (2005). Studies on the low-velocity impact response of woven hybrid composites, *Composite Structures*, **67(3)**, 253-262.

[39] Gustin, J., Joneson, A., Mahinfalah, M., & Stone, J. (2005). Low velocity impact of combination Kevlar/carbon fiber sandwich composites, *Composite structures*, **69(4)**, 396-406.

[40] Wang, X., Hu, B., Feng, Y., Liang, F., Mo, J., Xiong, J., & Qiu, Y. (2008). Low velocity impact properties of 3D woven basalt/aramid hybrid composites, *Composites Science and Technology*, **68(2)**, 444-450.

[41] Sayer, M., Bektaş, N. B., & Sayman, O. (2010). An experimental investigation on the impact behavior of hybrid composite plates, *Composite Structures*, **92(5)**, 1256-1262.

[42] Sayer, M., Bektaş, N. B., & Çallioğlu, H. (2010). Impact behavior of hybrid composite plates, *Journal of applied polymer science*, **118(1)**, 580-587.

[43] Sevkat, E., Liaw, B., Delale, F., & Raju, B. B. (2009). Drop-weight impact of plain-woven hybrid glass–graphite/toughened epoxy composites, *Composites Part A: Applied Science and Manufacturing*, **40(8)**, 1090-1110.

[44] Enfedaque, A., Molina-Aldareguía, J. M., Gálvez, F., González, C., & LLorca, J. (2010). Effect of glass fiber hybridization on the behavior under impact of woven carbon fiber/epoxy laminates, *Journal of composite materials*, **44(25)**, 3051-3068.

[45] Sevkat, E., Liaw, B., & Delale, F. (2013). Drop-weight impact response of hybrid composites impacted by impactor of various geometries, *Materials & Design*, **52**, 67-77.

[46] Sarasini, F., Tirillò, J., Valente, M., Ferrante, L., Cioffi, S., Iannace, S., & Sorrentino, L. (2013). Hybrid composites based on aramid and basalt woven fabrics: Impact damage modes and residual flexural properties, *Materials & Design*, **49**, 290-302.

[47] Sarasini, F., Tirillò, J., Ferrante, L., Valente, M., Valente, T., Lampani, L., ... & Sorrentino, L. (2014). Drop-weight impact behaviour of woven hybrid basalt–carbon/epoxy composites, *Composites Part B: Engineering*, **59**, 204-220.

[48] Valença, S. L., Griza, S., de Oliveira, V. G., Sussuchi, E. M., & de Cunha, F. G. C. (2015). Evaluation of the mechanical behavior of epoxy composite reinforced with Kevlar plain fabric and glass/Kevlar hybrid fabric, *Composites Part B: Engineering*, **70**, 1-8.

[49] Bandaru, A. K., Patel, S., Sachan, Y., Alagirusamy, R., Bhatnagar, N., & Ahmad, S. (2016). Low velocity impact response of 3D angle-interlock Kevlar/basalt reinforced polypropylene composites, *Materials & Design*, **105**, 323-332.

[50] Aktaş, M., Atas, C., İçten, B. M., & Karakuzu, R. (2009). An experimental investigation of the impact response of composite laminates, *Composite Structures*, **87(4)**, 307-313.

[51] Cheon, S. S., & Lim, T. S. (1999). Impact energy absorption characteristics of glass fiber hybrid composites, *Composite Structures*, **46(3)**, 267-278.

[52] Murugan, R., Ramesh, R., & Padmanabhan, K. (2014). Investigation on static and dynamic mechanical properties of epoxy based woven fabric glass/carbon hybrid composite laminates, *Procedia Engineering*, **97**, 459-468.

[53] Erkliğ, A., & Bulut, M. (2017). Experimental investigation on tensile and Charpy impact behavior of Kevlar/S-glass/epoxy hybrid composite laminates, *Journal of Polymer Engineering*, **37(2)**, 177-184.

[54] Bozkurt, Ö. Y., Erkliğ, A., & Bulut, M. (2018). Hybridization effects on charpy impact behavior of basalt/aramid fiber reinforced hybrid composite laminates, *Polymer Composites*, **39(2)**, 467-475.

[55] Hosur, M. V., Chowdhury, F., & Jeelani, S. (2007). Low-velocity impact response and ultrasonic NDE of woven carbon/epoxy—Nanoclay nanocomposites, *Journal of Composite Materials*, **41(18)**, 2195-2212.

[56] Iqbal, K., Khan, S. U., Munir, A., & Kim, J. K. (2009). Impact damage resistance of CFRP with nanoclay-filled epoxy matrix, *Composites Science and Technology*, **69(11)**, 1949-1957.

[57] Khan, S. U., Iqbal, K., Munir, A., & Kim, J. K. (2011). Quasi-static and impact fracture behaviors of CFRPs with nanoclay-filled epoxy matrix, *Composites Part A: Applied Science and Manufacturing*, **42(3)**, 253-264.

[58] Kostopoulos, V., Baltopoulos, A., Karapappas, P., Vavouliotis, A., & Paipetis, A. (2010). Impact and after-impact properties of carbon fibre reinforced composites enhanced with multi-wall carbon nanotubes, *Composites Science and Technology*, **70(4)**, 553-563.

[59] Ashrafi, B., Guan, J., Mirjalili, V., Zhang, Y., Chun, L., Hubert, P., ... & Johnston, A. (2011). Enhancement of mechanical performance of epoxy/carbon fiber laminate composites using single-walled carbon nanotubes, *Composites science and technology*, **71(13)**, 1569-1578.

[60] Alhazov, D., & Zussman, E. (2012). Study of the energy absorption capabilities of laminated glass using carbon nanotubes, *Composites Science and Technology*, **72(6)**, 681-687.

[61] Soliman, E. M., Sheyka, M. P., & Taha, M. R. (2012). Low-velocity impact of thin woven carbon fabric composites incorporating multi-walled carbon nanotubes, *International Journal of Impact Engineering*, **47**, 39-47.

[62] Reis, P. N. B., Ferreira, J. A. M., Zhang, Z. Y., Benameur, T., & Richardson, M. O. W. (2013). Impact response of Kevlar composites with nanoclay enhanced epoxy matrix, *Composites Part B: Engineering*, **46**, 7-14.

[63] Reis, P. N. B., Ferreira, J. A. M., Santos, P., Richardson, M. O. W., & Santos, J. B. (2012). Impact response of Kevlar composites with filled epoxy matrix, *Composite Structures*, **94(12)**, 3520-3528.

[64] Hossain, M. E., Hossain, M. K., Hosur, M., & Jeelani, S. (2014). Low-velocity impact behavior of CNF-filled glass-reinforced polyester composites, *Journal of Composite Materials*, **48(7)**, 879-896.

[65] Alomari, A., Aldajah, S., Hayek, S., Moustafa, K., & Haik, Y. (2013). Experimental investigation of the low speed impact characteristics of nanocomposites, *Materials & Design*, **47**, 836-841.

[66] Rahman, M. M., Hosur, M., Hsiao, K. T., Wallace, L., & Jeelani, S. (2015). Low velocity impact properties of carbon nanofibers integrated carbon

fiber/epoxy hybrid composites manufactured by OOA–VBO process, *Composite Structures*, **120**, 32-40.

[67] Siegfried, M., Tola, C., Claes, M., Lomov, S. V., Verpoest, I., & Gorbatikh, L. (2014). Impact and residual after impact properties of carbon fiber/epoxy composites modified with carbon nanotubes, *Composite Structures*, **111**, 488-496.

[68] Sivasaravanan, S., & Raja, V. B. (2014). Impact Characterization of Epoxy LY556/E-Glass Fibre/Nano Clay Hybrid Nano Composite Materials, *Procedia Engineering*, **97**, 968-974.

[69] Taraghi, I., Fereidoon, A., & Taheri-Behrooz, F. (2014). Low-velocity impact response of woven Kevlar/epoxy laminated composites reinforced with multi-walled carbon nanotubes at ambient and low temperatures, *Materials & Design*, **53**, 152-158.

[70] Islam, M. E., Mahdi, T. H., Hosur, M. V., & Jeelani, S. (2015). Characterization of Carbon Fiber Reinforced Epoxy Composites Modified with Nanoclay and Carbon Nanotubes, *Procedia Engineering*, **105**, 821-828.

[71] Boumbimba, R. M., Froustey, C., Viot, P., & Gerard, P. (2015). Low velocity impact response and damage of laminate composite glass fibre/epoxy based tri-block copolymer, *Composites Part B: Engineering*, **76**, 332-342.

[72] Boroujeni, A. Y., Skandani, A. A., Emami, A., & Al-Haik, M. A. R. W. A. N. (2015, November). Impact Performance of a Hybrid ZnO Nanorod/Carbon Nanotube/Carbon Fiber Reinforced Polymer Composite, *In American Society of Composites-30th Technical Conference*.

[73] Rafiq, A., Merah, N., Boukhili, R., & Al-Qadhi, M. (2017). Impact resistance of hybrid glass fiber reinforced epoxy/nanoclay composite, *Polymer Testing*, **57**, 1-11.

[74] Heydari-Meybodi, M., Saber-Samandari, S., & Sadighi, M. (2016). An experimental study on low-velocity impact response of nanocomposite beams reinforced with nanoclay, *Composites Science and Technology*, **133**, 70-78.

[75] Singh, N. K., Rawat, P., & Singh, K. K. (2016). Impact Response of Quasi-Isotropic Asymmetric Carbon Fabric/Epoxy Laminate Infused with MWCNTs, *Advances in Materials Science and Engineering*, 2016.

[76] Taraghi, I., & Fereidoon, A. (2016). Non-destructive evaluation of damage modes in nanocomposite foam-core sandwich panel subjected to low-velocity impact, *Composites Part B: Engineering*, **103**, 51-59.

[77] Rostamiyan, Y., Fereidoon, A., Mashhadzadeh, A. H., Ashtiyani, M. R., & Salmankhani, A. (2015). Using response surface methodology for modeling and optimizing tensile and impact strength properties of fiber orientated quaternary hybrid nano composite, *Composites Part B: Engineering*, **69**, 304-316.

[78] Mohan, T. P., Velmurugan, R., & Kanny, K. (2015). Damping characteristics of nanoclay filled hybrid laminates during medium velocity impact, *Composites Part B: Engineering*, **82**, 178-189.

[79] Ahmad, T., Raza, S. S., Aleem, E., Kamran, M., Manzoor, U., Makhdoom, A., ... & Mukhtar, S. (2017). Improvement in mechanical and thermal properties of unsaturated polyester-based hybrid composites, *Iranian Polymer Journal*, **26(4)**, 305-311.

[80] Kamar, N. T., Hossain, M. M., Khomenko, A., Haq, M., Drzal, L. T., & Loos, A. (2015). Interlaminar reinforcement of glass fiber/epoxy composites with graphene nanoplatelets, *Composites Part A: Applied Science and Manufacturing*, **70**, 82-92.

[81] Haq, M., Umer, R., Khomenko, A., Loos, A. C., & Drzal, L. T. (2014). Manufacturing and impact behavior of sandwich composites with embedded graphene platelets, In *The 19th International Conference on Composite Materials*, Montreal, Canada. July 28-August 2013.

[82] Ávila, A. F., Dias, E. C., Cruz, D. T. L. D., Yoshida, M. I., Bracarense, A. Q., Carvalho, M. G. R., & Ávila Junior, J. D. (2010). An investigation on graphene and nanoclay effects on hybrid nanocomposites post fire dynamic behavior, *Materials Research*, **13(2)**, 143-150.

[83] Gokuldass, R., & Ramesh, R. (2019). Mechanical and low velocity impact behaviour of intra-ply glass/kevlar fibre reinforced nano-silica and micro-rubber modified epoxy resin hybrid composite, *Materials Research Express*, **6** 055302.

[84] Kavitha, N. S., & Prakash, R. V. (2014). Size Scale Effects on Post-Impact Residual Strength of Hybrid Glass/Carbon/Epoxy Nano-composites, *Procedia Materials Science*, **3**, 2134-2141.

[85] Mohanty, A., & Srivastava, V. K. (2015). Effect of alumina nanoparticles on the enhancement of impact and flexural properties of the short glass/carbon fiber reinforced epoxy based composites, *Fibers and Polymers*, **16(1)**, 188-195.

[86] Asaee, Z., Mohamed, M., De Cicco, D., & Taheri, F. (2017). Low-velocity impact response and damage mechanism of 3D fiber-metal laminates reinforced with amino-functionalized graphene nanoplatelets, *Int. J. Compos. Mater*, **7(1)**, 20-36.

[87] Zhang, X. (1998). Impact damage in composite aircraft structures-experimental testing and numerical simulation, Proceedings of the Institution of Mechanical Engineers, *Part G: Journal of Aerospace Engineering*, **212(4)**, 245-259.,

[88] Yeter, E. (2014). Buckling behavior of laminated hybrid composites. PhD Thesis in Mechanical Engineering, Gaziantep University.

[89] ASTM. American Society for Testing and Materials. Standard Test Method for Measuring the Damage Resistance of a Fiber-Reinforced Polymer Matrix Composite to a Drop-Weight Impact Event. D7136/D7136M-15. West Conshohocken, PA.

[90] ASTM. American Society for Testing and Materials. Standard Test Method for Measuring the Damage Resistance of a Fiber-Reinforced Polymer-Matrix Composite to a Concentrated Quasi-Static Indentation Force. D6264/D6264M-17. West Conshohocken, PA.

[91] ASTM. American Society for Testing and Materials. Standard Test Methods for Flexural Properties of Unreinforced and Reinforced Plastics and Electrical Insulating Materials. D790-17. West Conshohocken, PA.

[92] ASTM. American Society for Testing and Materials. Standard Test Method for Tensile Properties of Plastics. D638-14. West Conshohocken, PA.

[93] Erkliğ, A. & Bulut, M. (2016). Experimental investigation on tensile and Charpy impact behavior of Kevlar/S-glass/epoxy hybrid composite laminates, *Journal of Polymer Engineering*, **37(2)**, pp. 177-184.

[94] Du, J., & Cheng, H. M. (2012). The fabrication, properties, and uses of graphene/polymer composites, *Macromolecular Chemistry and Physics*, **213(10-11)**, 1060-1077.

[95] Bulut, M. (2017). Mechanical characterization of Basalt/epoxy composite laminates containing graphene nanopellets, *Composites Part B: Engineering*, **122**, 71-78.

[96] Du, X., Zhou, H., Sun, W., Liu, H. Y., Zhou, G., Zhou, H., & Mai, Y. W. (2017). Graphene/epoxy interleaves for delamination toughening and monitoring of crack damage in carbon fibre/epoxy composite laminates, *Composites Science and Technology*, **140**, 123-133.

[97] Rafiee MA, Rafiee J, Wang Z, Song HH, Yu ZZ, Koratkar N. (2009). Enhanced mechanical properties of nanocomposites at lowgraphene content, *ACS Nano*;**3(12)**:3884–90.

[98] Zaman I, Kuan HC, Dai JF, Kawashima N, Michelmore A, Sovi A, et al. (2012). From carbon nanotubes and silicate layers to graphene platelets for polymer nanocomposites, *Nanoscale*;**4(15)**:4578–86.

[99] Zhang, J., Chaisombat, K., He, S., & Wang, C. H. (2012). Hybrid composite laminates reinforced with glass/carbon woven fabrics for lightweight load bearing structures, *Materials & Design* (1980-2015), **36**, 75-80.

[100] Pandya, K. S., Veerraju, C., & Naik, N. K. (2011). Hybrid composites made of carbon and glass woven fabrics under quasi-static loading, *Materials & Design*, **32(7)**, 4094-4099.

[101] Kumari, N., & Kumar, K. (2018). Mechanical behaviour of graphene and carbon fibre reinforced epoxy based hybrid nanocomposites for orthotic calipers, *Journal of Experimental Nanoscience*, **13(sup1)**, S14-S23.

[102] Awan, F. S., Fakhar, M. A., Khan, L. A., & Subhani, T. (2019). Study of Interfacial Properties of Carbon Fiber Epoxy Matrix Composites Containing Graphene Nanoplatelets, *Fibers and Polymers*, **20(3)**, 633-641.

[103] Jusoh, M. S. M., Santulli, C., Yahya, M. Y. M., Hussein, N. S., & Ahmad, H. A. I. (2016). Effect of stacking sequence on the tensile and flexural properties of glass fibre epoxy composites hybridized with basalt, flax or jute fibres, *Mater Sci Eng Adv Res*, **1(4)**, 19-25.

[104] Naveen, J., Jawaid, M., Zainudin, E. S., Sultan, M. T., & Yahaya, R. (2019). Effect of graphene nanoplatelets on the ballistic performance of hybrid Kevlar/Cocos nucifera sheath-reinforced epoxy composites, *Textile Research Journal*, 0040517519833970.

[105] Sánchez, M., Campo, M., Jiménez-Suárez, A., & Ureña, A. (2013). Effect of the carbon nanotube functionalization on flexural properties of multiscale carbon fiber/epoxy composites manufactured by VARIM, *Composites Part B: Engineering*, **45(1)**, 1613-1619.

[106] Jang, B. Z., Chen, L. C., Wang, C. Z., Lin, H. T., & Zee, R. H. (1989). Impact resistance and energy absorption mechanisms in hybrid composites, *Composites Science and Technology*, **34(4)**, 305-335.

[107] Doğan, N. F., Bulut, M., Erklig, A., & Bozkurt, Ö. Y. (2019). Mechanical and low velocity impact characterization of carbon/glass hybrid composites with graphene nanoplatelets, *Materials Research Express*, **6** 085304.

[108] Reddy, T. S., Reddy, P. R. S., & Madhu, V. (2017). Response of E-glass/Epoxy and Dyneema® Composite Laminates Subjected to low and High Velocity Impact, *Procedia engineering*, **173**, 278-285.

[109] Qin, W., Vautard, F., Drzal, L. T., & Yu, J. (2015). Mechanical and electrical properties of carbon fiber composites with incorporation of graphene nanoplatelets at the fiber–matrix interphase, *Composites Part B: Engineering*, **69**, 335-341.

[110] Peterson, A. M., Jensen, R. E., & Palmese, G. R. (2011). Thermoreversible and remendable glass–polymer interface for fiber-reinforced composites, *Composites Science and Technology*, **71(5)**, 586-592.

[111] Mohanty, A. K., Khan, M. A., & Hinrichsen, G. (2000). Surface modification of jute and its influence on performance of biodegradable jute-fabric/Biopol composites, *Composites Science and Technology*, **60(7)**, 1115-1124.

[112] Jabbar, A., Militký, J., Wiener, J., & Karahan, M. (2016). Static and dynamic mechanical properties of novel treated jute/green epoxy composites, *Textile Research Journal*, **86(9)**, 960-974.

[113] Kowsika, M. V., & Mantena, P. R. (1999). Static and low-velocity impact response characteristics of pultruded hybrid glass-graphite/epoxy composite beams, *Journal of Thermoplastic Composite Materials*, **12(2)**, 121-132.

[114] Feraboli, P., Ireland, D., & Kedward, K. (2004). The role of force and energy in low velocity impact events, In *45th AIAA/ASME/ASCE/AHS/ASC Structures, Structural Dynamics & Materials Conference* (p. 1841).

[115] Sjoblom, P. O., Hartness, J. T., & Cordell, T. M. (1988). On low-velocity impact testing of composite materials, *Journal of composite materials*, **22(1)**, 30-52.

CURRICULUM VITAE

PERSONAL INFORMATION

Name and Surname: Nurettin Furkan DOĞAN

Nationality: T.C.

E-mail: nfurkandogan@gantep.edu.tr

EDUCATION

	Graduate School	Year
Ph.D.	Gaziantep University, Mechanical Engineering Department, Mechanic Division	2019
M.Sc.	Gaziantep University, Mechanical Engineering Department, Mechanic Division	2015
B.Sc.	Gaziantep University, Mechanical Engineering Department	2012
High School	Gaziantep Anatolian High School	2006

WORK EXPERIENCE

	Place	Enrollment
2013-Present	Gaziantep University, Mechanical Engineering Department	Research Asst.
2012-2013	Kilis 7 Aralık University, Mechanical Engineering Department	Research Asst.

PUBLICATIONS

Papers Published in International indexed Journals

1) DOĞAN NURETTİN FURKAN, BULUT MEHMET, ERKLİĞ AHMET, BOZKURT ÖMER YAVUZ (2019). Mechanical and low velocity impact characterization of carbon/glass hybrid composites with graphene nanoplatelets.Materials Research Express, 6(8), 85304, Doi: 10.1088/2053-1591/ab1c03 (Yayın No: 5020424)

2) ERKLİĞ AHMET, DOĞAN NURETTİN FURKAN, BULUT MEHMET (2017). Charpy Impact Response of Glass Fiber Reinforced Composite with Nano Graphene Enhanced Epoxy. Periodicals of Engineering and Natural Sciences (PEN), 5(3), Doi: 10.21533/pen.v5i3.121 (Yayın No: 4390278)

3) BULUT MEHMET, ERKLİĞ AHMET, DOĞAN NURETTİN FURKAN (2017). On adhesive properties of perlite and sewage sludge ash with epoxy resin bonded single-strap repairs. Materials Research Express, 4(8), 85302, Doi: 10.1088/2053-1591/aa8231 (Yayın No: 3725159)

4) KANBER BAHATTİN, DOĞAN NURETTİN FURKAN (2013). Comparison of PIM and RPIM Solutions of Elasto Plastic Thick Beams. International Journal of Aerospace and Lightweight Structures (IJALS), 3(2), 241, Doi: 10.3850/S2010428613000640 (Yayın No: 2856162)

Papers Published in National indexed Journals

1) DOĞAN NURETTİN FURKAN, ERKLİĞ AHMET (2018). On the effect of nano particle inclusion in fiber reinforced composite tensile and flexural behavior. International Advanced Researches and Engineering Journal, 2(3), 240-244. (Kontrol No: 4654554)

International Conference Papers Published in Proceedings

1) ERKLİĞ AHMET, OĞUZ ZEYNAL ABİDİN, DOĞAN NURETTİN FURKAN (2019). Effect of Seawater Aging Condition on Tensile Properties of Glass-Epoxy Composites. 6th International Multidiciplinary Studies Congress (Tam Metin Bildiri/Sözlü Sunum) (Yayın No:5037231)

2) ERKLİĞ AHMET, OĞUZ ZEYNAL ABİDİN, DOĞAN NURETTİN FURKAN (2019). Effect of Distilled Water Aging Condition on Tensile Properties

of Glass-Epoxy Composites. 6th International Multidiciplinary Studies Congress (Tam Metin Bildiri/Sözlü Sunum) (Yayın No:5037232)

3) ERKLİĞ AHMET, DOĞAN NURETTİN FURKAN, OĞUZ ZEYNAL ABİDİN (2019). Charpy impact response of Glass/Aramid hybrid fiber reinforced epoxy filled with Graphene Nano-Platelets. III. Uluslararası AVRASYA Multidisipliner Çalışmalar Kongresi, 542-548. (Tam Metin Bildiri/Sözlü Sunum) (Yayın No:5026928)

4) ERKLİĞ AHMET, DOĞAN NURETTİN FURKAN, OĞUZ ZEYNAL ABİDİN (2019). On the Low-Velocity Impact Behavior of Nanoparticle Filled Glass/Basalt Hybrid Composites. III. Uluslararası AVRASYA Multidisipliner Çalışmalar Kongresi, 549-556. (Tam Metin Bildiri/Sözlü Sunum) (Yayın No:5026930)

5) ERKLİĞ AHMET, DOĞAN NURETTİN FURKAN (2018). Flexural Behavior of Nano Graphene Reinforced Hybrid Composite Laminates. The Internatinonal Conference on Materials Science Mechanical and Automation Engineerings and Technology, 608-608. (Özet Bildiri/Sözlü Sunum) (Yayın No:4680273)

6) ERKLİĞ AHMET, DOĞAN NURETTİN FURKAN (2018). Charpy Impact Behavior of Nano Graphene Reinforced Hybrid Composite Laminates. The Internatinonal Conference on Materials Science, Mechanical and Automotive Engineerings and Technology, 513-513. (Özet Bildiri/Sözlü Sunum) (Yayın No:4680285)

7) ERKLİĞ AHMET, DOĞAN NURETTİN FURKAN (2017). On the Effect of Nano Particle Inclusion in Fiber Reinforced Composite Tensile and Flexural Behavior. International Advanced Researches Engineering Congress-2017 (Özet Bildiri/Sözlü Sunum) (Yayın No:3724941)

8) ERKLİĞ AHMET, DOĞAN NURETTİN FURKAN (2017). On the Effect of Nano Particle Inclusion in Fiber Reinforced Composite Vibration Behavior. International Advanced Researches Engineering Congress-2017 (Özet Bildiri/Sözlü Sunum) (Yayın No:3724923)

9) ERKLİĞ AHMET, BULUT MEHMET, DOĞAN NURETTİN FURKAN (2017). Vibration Properties of Intraply Woven Carbon/Aramid Fiber Reinforced Composites with Nano Clay Particles. ICAIE 2017- International Conference on

Advances and Innovations in Engineering (Tam Metin Bildiri/Sözlü Sunum) (Yayın No:3662852)

10) ERKLİĞ AHMET, DOĞAN NURETTİN FURKAN, BULUT MEHMET (2017). On the Vibration Behavior of Intraply Woven Carbon/Kevlar Reinforced Composites with Nano Silica Particle. 3.International Conference on Engineering and Natural Sciences, 1258-1262. (Tam Metin Bildiri/Sözlü Sunum) (Yayın No:3724829)

11) ERKLİĞ AHMET, DOĞAN NURETTİN FURKAN, BULUT MEHMET (2017). Charpy Impact Response of Glass Fiber Reinforced Composite with Nano Graphene Enhanced Epoxy. 3.International Conference on Engineering and Natural Sciences, 1263-1267. (Özet Bildiri/Sözlü Sunum) (Yayın No:3724878)

12) KÜTÜK MEHMET AKİF, DOĞAN NURETTİN FURKAN, ALDULAİMİ OMAR (2016). Tensile Strength of Double Lap Joints Bonded With A Microparticle Reinforced Adhesive. International Conference on Engineering and Natural Sciences (ICENS 2016), 1(2) (Tam Metin Bildiri/Sözlü Sunum) (Yayın No:2856161)

13) KÜTÜK MEHMET AKİF, DOĞAN NURETTİN FURKAN (2016). Kompozit Malzemelerin Yapıştırılmasında Parçacık Katkılı Yapıştırıcıların Yapıştırma Performansına Etkisi. 4th International Conference on Welding Technologies and Exhibition, 2(4), 1291-1301. (Tam Metin Bildiri/Sözlü Sunum) (Yayın No:2861154)

14) KANBER BAHATTİN, DOĞAN NURETTİN FURKAN (2013). Comparison of PIM and RPIM solutions of Elasto-plastic Thick Beams. 5th Asia Pasific Congress on Computational Mechanics (Tam Metin Bildiri/Sözlü Sunum) (Yayın No:3435415)

National Conference Papers Published in Proceedings

1) KANBER BAHATTİN, DOĞAN NURETTİN FURKAN (2015). İndirgenmiş Noktasal İntegrasyon Kullanılarak Kalın Kirişlerin Elasto plastik Davranışlarının İncelenmesi. Ulusal Mekanik Kongresi (Tam Metin Bildiri/Sözlü Sunum) (Yayın No:2122898)

2) KANBER BAHATTİN, DOĞAN NURETTİN FURKAN, TUFIK OTHMAN (2013). İNCE KİRİŞLERİN ELASTİK DAVRANIŞLARININ NİY VE RNİYYÖNTEMLERİ İLE İNCELEMESİ. 18. Ulusal Mekanik Kongresi, 340-348. (Tam Metin Bildiri/Sözlü Sunum) (Yayın No:2861163)

TASKS IN PROJECTS

1) Jüt/cam fiber nanosilika katkılı hibrid kompozitlerin mekanik özelliklerinin araştırılması, Yükseköğretim Kurumları tarafından destekli bilimsel araştırma projesi, Araştırmacı:Hassan Wasan Falah,Araştırmacı:DOĞAN NURETTİN FURKAN,Yürütücü:ERKLİĞ AHMET, , 07/03/2018 - 14/11/2018 (ULUSAL)

2) Elyaf Sarma İşleminde Üretim Hızını Ve Esnekliğini Artırmaya Yönelik Yeni Bir Yöntem Uygulaması, -Tübitak 1005, Yürütücü:ERKLİĞ AHMET,Bursiyer:BULUT MEHMET, Bursiyer:DOĞAN NURETTİN FURKAN, Araştırmacı:BOZKURT ÖMER YAVUZ, Bursiyer:ÖZBEK ÖZKAN, , 01/09/2015 - 22/02/2018 (ULUSAL)

3) Cam/Aramid Hibrit Fiber Takviyesi ile birlikte Nano Grafen Katkısının Kompozit Plakaların Mekanik Özelliklerine Etkisinin Araştırılması, Yükseköğretim Kurumları tarafından destekli bilimsel araştırma projesi, Yürütücü:ERKLİĞ AHMET, Araştırmacı:DOĞAN NURETTİN FURKAN , 23/02/2018 – 05/07/2019 (ULUSAL)